Machbarkeitsstudie eines Sonnenschildes im Einflussbereich des Sonne Erde L1 Lagrange Punktes

Feasibility study of a sunshade in the vicinity of the Sun Earth L1 Lagrange Point

Master Thesis by
B.Sc. Sebastian Fix
IRS-21-S-006

Supervisors:
Prof. Dr. rer. nat. Reinhold Ewald
M.Sc. Markus Graß

Institute of Space Systems
University of Stuttgart
February 2021

Please do not distribute without the author's consent

Abstract

Shading the Earth with one or several thin structures positioned at the Sun Earth L1 Lagrange Point is a concept that was proposed to counter global warming [1]. The technological feasibility of producing these sunshades has been reviewed in this thesis. Technologies for lunar in-situ resource utilisation, manufacturing of the sunshades in space, and ways to produce solar cells for powering production facilities and sunshades have been examined. The state-of-the-art of these technologies and trends for the future were applied to a roadmap proposing steps to be taken on the way towards sunshade implementation. This has shown that the trend of in-space manufacturing and international goals for lunar exploration can be utilised for accelerated sunshade development. Many technologies which are required to manufacture satellite structures in space or to operate sustainable lunar exploration are similar to those technologies required for producing sunshades in space. The manufacturing process of thin metallic foil and solar cells from space resources still must be demonstrated. However, if pursued near-term, the timeframe for technology demonstration is still feasible and first sunshades could be operated by 2060. Advancing the development of sunshade production technologies not only allows for reduction of the global warming, but for many other applications that would facilitate ground-breaking space operations.

Zusammenfassung

Um die globale Klimaerwärmung aufzuhalten, wurde vorgeschlagen, die Sonne mithilfe einer oder mehrerer dünner Strukturen abzuschirmen [1]. In dieser Thesis wurde die technologische Machbarkeit der Produktion dieser Sonnenschilde überprüft. Untersucht wurden Technologien zur Nutzung von Mondressourcen, Fertigung der Schilde im Weltall, sowie Möglichkeiten Solarzellen herzustellen, welche Produktionsanlagen und Sonnenschilde mit Energie versorgen. Der Stand der Technik und Trends für die Zukunft wurden verwendet, um einen Strategieplan zu entwerfen, der Handlungsschritte vorschlägt, die den Betrieb der Sonnenschilde ermöglichen. Daraus ging hervor, dass der Trend hin zur Weltraumproduktion und internationale Ziele für die Mondexploration genutzt werden können, um die Entwicklung der Sonnenschilde voranzutreiben. Viele Technologien, die benötigt werden, um Satellitenstrukturen im Weltall herzustellen, oder nachhaltig Mondforschung zu betreiben, gleichen denen, die benötigt werden, um Sonnenschilde im Weltall herzustellen. Die Fähigkeit, aus Mondressourcen dünne Metallfolien und Solarzellen zu produzieren, muss nachgewiesen werden; jedoch ist der Zeitrahmen zur Technologiedemonstration realisierbar, sofern diese zeitnah verfolgt wird, und die ersten Sonnenschilde könnten ab 2060 einsatzbereit sein. Die Unterstützung der Technologieentwicklung für die Produktion der Sonnenschilde ermöglicht nicht nur die globale Klimaerwärmung abzuschwächen, sondern auch viele weitere Anwendungen, welche bahnbrechende Raumfahrtaktivitäten vereinfachen würden.

Contents

List of Symbols

Latin Symbols

A_{Sh}	m^2	Shading Area
a_{SRP}	$\frac{\mathrm{m}}{\mathrm{s}^2}$	Solar Radiation Pressure Acceleration
f	–	Relative Reduction of Solar Radiation
M_{Sh}	kg	Sunshade Mass
RF	$\frac{\mathrm{W}}{\mathrm{m}^2}$	Radiative Forcing
R_{Sh}	m	Radius of the Sunshade
r_{Sh}	m	Distance between Sunshade and the Earth
S	$\frac{\mathrm{W}}{\mathrm{m}^2}$	Solar Insolation of the Earth's Surface
ΔS	$\frac{\mathrm{W}}{\mathrm{m}^2}$	Solar Radiation Reduction
ΔT	K	Temperature Change
Δv	$\frac{\mathrm{m}}{\mathrm{s}}$	Change of Velocity

Greek Symbols

α_p	–	Planetary Albedo
ϵ	–	Emissivity
ϵ_B	–	Emissivity of the Back Surface
ϵ_F	–	Emissivity of the Front Surface
η	–	Specular Reflectivity
κ	–	Factor of Optical Properties of a Surface
λ	$\frac{\mathrm{W}}{\mathrm{m}^2\ \mathrm{K}}$	Climate Sensitivity
ρ	$\frac{\mathrm{kg}}{\mathrm{m}^3}$	Density
ρ_{Sh}	$\frac{\mathrm{kg}}{\mathrm{m}^2}$	Sunshade Average Areal Density
Ω_S	sr	Solid Angle of the Sun as seen from the Earth
ω_E	$\frac{\mathrm{rad}}{\mathrm{s}}$	Angular Velocity of the Earth around the Sun

Constants

G	$6.674 \cdot 10^{-11}$	$\frac{\mathrm{m}^3}{\mathrm{kg\ s}^2}$	Gravitational Constant
M_E	$5.974 \cdot 10^{24}$	kg	Mass of the Earth
M_S	$1.989 \cdot 10^{30}$	kg	Mass of the Sun
P_E	$4.56 \cdot 10^{-6}$	$\frac{\mathrm{N}}{\mathrm{m}^2}$	Solar Radiation Pressure at 1 AU
R_S	$6.957 \cdot 10^{8}$	m	Radius of the Sun
r_S	$1.49598 \cdot 10^{11}$	m	Distance between the Earth and the Sun
S_0	$1371\ (\pm 10)$	$\frac{\mathrm{W}}{\mathrm{m}^2}$	Solar Constant

List of Abbreviations

AM	Additive Manufacturing
AOCS	Attitude and Orbit Control System
AR5	Fifth Assessment Report
ARC	Anti-reflection Coating
CDR	Carbon Dioxide Removal
DARPA	Defense Advanced Research Projects Agency
EBF3	Electron-beam Free-form Fabrication
EL3	European Large Logistics Lander
ESA	European Space Agency
ETDP	Exploration Technology Development Program
ETW	Electrostatic Travelling Wave
FabLab	Multi-Material Fabrication Laboratory
FDM	Fused Deposition Modelling
GEO	Geostationary Earth Orbit
GER	Global Exploration Roadmap
GHG	Greenhouse Gas
ILR	Ionic Liquid Reduction
IPCC	Intergovernmental Panel on Climate Change
IPSS	International Planetary Sunshade
ISECG	International Space Exploration Coordination Group
ISM	In-space Manufacturing
ISRU	In-situ Resource Utilisation
ISS	International Space Station
LEO	Low Earth Orbit
MCB	Marine Cloud Brightening
MEV	Mission Extension Vehicle

MRE	Molten Regolith Electrolysis
MRV	Mission Robotic Vehicle
MSE	Molten Salt Electrolysis
NASA	National Aeronautics and Space Administration
NATO	North Atlantic Treaty Organisation
NEA	Near Earth Asteroid
NIAC	NASA Innovative Advanced Concepts
NIR	Near-infrared
NOAA	National Oceanic and Atmospheric Administration
NRL	U.S. Naval Research Laboratory
NSS	National Space Society
OSAM	On-orbit Servicing, Assembly, and Manufacturing
P/L	Payload
PILOT	Precursor ISRU Lunar Oxygen Testbed
ppb	parts per billion
ppm	parts per million
ProSPA	PROSPECT Sample Processing and Analysis
PROSPECT	Package for Resource Observation and in-situ Prospecting for Exploration, Commercial exploitation and Transportation
PTFE	Polytetrafluorethylene
PVD	Physical Vapour Deposition
RCP	Representative Concentration Pathways
RF	Radio Frequency
SAI	Stratospheric Aerosol Injection
SAR	Sulphuric Acid Reduction
SBIR	Small Business Innovation Research
SEL	Sun-Earth Lagrange Point
SEL_A	Artificial Sun-Earth Lagrange Point
SLA	Stereo Lithography
SLD	Solar Limb Darkening
SLM	Selective Laser Melting
SLS	Selective Laser Sintering
SLS	Space Launch System
SPIDER	SPace Infrastructure DExterous Robot
SPS	Solar Power Satellite
SRM	Solar Radiation Management
SRP	Solar Radiation Pressure
TRC	Twin Roll Casting

TRL	Technology Readiness Level
UAM	Ultrasonic Additive Manufacturing
UNEP	United Nations Environmental Programme
UNFCCC	United Nations Framework Convention on Climate Change
VPP	Vapour Phase Pyrolysis
WMO	World Meteorological Organization
WPT	Wireless Power Transmission

Chapter 1

Introduction

Global efforts for climate change mitigation focus on the reduction of greenhouse gas emissions and the development of techniques to remove excessive carbon from the atmosphere. Latest reports on the global climate show only moderate success and predict that the goals defined within the Paris Agreement will likely be missed [2]. Other concepts exist that aim to counter global warming by manipulating the incidence of solar radiation on the Earth's atmosphere. One of these ideas is to create a cooling effect by placing objects into space that would cast a shade onto the Earth.

Solar Radiation Management (SRM) is mostly criticised for being a distraction within the climate change mitigation efforts dialogue [3]. Publicly, it could be perceived as just another human climate intrusion trying to correct past wrongdoings by constructing another piece in a house of cards that will eventually fail. However, this form of geoengineering should not be seen as an alternative to carbon reduction, but as supplementary addition on the way towards sustainability. Should sufficient deceleration of the global temperature rise not be achieved in time and therefore catastrophic destabilisation of the climate be imminent, an optional plan B must be at hand that can be incepted rapidly. At that time, an endeavour of SRM scale cannot be accomplished starting from scratch with only scholarly work performed. The technical systems must be developed and demonstrated, parallel to multilateral governance frameworks that must be formulated based on thorough ethical discussions. An SRM system should not draw attention from creating a sustainable world, it shall rather for a limited duration buy time for humanity to adapt to a future way of living. Therefore, an appropriate dialogue with politics and the public should focus on promoting the potential of SRM for future climate scenarios, raising awareness of the strictly secondary role, while outlining sophisticated concepts for realisation. For the space community this means that models including technology research and development, manufacturing, infrastructure, logistics, and operation must be created, optimising implementation time, cost, climate effect, lifetime, and reliability of space-based sun shading schemes.

The goal of this thesis is to assess the technical feasibility of a sunshade in the vicinity of Sun-Earth Lagrange Point $(SEL)_1$. Sunshade production and resource supply are the main elements examined herein. Starting from the requirement for temperature reduction, the requirements for those system elements shall be derived. To evaluate the feasibility a state-of-the-art review of technologies enabling sunshade manufacturing and eventually operation will be performed. With that knowledge a roadmap towards implementation of a sunshade at SEL_1 will be created, pointing out opportunities to integrate ongoing scientific and commercial efforts, technology fields that require particular attention, and recommendations for near-term technology demonstration missions.

A second thesis has been performed in parallel, considering logistical aspects of sunshade production and operation, so that a full overview can be presented in a short time [4].

As a background for space-based sun shading, the next chapter will give an overview of the state of the global climate, as well as trends for the future. Several concepts for SRM will be compared and the potential of space-based solar geoengineering will be presented. Different concepts for space-based sun shading and their effect on the global climate are discussed therein.

Chapter 3 will present requirements for a sunshade positioned at SEL_1. The determination of size, position, and mass of a sunshade will be described, as well as constraints for material availability and the timeframe for implementation.

The requirements for the sunshade define the requirements for the production systems. Chapter 4 will explore ways to extract construction material from space resources and assess their potential. After that, chapter 5 will review technologies that enable the manufacturing and assembly of sunshade components as well as means to supply it with electrical power. Chapter 6 will give an impression of the scale of production required by presenting sunshade concepts from materials that were extracted by systems reviewed in chapter 4 and manufactured with systems reviewed in chapter 5.

With the constraints defined and the technologies reviewed, the concept of a roadmap that proposes steps towards the implementation of a sunshade at SEL_1 will be proposed in chapter 7. Required development efforts, possibilities to spin in existing technologies, and future spin-off potentials for sunshade technologies will be pointed out.

Chapter 2

Background

2.1 Climate Change

In the last 20 years the number of severe weather events has doubled compared to the previous 20 years. This rise can be explained primarily by the rising global surface temperatures as part of climate change. Especially the numbers of wildfires, floods, and extreme temperatures rose by 46%, 143%, and 223%, respectively, as can be seen in figure 2.1. The anthropogenic emissions of CO_2, CH_4, and N_2O are assumed to intensify the greenhouse effect, increasing the rate of solar energy trapped in the Earth's atmosphere [5]. As can be seen in figure 2.2, those emissions have increased significantly over the last decades [2]. The predicted temperature rise can already be observed, considering that the past six years are likely to be the six warmest years on record [7]. In its report on the state of the global climate the World Meteorological Organization (WMO) also lists constantly increasing side effects in 2019 and 2020: sea level rise, high marine temperature and heatwaves, decreasing arctic sea-ice and Greenland ice sheet, heavy rain and extensive flooding, a record number of North Atlantic hurricanes, severe drought, and population movements in consequence of the aforementioned weather events [7]. Not only did the number of events and people killed or otherwise affected increase during that time span, but also did the economic losses as a consequence of these catastrophes rise from previously $US 1.63 trillion in 1980 – 1999 to $US 2.97 trillion in 2000 – 2019 [6].

These statistics substantiate the urge for action against climate change, of which the effects can already be proven. While governments fear to experience economic deceleration or recession through strict climate policies, the previously mentioned economic costs receive little attention. Weighing them in when financially quantifying measures for climate change mitigation might put expensive efforts into a new perspective. Apart from that, the objective of preventing calamity and millions of deaths is obvious.

Increased concentrations of greenhouse gases (GHGs) change the radiative budget of the Earth's atmosphere. The amount of light shining onto the Earth and the part absorbed and

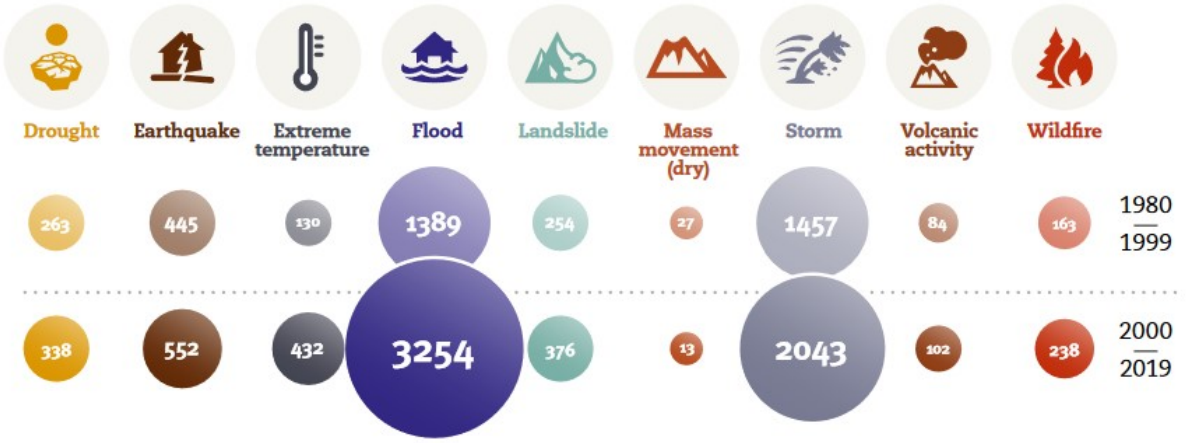

Figure 2.1: Total disaster events by type: 1980 – 1999 vs. 2000 – 2019 [6]

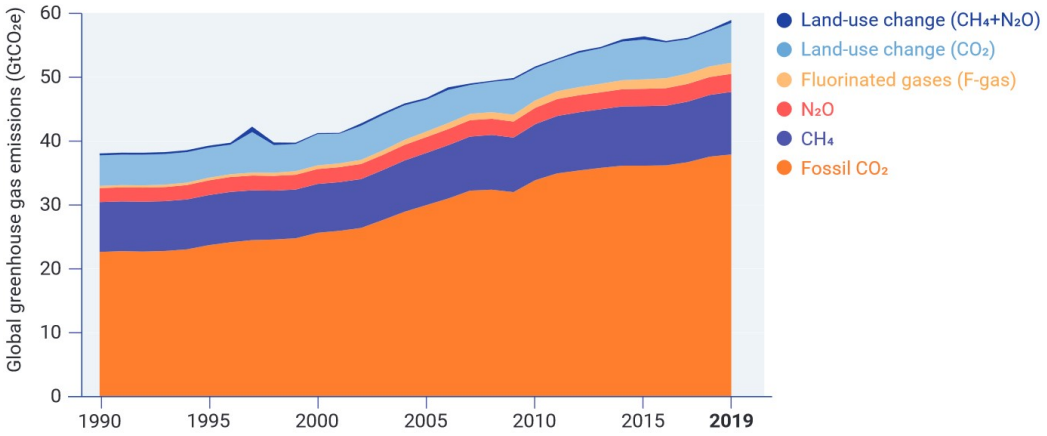

Figure 2.2: Global GHG emissions from all sources [2]

trapped in the planetary mantle and atmosphere, resulted to an equilibrium temperature of about 14 °C for centuries. With increasing greenhouse gas concentrations, the amount of radiation trapped in the atmosphere increases, leading to higher atmospheric temperatures. This can be expressed analytically as an additional source in the Earth's thermal equilibrium equation and is called radiative forcing (given in $\frac{\mathrm{W}}{\mathrm{m}^2}$). If radiative forcing is exerted on a planet's atmosphere, the mean temperature changes until a new equilibrium is reached and subsequently the radiative forcing is zero. Knowing this, the air temperature can be changed anthropogenically by controlling the radiative budget, i.e., GHG concentration and solar irradiation.

Within the Fifth Assessment Report (AR5) by the Intergovernmental Panel on Climate Change (IPCC) four Representative Concentration Pathways (RCP) were presented; pathways for atmospheric GHG concentrations until the end of the 21$^{\mathrm{st}}$ century, as shown in figure 2.3 [5].

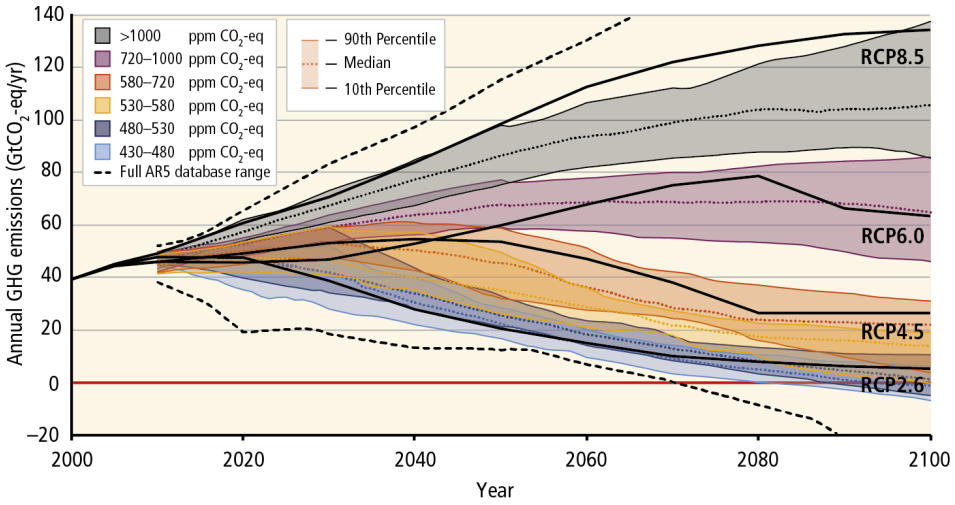

Figure 2.3: GHG emission pathways 2000 – 2100: All AR5 scenarios [5]

They are labelled according to the predicted radiative forcing for each scenario. Radiative forcings of 2.6 $\frac{W}{m^2}$, 4.5 $\frac{W}{m^2}$, 6.0 $\frac{W}{m^2}$, and 8.5 $\frac{W}{m^2}$ on the Earth's atmosphere serve as baseline scenarios for temperature predictions.

The results of the IPCC's Fifth Assessment Report were the groundwork for the agreement formulated at the 21st Conference of the Parties of the United Nations Framework Convention on Climate Change (UNFCCC) in 2015, known as the Paris Agreement. Central to the agreement is the goal to keep the increase of the global mean temperature under 2 °C with the pursuit of a maximum of 1.5 °C above pre-industrial levels, in order to prevent tipping points that may change the climate irreversibly [8]. To tackle climate change at its roots, the main focus of climate change mitigation lies on the reduction of GHG emissions. Governments promote renewable energies and electric transportation to reach carbon neutrality within the next few decades. But even after the Paris Agreement was signed, GHG emissions still rise globally, raising concerns about the effectiveness of current efforts. In the United Nations Environmental Programme (UNEP) 2020 Emissions Gap Report a course towards a 3 °C temperature rise is predicted with current climate policies. Even the global reduction of human activities (especially transportation) as a consequence of the COVID-19 pandemic created 'only a small dip' in CO_2 emissions. Low-carbon economic recovery funding on the other hand, could have significant impact on emissions in the next decades [2].

With the little success of emissions reduction, additional action must be considered. There is no alternative to a carbon-free economy and to carbon capture in the future. Eventually the atmospheric concentration of GHG must be restored to pre-industrial levels. The pollution must be limited and carbon in the atmosphere must be stored biologically or synthetically, reversing the anthropogenic atmosphere alteration. Afforestation, biomass energy production with CO_2

sequestration, land- and ocean-based weathering, ocean fertilisation, and direct air capture are several concepts for Carbon Dioxide Removal (CDR) that have been formulated [9]. These methods have the capability to create negative global net emissions, if applied on a large scale. The main disadvantage are the low efficiencies of carbon capturing technologies and therefore large spatial deployment requirements that may create conflict with other land use interests, or on the other hand it may take too long until an effect on the atmospheric GHG concentration is achieved [9]. The time scale for carbon removal can be compared to industrial carbon injection which occurred over centuries [10]. With that in mind, the goal of limiting the increase of the global mean temperature to 2 °C by only carbon concentration manipulation seems improbable to be achieved and secondary action must be taken into serious consideration if the catastrophic consequences of climate change tipping points should be prevented. While the current climate change mitigation concentrates on controlling the atmospheric GHG concentration, other approaches aim to alter the solar radiation incident on the Earth's environment. This is called solar radiation management.

2.2 Solar Radiation Management

The general idea of SRM is to reduce radiative forcing by diverting solar light before it can significantly contribute to the Earth's atmospheric energy balance. The concepts distinguish themselves from each other by how and where this is achieved (see fig. 2.4). Several concepts have been studied that aim to modify the Earth's albedo and by that increase the amount of light reflected back into space by the atmosphere and the surface. Surface albedo enhancement includes planting highly reflective crops [11, 12], covering urban roofs and paved surfaces with reflective material [13, 14], and injecting small bubbles over large areas of oceans to increase the oceanic albedo [15]. Marine Cloud Brightening (MCB) increases the atmospheric albedo by artificial, particle-based creation of ocean clouds [16, 17]. Based on the effects of volcanic eruptions, the idea of Stratospheric Aerosol Injection (SAI) has been formulated [18, 19]. The atmospheric albedo would be increased by injecting sulphate aerosols into the lower stratosphere.

While these albedo modification techniques require large-scale changes of landscapes or interference with the atmosphere, space-based approaches aim to reduce the solar light before it even reaches the Earth. The result is a change of the solar constant rather than a change of the planetary albedo.

Each SRM method introduces its own risks and benefits. Land surface and marine cloud albedo enhancement could only achieve nonuniform or partial cancellation of CO_2 induced radiative forcing [20, 21]. This is different with SAI, since the right choice of locations for the release of aerosols enables to create a uniform global aerosol layer [22]. By variation of the injection rate spatial and temporal control can be achieved [23]. The response time of this control would be much longer compared to MCB [22]. Techniques with short response times would not fall

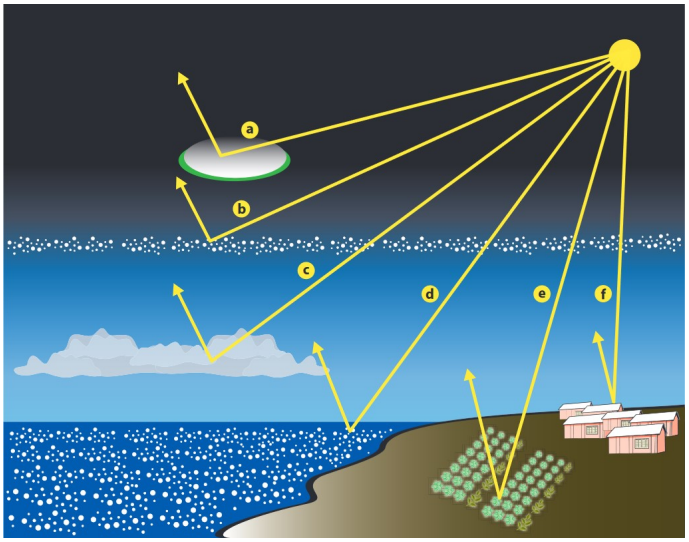

Figure 2.4: Concepts of solar radiation management [9]

under the term climate control but would rather be classified as weather control. This is a very delicate matter within the geoengineering community, as such technologies could be used for military purposes. Therefore, technologies that have a global effect and only allow for inert surface temperature control appear to be the safest [24]. Additionally, the costs for continuous aerosol injection operations would be lower than for any other method [24]. For these reasons, SAI is seen as the most promising Earth-based SRM-method to reduce carbon induced temperature rise [9, 20, 22, 24].

Space-based methods have received significantly less attention within geoengineering discussions. Considering the radiative forcing potential, together with SAI they are the most efficient methods and provide sufficient uniformity with scalability to the global application [20]. However, they are seen as too expensive, demanding, or fanciful [3]. Their high research and development demands compared to Earth-based technologies make them the least timely [24]. Nevertheless, space-based geoengineering has several advantages over Earth-based techniques. An additional anthropogenic interference with the Earth's atmosphere by aerosol injection is raising concerns regarding the effects on the stratospheric ozone, high-altitude tropospheric clouds, and the biological productivity [24]. This would be eliminated with technologies deployed in space. The reduced dependency on uncertain atmospheric dynamics and the fact that only a single parameter would be changed globally (the solar radiation flux) promise easier modelling and higher predictability [3, 10]. Furthermore, space-based concepts are the only ones allowing for implementation in structured phases, and in some cases full controllability and full reversibility once implemented. Scientific showstoppers could not yet be identified, only economic and technological challenges have been reported.

2.3 Space-based Sun Shading

Just as for Earth-based solar radiation management, different space-based geoengineering concepts have been formulated. The following sections summarise results of studies performed on several space-based sun shading concepts and weigh the challenges for the implementation against benefits once implemented.

2.3.1 Lagrange Point Sunshade

In 1989, Seifritz [1] and Early [26] were the first to propose sunshades placed in space to counter global warming. Seifritz presented the idea of placing thin reflective aluminium screens at SEL_1. A sunshade located at this semi-stable position could be operated with minimal propulsion effort and would constantly cast a shade onto the Earth. This constellation is shown in figure 2.5. Later that year, Early presented his calculation for a sunshade made from thin glassy lunar material located at the same position. The glass shade with lens properties would not completely block the solar light but would rather scatter it transparently at a sufficient angle. He did also consider the influence of the Solar Radiation Pressure (SRP) onto the shade, as well as the absorption and re-emission of thermal energy. McInnes [27] used an advanced energy balance for the Earth and estimated a required solar light reduction of 1.7% to counter climate change. He also determined the optimal position of a shade in between the Earth and the Sun in terms of overall mass. When considering the push from the solar radiation pressure, a new equilibrium position is obtained, that is located further away from the Earth than the conventional SEL_1 point (1.5×10^6 km) in order to counter the SRP push with an increased gravitational pull by the Sun. The minimal mass would be achieved when the shade is stable at 2.36×10^6 km from the Earth. A more detailed analysis will be presented in chapter 3.2.2. McInnes proposes that the sunshade should be fabricated from an M-type asteroid extracting iron and carbon materials. In 2009, he presented

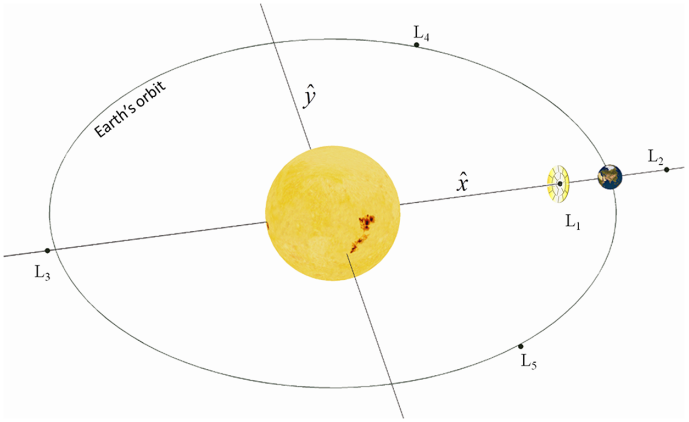

Figure 2.5: Sunshade disk near the Sun-Earth Lagrange Point L1 [25]

new calculations with optimised shade designs. A carbonaceous coating could create lower shield reflectivity which shall reduce SRP displacement and therefore the sunshade mass [28]. Furthermore, he presented an estimation for the manufacturing requirements. An 800 kg solar reflector with a 500 m radius disc would concentrate enough solar energy to enable processing an asteroid of 145 m radius and separate materials within about 150 days. Such a reflector could easily be launched from Earth. The most sophisticated model of a sunshade has been created by Sánchez and McInnes in 2015 [25]. Their study included computer modelling of shade orbit dynamics and atmospheric climate response. The effect of a sunshade located directly on the Sun-Earth-line was simulated using a three-dimensional climate model. Results showed that the polar regions experienced less radiation reduction than equatorial regions. This non-uniformity might still cause unwanted damage on the Earth, so they simulated a shade that oscillates vertically. The vertical movement could reduce the worst local mean temperatures with only slight losses for the global mean. The natural orbital period of this vertically oscillating shade close to SEL_1, which is longer than the Earth's period around the Sun, was modified by active control, utilising the solar radiation pressure. Required control mechanics for the sunshade were presented. To improve the model even further, a numerical optimisation method was used to calculate the optimal configuration of two sunshades that would account for the same total shading area, however would have different size, orbits, orbital periods, and orbit control, to maximise the climate performance. The simulated shades returned nearly 40% of the Earth's surface to within 0.1 °C of the pre-global warming temperature, compared to 10% achieved with classical geoengineering scenarios [25]. 50% were later achieved by allowing the accumulated disk size to change. Two disks with radii of 1522 km and 880 km were obtained for the best climate performance.

A different sun shading approach was formulated by Angel in 2006 [29]. To reduce the technological advancements required to manufacture and operate a sunshade at SEL_1, he proposed that trillions of smaller shades should be manufactured on the Earth and then be launched to space. Autonomous random placement in a large cloud envelope reduces the need for station keeping but increases the number of satellites needed to compensate for self-shadowing and of-axis displacement from the Sun-Earth-line. The small satellites could be launched with an electromagnetic railgun, preventing further pollution from chemical rocket exhaust, but creating huge electrical power supply demands on the Earth. 20 million launches with 1 t of sunshade payload each have been estimated. The small shades with a diameter of 1 m could be manufactured with high quality on Earth. A hole pattern was proposed that would scatter the solar light refractively and therefore reduce the impulse by the solar radiation, similar to the concept of Early [26]. Subsequently the system mass and the number of launches could be reduced. Angel's concept is currently the lowest-mass proposal.

Kennedy, et al. [30] presented a secondary use for the sunshade at SEL_1. Their idea is to partially utilise the light that is blocked by the shade. Photovoltaic cells shall convert the

absorbed solar energy into electrical power that is then transmitted towards the Earth. A continuous power of ∼10 TW that would be available on Earth has been estimated[1]. Today's total energy consumption is ∼18 TW [31]. Even with rising energy consumption in the future, the amount of energy provided by the sunshade could significantly help powering a carbon-free economy, creating a self-sustaining business case for the sunshade. High economic payback however comes with the price of an extremely heavy and therefore expensive sunshade, for solar cells, transmitter, receiver, and power conversion systems adding to the system mass.

2.3.2 Dust Clouds

Technological challenges have been a major adversary for space-based geoengineering. As mentioned above, simple shade designs or manufacturing on Earth were sought to reduce the technological requirements to a minimum. The most extreme example of technologically simple space-based sun shading has been proposed by Bewick, et al. in 2012 [32].

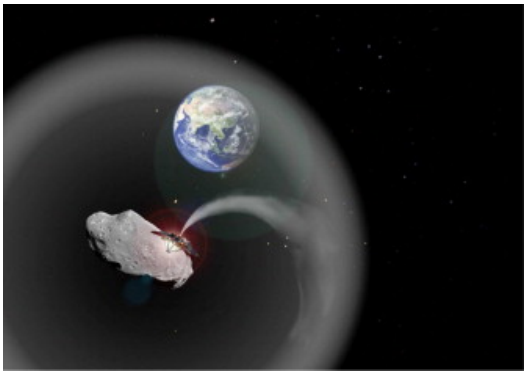

Figure 2.6: Impression of an SEL_1 positioned dust cloud for space-based geoengineering [32]

The idea is to create a cloud of dust particles at SEL_1 instead of thin-film reflectors. The only technologies required would be the capturing of a nearby source asteroid, material extraction from this asteroid, and distribution of the dust so that enough shading is achieved. They analysed and simulated dynamics of different dust types in the Lagrange Point radiation environment to predict cloud development. Adverse to the reduced engineering costs is the high mass required to constantly replenish dissipated dust. Later that year, the same authors presented a similar concept with the difference that the dust cloud may be gravitationally anchored by the asteroid used for dust production [33]. This anchor however represents a significant contribution to the mass to be transported to SEL_1.

Another concept for sun shading not taking place at or around SEL_1 has been formulated by Struck [34]. He assessed the feasibility of dust clouds artificially formed around Lagrange Points 4 and/or 5 of the Earth-Moon-System. The resulting toroidal orbits would spiral around the lunar orbit, in advance or behind the Moon. The clouds would shade the Earth on a monthly basis. The shading of one cloud would need to be much larger to achieve the required shading summed up over the year. Therefore, the required mass is higher than that of SEL_1 concepts. Also, the effects of the intensive cyclic solar light reduction on the Earth's ecological systems would have to be considered.

[1] Of 700,000 km^2 total sunshade area only 130,000 km^2 (∼18%) were covered with solar cells

2.3.3 Earth Rings

A concept that is situated much closer to the Earth was first presented by Mautner [36]. He proposed to counter climate change by forming rings around the Earth similar to Saturn's rings, as displayed in figure 2.7. They may be realised with structurally supported thin reflective films, thin absorbing films, or simple absorbent dust grains. Pearson, et al. [37] later performed a more detailed analysis of this Low Earth Orbit (LEO) concept. In their study a particle ring system and a ring-shaped constellation of several controlled reflective spacecraft were examined. Their performance was evaluated using a one-dimensional climate model. The particle ring would be optimal at 1.3 – 1.6 Earth radii and the spacecraft ring at 1.2 – 1.5. For cost determination, the launch of Earth, lunar, and asteroid material has been compared and Earth material has been excluded for its higher launch costs. Shading particles would be a significant source of micro-meteorites that would influence the lifetime of LEO satellites, but as for SEL_1 dust clouds, require much less manufacturing technology advancement and Earth launches. The controllability of the reflective satellites was mentioned as being advantageous for the active satellite constellation. In case of a required change of shading it may be easily adjusted by re-configuring the orbital constellation.

Bewick, et al. [35] derived Earth orbits with minimal mass loss for dust rings. With inclusion of the SRP effect and the Earth's J_2 perturbation on the dust grains an envelope of frozen heliotropic equilibrium orbits could be determined that would minimise the mass loss from the dust ring. The spatial and seasonal distribution of insolation reduction was simulated. By far the largest amount of shading is achieved in the tropical regions, while in the other regions no shading was obtained, as can be seen in figure 2.8. They also estimated the thermal influence the ring would have onto the Earth either by reflection from the back side of the ring onto the

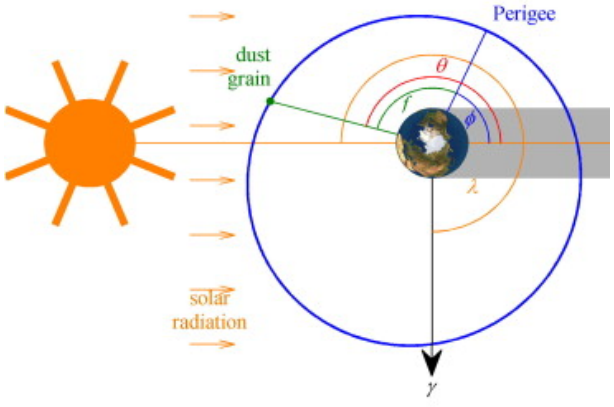

Figure 2.7: Geometry of a dust ring orbit [35]

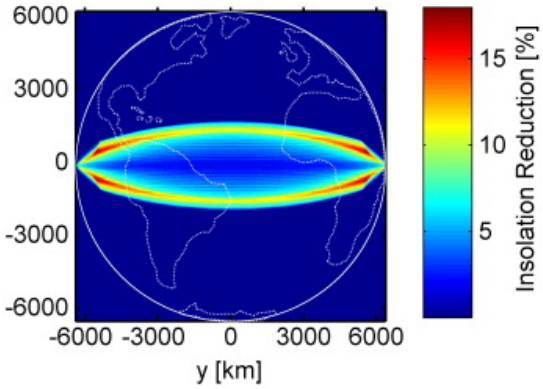

Figure 2.8: Insolation change over the Earth's surface over the course of a year, as seen from the Sun [35]

Earth's night side, or by infrared radiation of absorbed solar energy. Values of 2.3 $\frac{W}{m^2}$ and 4 $\frac{W}{m^2}$, respectively, were presented.

2.3.4 Discussion

Table 2.1 shows an overview of some well-defined sunshade concepts. The shading describes the fraction of the sunlight that is blocked by the shade. For the case of the SEL_1 positioned shades the overall mass usually scales linearly with this shading requirement (see also chapter 3.2). The area of the sunshades is only given for the SEL_1 screens and the satellite ring around the Earth, since the other ones achieve solar light reduction by means of a volume rather than a plane.

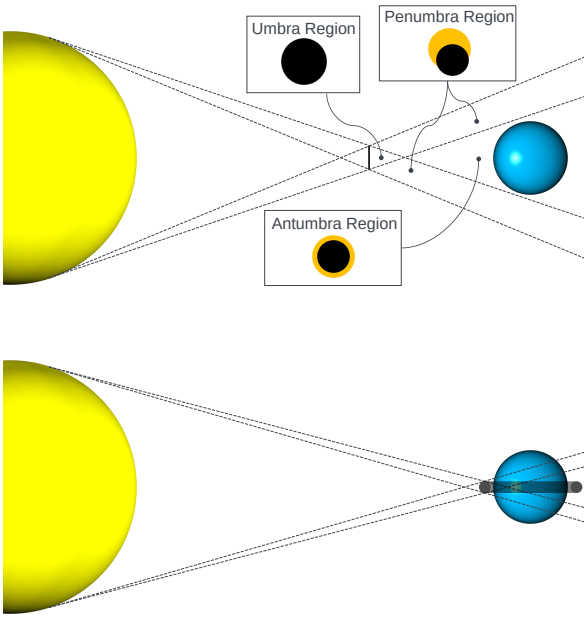

Figure 2.9: Shadow regions for a sunshade positioned at SEL_1 (top) and in Earth orbits (bottom)

The most obvious advantage of SEL_1 sunshades is the orbit mechanics of the Lagrange Point itself. If not spread out too far, all the shade mass positioned there would have a constant shadowing effect on the Earth with minimal control requirements. Systems orbiting the Earth only have a fraction of their mass influencing the atmosphere. The usually higher mass requirements for Earth vicinity concepts are evidence of this low efficiency[2].

The shadowing effect of an SEL_1 placed sunshade would also be more uniform than with Earth vicinity concepts, as can be seen in figure 2.9. Due to the small size of the shade compared to the Sun, the umbra shadow (full shadow) would not reach the Earth. Only antumbra or penumbra shadow is cast on the Earth. Earth rings for example would have an excessive (maybe even full) shading onto tropical regions in order to achieve a sufficient shading for the whole planet. These dramatic impacts on the local thermal balance could have unpredictable consequences for the hydrological cycle, oceanic currents, or local vegetation and animal life. The political discussion on such a measurement could be very complicated.

The close proximity of shading systems around the Earth and therefore short reaction times for service operations comes with the cost of interference with Earth orbit traffic. Adding millions of tonnes of mass to LEO or Geostationary Earth Orbit (GEO) would increase the risk of collisions that could initiate a catastrophic Kessler syndrome. The lifetime of satellites as

[2]Mass efficiency: Achieved shading per sunshade mass deployed

Author	Shading	Mass [kg]	Area [km^2]
SEL_1 Shade			
Early, 1989 [26]	2%	1.0×10^{11}	1.3×10^7
McInnes, 2002 [27]	1.7%	4.16×10^{11}	1.0×10^7
Angel, 2006 [29]	1.8%	2.0×10^{10}	4.6×10^6
McInnes, 2009 [28]	1.7%	2.6×10^{11}	6.57×10^6
	1.7%	5.2×10^{10}	6.57×10^6
Kennedy, 2013 [30]	0.25%	$3.1 - 3.6 \times 10^{11}$	$5.5 - 11 \times 10^5$
Sánchez, 2015 [25]	1.7%	$4 - 24 \times 10^{10}$	6.46×10^6
Dust Clouds			
Struck, 2007 [34]	1.4%	2.1×10^{14}	-
Bewick, 2012a [32]	1.7%	1.87×10^{10}/yr	-
Bewick, 2012b [33]	1.7%	1.3×10^{16}	-
Earth Rings			
Pearson, 2006 [37]	1.6%	2.0×10^{12}	-
	1.6%	5.0×10^9 [1]	5.0×10^6
Bewick, 2013 [35]	1.7%	2.0×10^{12}	-

Table 2.1: Concepts for space-based sun shading

well as communication pathways would be affected by orbital dust. Finally, aesthetic concerns can be raised for night sky flickering by shades or dust particles in Earth orbits. Astronomical observations from the Earth could be affected and may even be impossible considering the high thermal radiation reflected from dust rings. Aesthetic concerns could also be raised for systems shading the Sun from SEL_1, although they are expected to be rather insignificant since a large disc may only be seen with protective measures and optical enlargement. In case of a fleet of smaller discs it could even be impossible to see with standard devices.

A sunshade positioned at SEL_1 would not interfere with Earth orbit operations, would not represent a serious threat to any ongoing space operations, would minimise the aesthetic intrusion, and maximise mass efficiency with the most extensive global climate effect. SEL_1 therefore seems to be the optimal location for a space-based sunshade.

Shading the Earth with a dust cloud has the advantage of few technologies that would have to be developed, of which capturing and redirecting an asteroid of sufficient mass is probably the greatest challenge.

A system that shades the Sun must allow for immediate termination or adaptation to new climate situations. Active systems could be controlled directly. They could be removed from

[1] assuming a total areal density of 1 $\frac{g}{m^2}$

the position in between the Sun and the Earth and be placed in a higher parking orbit. In the SEL_1 environment this manoeuvre could be performed by utilising the solar wind. A passively shading dust cloud will quickly dissipate at the semi-stable Lagrange Point. If the constant replenishment of dust is stopped or adjusted, the termination or adaptation of the shade is achieved. Using an asteroid to anchor this dust cloud however represents a challenge in regards of shading termination. The propulsion demand to remove this asteroid again would be very large. Thus, in terms of safety and controllability, the anchor concept is unfavourable. The anchor asteroid also greatly increases the overall mass that has to be transported to SEL_1. Yet the requirements for material extraction and dust cloud generation on the other hand are much smaller.

Studies performed on a perfectly uniform solar geoengineering model have shown, that the climate is not reset to pre-industrial standards when reduction of the global mean temperature is achieved [38]. The poles will experience less cooling, while the tropics will be cooled excessively. This leads to decreased latent heat evaporation due to cooler tropical oceans and reduced poleward heat transport in both hemispheres since the meridional temperature gradient is smaller. The global annual precipitation would decrease by 5%, primarily in the tropics. The less intensive hydrological cycle would lead to a reduction in cloud formation and the planetary albedo would be reduced. Seasonal and diurnal temperature cycles would have smaller amplitudes. While storm track intensities and local mean temperatures would be reduced as desired, the numerous negative side-effects cannot be neglected when developing a geoengineering system. A more detailed distribution of radiative forcing reduction may prevent some of the side-effects caused by uniform solar geoengineering.

MacMartin, et al. [39] ascertained that, with simple spatial and seasonal variation of solar light reduction, the worst-case local mean temperature and precipitation changes can be reduced by 30%, without a significant degradation of the global mean. The results of Sánchez, et al. [25] showed the capability of a constellation of sunshade discs to achieve those shading variations. The local mean temperatures were improved significantly. An assembly of several shades might allow for optimal climate control. Due to the low gravitational potential and therefore long periods of orbits in the Lagrange Point vicinity [25], the sunshade control would not allow for quick local weather control on the Earth, but for seasonal and spatial shading variations.

The controllability of thin-sail sunshades that allows for optimised climate feedback and quick decommissioning might justify taking on the challenge of maturing many technologies, rather than implementing a less challenging system that has more negative side-effects. A discussion on a geoengineering project that will affect the whole planet must include every nation. Countries that are negatively affected by side-effects of passive shading systems will object to the implementation which may even cause conflict. Realisation of a dust cloud shade might not be possible at the political stage, however actively controllable sunshades placed at SEL_1 can be presented as the option that serves everyone with no or at least minimal damage. Table 2.2

gives an overview over the evaluation of the sunshade concepts discussed here. It shows the many advantages of controllable sunshade sails positioned at SEL_1 over Earth vicinity concepts and SEL_1 dust clouds. The technical challenges will be larger than for other solar radiation management approaches, but when getting started as early as possible this sunshade concept could play a significant role for the prevention of severe climate change.

	Lagrange Point Sunshade	SEL_1 Dust Clouds	Earth Rings/Clouds
Mass Efficiency	+ +	+	-
Development Effort	-	+	+
Climate Effect	+ + +	+	+/-[1]
Controllability	+ +	+	+/-[2]
Interference with Space Operations	+ +	+ +	-
Aesthetic Concerns	+	+	-

Table 2.2: Concepts for space-based sun shading

[1] Reduction of the average surface temperature, but dramatic local alterations

[2] Controllable spacecraft / uncontrollable dust

Chapter 3

Lagrange Point Sunshade Requirements

Constructing a sunshade that consists of several controllable thin screens placed in the vicinity of the Sun Earth L1 Lagrange Point has been reviewed as the most promising concept of space-based solar radiation management. The following sections will determine constraints and requirements for realising such a sunshade system. The requirement for solar light reduction will be defined on the basis of the IPCC's climate predictions. With that, the size of the sunshades will be derived geometrically and the influence of certain sunshade properties on the position and mass of the system will be described. With the scale of the sunshades, considerations on the source of construction material, as well as temporal constraints for development, demonstration and construction will be outlined. As a result, a preliminary overview of all system elements involved in sunshade implementation is presented.

3.1 Shading Requirement

The solar radiation flux in the Earth's distance to the Sun S_0 is 1371 $\frac{\mathrm{W}}{\mathrm{m}^2}$ [40]. This two-dimensional value must be translated into the average solar insolation S onto the Earth's three-dimensional surface. The solar constant describes the radiation power onto a flat surface that is perpendicular to the Sun, such as for example a satellite's solar array or the planar projection of the Earth. Figure 3.1 shows how the solar light is distributed over the actual curved surface of the Earth, which is 4 times larger than its projection. Therefore, the average solar insolation on the Earth's body is only a fourth of S_0, thus $S = 342.75\ \frac{\mathrm{W}}{\mathrm{m}^2}$. This value is further reduced by the effect of the planetary albedo. For the Earth this is $\alpha_p = 0.313$ [20]. Therefore, the solar light contribution to the Earth's thermal balance is only 235.5 $\frac{\mathrm{W}}{\mathrm{m}^2}$. The RCPs estimated by the IPCC range from 2.6 $\frac{\mathrm{W}}{\mathrm{m}^2}$ to 8.5 $\frac{\mathrm{W}}{\mathrm{m}^2}$ of radiative forcing (see fig. 2.3), which now adds to the thermal balance as a consequence of higher CO_2 concentrations in the atmosphere [5].

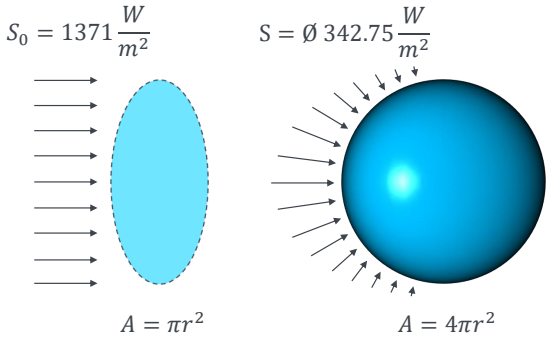

Figure 3.1: Transformation of the solar constant

Full Compensation

To counter the effects of climate change and re-establish thermal equilibrium in the Earth's atmosphere to pre-industrial conditions only with space-based measures, this radiative forcing must be countered. Due to the effect of the albedo, the radiation that must be blocked is higher than the intended change of radiative forcing. In accordance with relevant literature [20], the reduction in solar insolation ΔS to counter radiative forcing RF with space-based measures can be determined with

$$\Delta S = \frac{RF}{(1 - \alpha_p)} \,. \tag{3.1}$$

Furthermore, the relative fraction of light to be reduced by a sunshade f is then obtained with

$$f = \frac{\Delta S}{S} \,. \tag{3.2}$$

Table 3.1 shows the resulting fraction of solar radiation that needs to be blocked for each RCP scenario. It ranges from 1.1% to 3.6%. Most previous studies assumed a doubling of CO_2 concentrations and 4.17 $\frac{\mathrm{W}}{\mathrm{m}^2}$ radiative forcing [28, 29, 37, 41]. Latest trends, presented by the National Oceanic and Atmospheric Administration (NOAA) [42], justify this assumption.

Pathway		RCP2.6	[28, 29, 37, 41]	RCP4.5	RCP6.0	RCP8.5
RF	$[\frac{\mathrm{W}}{\mathrm{m}^2}]$	2.6	4.17	4.5	6.0	8.5
ΔS	$[\frac{\mathrm{W}}{\mathrm{m}^2}]$	3.78	6.07	6.55	8.73	12.37
f	[-]	1.1%	1.77%	1.9%	2.6%	3.6%

Table 3.1: Insolation reduction requirements for 2014 IPCC report scenarios

Emergency Blanket for Paris Agreement Goals

A different approach is not to aim for full compensation of all radiative forcing caused by increased carbon-dioxide concentrations in the atmosphere, but to limit the temperature increase to a certain level. Carbon reduction is the primary and ultimate goal that should be pursued with greatest effort. The deployment of a space-structure would serve as an emergency blanket to prevent tipping points in the climate. As soon as the carbon is lowered sufficiently the sunshade could be disabled. The secondary role of the sunshade reduces the dependency on the space system and therefore the severity of abrupt termination due to any reasons.

To derive a shading requirement for a sunshade, it must now be examined how a change of radiative forcing by the sunshade is affecting the global mean surface temperature ΔT.

$$\Delta RF = \lambda \cdot \Delta T \tag{3.3}$$

The factor λ in equation 3.3 is called climate sensitivity. Recently, the climate sensitivity was assessed on the basis of feedback process understanding, historical climate records, and paleoclimatic records [43]. According to this analysis, λ results to

$$\lambda = \frac{RF}{\Delta T} = 1.23 \ \frac{\mathrm{W}}{\mathrm{m^2 K}} \, . \tag{3.4}$$

If it is now assumed, that the shade's task is to reduce the temperature on the Earth by 1 K, the climate sensitivity can be used to determine the amount of radiative forcing on the Earth that will be reduced by the shade. A radiative forcing reduction of 1.23 $\frac{\mathrm{W}}{\mathrm{m^2}}$ is obtained. Now equation 3.1 yields 1.79 $\frac{\mathrm{W}}{\mathrm{m^2}}$ of solar insolation reduction ΔS and therefore, $f = 0.52\%$ of sunlight that must be blocked.

Chapter 1 addressed the role of SRM in a modern socio-political context. Unlike many sun shading concepts in literature, a secondary role of SRM is anticipated here. The global mean temperature reduction of 1 K serves as an orientation that can be adjusted easily on a model basis and all the systems can be scaled accordingly, if required. Henceforth in this report, the requirement for solar light reduction by the shade will be 0.52% .

3.2 Sunshade Size

3.2.1 Geometry

Given the 0.52% of solar radiation that has to be blocked in an emergency blanket scenario, the shading area can be derived geometrically. The solid angle Ω_S subtended by the Sun as seen from the Earth is

$$\Omega_S = \frac{\pi R_S^2}{r_S^2}, \tag{3.5}$$

where R_S is the radius of the Sun and r_S is the distance between the Earth and the Sun, i.e., 1 AU (149.6×10^9 m). It can now be said, that in order to reduce the solar radiation on the Earth by a fraction of f the sunshade must subtend the fraction f of the Sun's solid angle. Figure 3.2 displays this geometric approach as defined in equation 3.6.

$$\Omega_{Sh} = f \cdot \Omega_S \tag{3.6}$$

$$\frac{\pi R_{Sh}^2}{r_{Sh}^2} = f \cdot \frac{\pi R_S^2}{r_S^2} \tag{3.7}$$

$$R_{Sh}(r_{Sh}) = R_S \frac{r_{Sh}}{r_S}\sqrt{f} \tag{3.8}$$

Equation 3.8 is obtained by rearranging equation 3.7. It shows the linearity between the shade's radius R_{Sh} and the shade's distance r_{Sh} to the Earth.

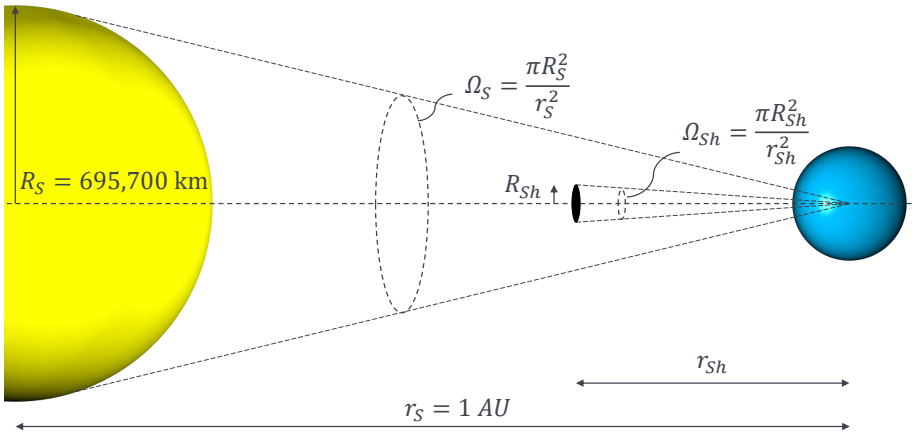

Figure 3.2: Solid angle derivation
(angles and distances not to scale)

The shade area A_{Sh}, calculated with equation 3.9, grows quadratically with distance to the Earth, as can be seen in figure 3.3.

$$A_{Sh}(r_{Sh}, f) = \pi R_{Sh}^2 \tag{3.9}$$

This area is not restricted to a circular shape as for the geometric derivation. Rectangular or hexagonal shapes with the same total area have the same blocking effect. Also splitting the shading area into several smaller elements is possible.

The intensity of the solar light is higher than average in the centre of the solar disc and lower than average at the edges. This is called Solar Limb Darkening (SLD). Figure 3.4 shows the effect of SLD on the intensity of light reduction when Sun, shade, and observer are not in line. If a sunshade is positioned directly in line with the Sun and the observer, the largest fraction of light is blocked. The required area of the disc is smaller than calculated without considering SLD. For a single large sunshade in central position, mass savings of up to ∼21% could be modelled [25]. If the sunshade moves away from the central position, the light reduction and therefore the efficiency of the sunshade decreases, so that the required area could even be larger than without considering SLD. If there are more shades distributed over the solar disc, the effects of solar limb darkening might be cancelled out. This is assumed for the present report.

The sunshades should at all times be in front of the Sun for any viewers location on the Earth, i.e., antumbra shadow. If a shade moves, for example, very far below the Sun-Earth-line, a viewer from the Earth's north pole might see the edges of the sunshade pass over the lower edge of the Sun (penumbra shadow). The part of this shade that is not in front of the Sun

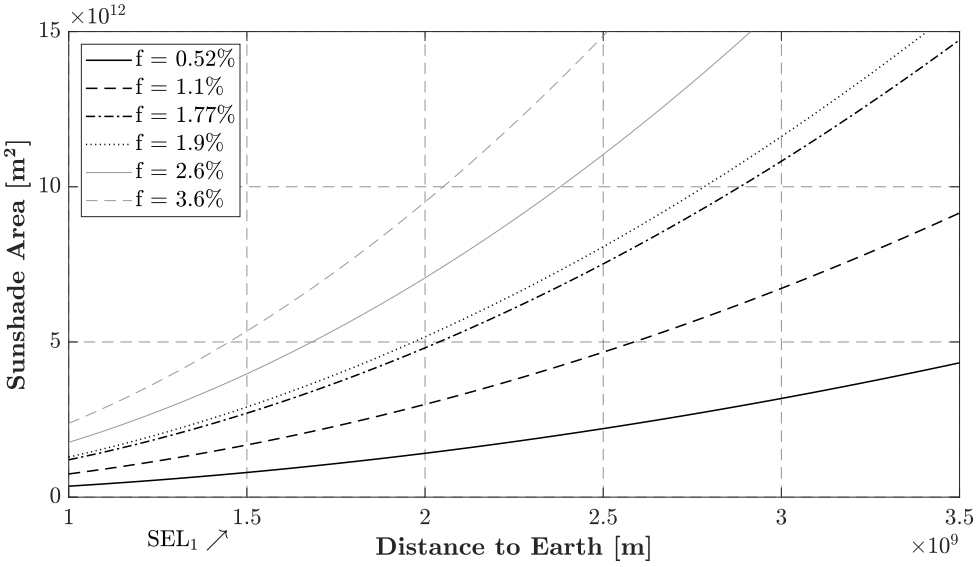

Figure 3.3: Required sunshade area to block different amounts of sunlight

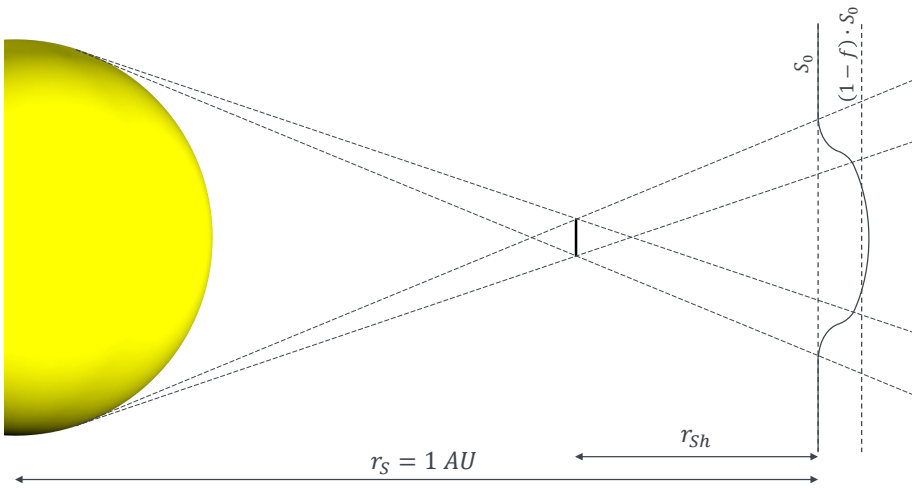

Figure 3.4: Schematic of the effect of the solar limb darkening on the shading distribution as a function of distance to the Sun-Earth line

would have no effect on the north pole, even if it is still shading the equator. The efficiency of the shade would decrease, and subsequently additional shading area would have to be provided compensating for the part of the shade area that is not shielding the corresponding location on the Earth. This effect can be seen in figure 3.4, where the solar radiation increases significantly in the penumbra region. This also is the case for a large cloud of very small spacecraft that is widely distributed to avoid collisions and self-shadowing [29].

These geometrical considerations for the shading efficiency must be taken into account for detailed analysis. Climate simulations should determine the optimal sunshade configuration. Sánchez, et al. [25] have made an excellent example for this. It should be explored further how number, size, shape, and orbital dynamics of several sunshades can improve the results presented there. Furthermore, these climate simulations should consider an incrementally-increasing sunshade area, due to the long production time expected. A strategy for step-by-step sunshade deployment should be defined.

3.2.2 Solar Radiation Pressure Effect

As discussed in chapter 2.3, the optimal position for a sunshade in space would be Lagrange Point 1 within the Sun-Earth-gravitational system. An object placed at this semi-stable point would offer constant solar shading of the Earth with minimal Δv requirements. More details can be found in the parallel thesis [4]. With the previous derivations, a sunshade blocking 0.52% of sunlight at this position would have a radius of 503 km and an equivalent area of 795,000 km^2 .

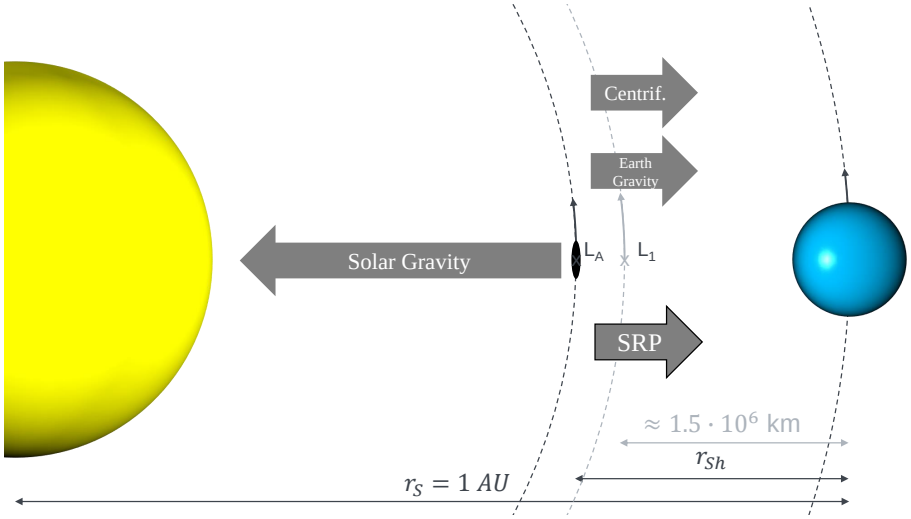

Figure 3.5: Displacement effect on the equilibrium position by the solar radiation pressure

The analytical model of the semi-stable Lagrange Points does not consider the effect of the pressure of the solar radiation exerted on a surface facing the Sun. The SRP force disturbs the momentum equilibrium for light structures, as can be seen in figure 3.5. Sánchez, et al. [25] defined a lightness parameter that quantifies the significance of the SRP as a ratio of SRP force to solar gravity, similar to the ballistic coefficient used for aerodynamic modelling. A sunshade placed in between the Earth and the Sun would certainly be a 'light' structure, since low total mass would reduce the production effort and consequently the cost for construction. To cancel out the additional effect of the SRP the shade moves closer to the Sun, increasing the inwards pull of the solar gravitation and reducing the outwards pull from the Earth and the centrifugal acceleration. In order to determine the new Artificial Sun-Earth Lagrange Point (SEL_A), the definition for the equilibrium location must be adjusted by adding the SRP force as an additional factor. According to McInnes [28], the SRP acceleration a_{SRP} can be defined as:

$$a_{SRP} = \frac{2\kappa P_E A_{Sh}}{M_{Sh}} \left(\frac{r_S}{r_S - r_{Sh}} \right)^2 , \tag{3.10}$$

where P_E is the solar radiation pressure in a distance of one astronomical unit from the Sun, M_{Sh} is the mass of the sunshade, and κ describes the optical reflectance and re-emission properties as follows:

$$\kappa = \frac{1}{2} \left[(1+\eta) + \frac{2}{3}(1-\eta) \frac{\epsilon_F - \epsilon_B}{\epsilon_F + \epsilon_B} \right] . \tag{3.11}$$

η is the specular reflectivity, ϵ_F is the emissivity of the frontal, Sun facing surface and ϵ_B is the emissivity of the rear, Earth facing surface. Together with Sun gravity, Earth gravity, and

the centrifugal acceleration, the new equilibrium is defined as

$$\frac{GM_E}{r_{Sh}^2} - \frac{GM_S}{(r_S - r_{Sh})^2} + \omega_E^2(r_S - r_{Sh}) + \frac{2\kappa P_E A_{Sh}}{M_{Sh}}\left(\frac{r_S}{r_S - r_{Sh}}\right)^2 = 0\,. \tag{3.12}$$

Here, G is the gravitational constant, M_E and M_S are the mass of the Earth and the Sun, and ω_E the angular velocity of the Earth around the Sun determined with

$$\omega_E = \sqrt{\frac{GM_S}{r_S^3}}\,. \tag{3.13}$$

Rearranging eq. 3.12 allows to determine the sunshade mass, with $g_{L1}(r_{Sh})$ as a function including the conventional Lagrange Point accelerations:

$$M_{Sh}(r_{Sh}, \kappa, f) = \frac{2\kappa P_E A_{Sh}(r_{Sh}, f)}{-g_{L1}(r_{Sh})}\left(\frac{r_S}{r_S - r_{Sh}}\right)^2 \tag{3.14}$$

Inserting equations 3.8 and 3.9 delivers

$$M_{Sh}(r_{Sh}, \kappa, f) = \frac{2\kappa P_E \pi f R_S^2 \left(\frac{r_{Sh}}{r_S}\right)^2}{-g_{L1}(r_{Sh})}\left(\frac{r_S}{r_S - r_{Sh}}\right)^2. \tag{3.15}$$

It can be seen that κ and f are constants in equation 3.15. The sunshade mass has linear dependency on both. Two factors in equation 3.14/3.15 that have an effect on the position and mass are defined by the design of the sunshades: the areal density $\rho_{Sh} = M_{Sh}/A_{Sh}$, which describes the mass of a sunshade per square meter, and κ, which depends on the reflectivity and the combination of frontside and backside emissivity. The plot of this equation in figure 3.6 shows that the shade mass has a minimum at a certain position. To stabilise a sunshade close to SEL_1 it must be very heavy to counter the SRP acceleration; the required mass grows to infinity. Reducing the sunshade's overall mass by reducing the areal density increases the displacement effect of the SRP, moving the shade closer to the Sun. The increased distance to the Earth geometrically requires the shade area to increase in order to provide sufficient shading. At a certain point the mass increasing effect of the increase of the shade area outweighs the mass decreasing effect of the reduction of areal density. A position of minimal mass for the shade is obtained. In accordance with previous studies [28, 29], it results to $2.36 \cdot 10^9$ m from the Earth and does not depend on the surface properties of the sunshade and the required shading[1]. At this position the sunshade would have a radius of 791 km and an equivalent area of 1.968×10^6 km^2 . Minimal mass is of great interest since the scale of space-based geoengineering presents a huge production challenge. Ways to reduce the required mass to shade a certain amount of light could facilitate sunshade implementation. While changing κ and f results in linear scaling of the graph

[1] κ and f are constants in equation 3.15. To determine the position of minimal mass, this equation must be differentiated and afterwards set equal to zero. When solving the equation for r_{Sh}, both constants are eliminated.

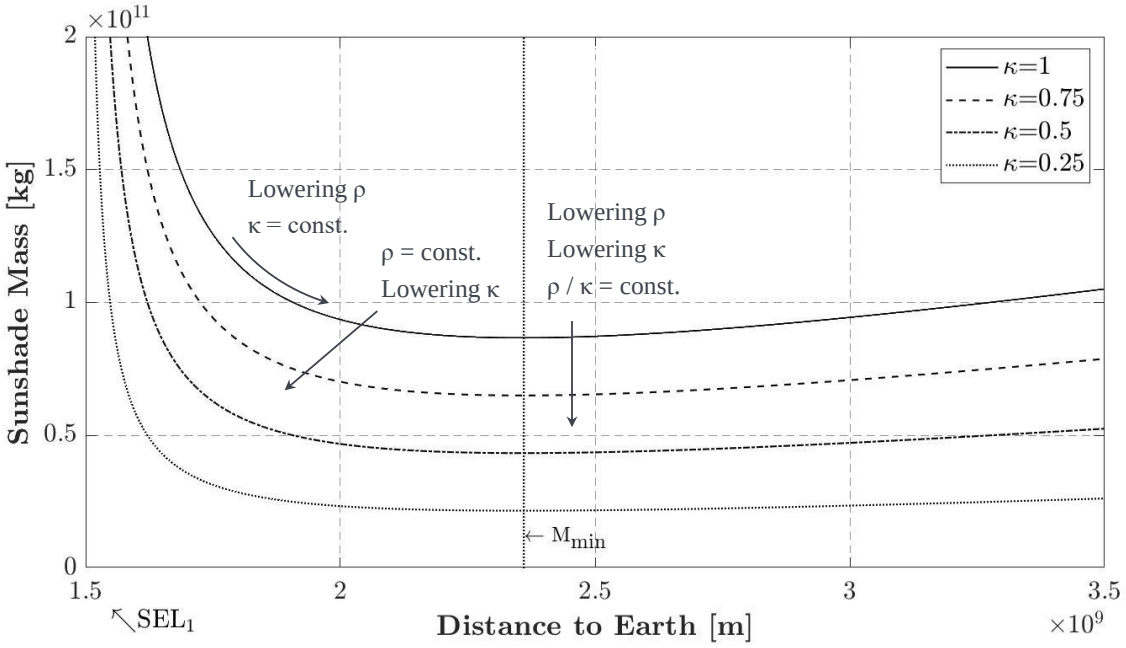

Figure 3.6: Shade mass to block $f = 0.52\%$ of sunlight with different κ

in figure 3.6, it is the ratio of areal density to the optical factor that defines the position on the graph. At the position of minimal mass, a sunshade with reflection and re-emission that result to $\kappa = 1$ would be in equilibrium if its areal density is 44.1 $\frac{\mathrm{g}}{\mathrm{m}^2}$. The ratio of density to the optical factor would be

$$\left.\frac{\rho_{Sh}}{\kappa}\right|_{M_{min}} = 0.0441 \, \frac{\mathrm{kg}}{\mathrm{m}^2} \, . \tag{3.16}$$

The total system mass for shading 0.52% of the sunlight would be $87{\times}10^6$ t . If the areal density is reduced further, the total sunshade mass would increase. To counter that, the reflectivity of the shade surface must be reduced resulting in lower κ, so that the ratio ρ_{Sh}/κ remains at 0.0441 $\frac{\mathrm{kg}}{\mathrm{m}^2}$. Very low density and therefore very low total mass is only feasible with low κ.

With the goal to reduce the total sunshade mass and therefore the production effort for a given amount of shading, it must be examined how far both parameters could be lowered with future manufacturing capabilities.

3.3 Material Source

A space construction on the scale of a sunshade raises questions about the source of materials. Tens or hundreds of million tonnes would need to be transported to Lagrange Point 1 of the Sun Earth system.

Earth Materials

The conventional way to launch material from the Earth poses a threat to the environment due to the many rocket launches necessary. Rockets carrying 50 – 100 tonnes have been announced by several rocket developers. The National Aeronautics and Space Administration's (NASA) *Space Launch System (SLS)* will be designed to lift 46 t of payload into deep space [44]. The Russian *Yenisei* rocket and the Chinese *Long March 9* are expected to have comparable super heavy-lift capabilities [45]. However, it is SpaceX's *Starship* that is the most attractive for launching millions of tonnes into space, since it will be fully reusable and therefore much less expensive. A LEO lift capability of at least 100 t has been announced [46]. Should a future logistical architecture allow for low-Earth orbit refuelling, this payload could be transported to SEL_1 completely. $87{\times}10^6$ t of shade mass would mean 870,000 *Starship* launches. If the sunshades were to be built in a period of a decade it would result in about 240 launches per day. These large numbers of Earth launches raise concerns about environmental impacts. It is commonly agreed that when launching a space sunshade from the Earth with chemical rocket propulsion it would cause more damage to the environment than it seeks to prevent [47].

Unconventional launch technologies have been considered as an alternative. Angel [29] proposed to launch stacks of shades from the Earth with a railgun. One tonne of payload in a two-tonne capsule would be electromagnetically accelerated to escape velocity directly on the Earth's surface. The requirements for short time high energy release would present a serious challenge for the launch facility infrastructure. Several of those facilities would be needed. The high energy demand and complex infrastructure are inferior to other alternatives, which is why electromagnetic launch from the Earth has not been pursued seriously in the past.

Space Resources

Apart from the Earth, the Moon and asteroids are bodies in space that present a multitude of materials that, when accessed and extracted, could be used for the production of space systems. McInnes [28] has proposed to capture a nearby M-type asteroid that in large parts carries iron and carbon. The iron could be used for shade foil production, the carbon as coating to reduce the surface reflectivity. Asteroids have the advantage of low gravity which reduces the propulsion demand to transfer extracted material. Accessible asteroid resources that require lower energies to be transported into an Earth orbit than those required to exploit the Moon are in the order of 10^{14} kg [48]. The S-type asteroids additionally provide a source of silicon that can be used for solar cell production [49]. Water for propellant supply is available on hydrated carbonaceous asteroids [49].

While the energy demand is low, the time to travel to an asteroid is usually high. Transfer windows to closer Near Earth Asteroids (NEA) create restrictions for mission operations. More favourable would be to capture an asteroid and place it into an easily accessible orbit. After

the large and complex effort of asteroid capturing, the access to the material source would be improved significantly. Location in an Earth orbit would create great flexibility for resource extraction. While extracted material for shade production would eventually need to be transported to SEL_1, by-products such as oxygen and water could be used directly around the Earth. Transfer of large masses from Earth orbits to the Lagrange Point could be avoided by placing the asteroid(s) directly at SEL_1. This would also reduce the risk of catastrophic consequences in case of a failure during asteroid redirection towards Earth. The transfer cost for resource extraction systems would be larger, however the material itself would, after manufacturing, only need to be commissioned to a desired operational orbit. Over these short distances, light sailing operations might even allow to perform the commissioning without any need for a propellant [4].

The utilisation of asteroids promises a great potential for large-scale space construction. Asteroid capturing is the crucial technology that would need to be demonstrated and matured sufficiently before major sunshade production operations could be initiated.

However, there already is a large boulder captured in the Earth's gravitational system. The Moon poses a huge resource for manufacturing materials. The lunar surface is covered by a layer of fine-grained material with a mixture of rocks consisting of fine-grained mineral and glass particles, called regolith [50]. The main components in the lunar regolith are oxygen, silicon, aluminium, and iron [51]. With aluminium a low-density metal with excellent mechanical behaviour could be provided, that might be superior to the use of heavy iron. Additionally, titanium, calcium, and magnesium present useful elements for many high-performance alloys [51]. Figure 4.1 shows the distribution of these elements for different locations on the Moon.

Other trace elements in the lunar regolith have been detected [50, 52]. Their variety is great and in some cases their value is as well. Enhanced levels of rare Earth elements (also known as lanthanides) and several others have been reported within lunar material samples [51]. Despite the occurrence given in parts per million (ppm) or even parts per billion (ppb), the existence of these trace elements might come to use in case of hundreds of million tonnes of regolith processed for a sunshade. For example, the existence of uranium and thorium has been considered for applications within nuclear power generation [51]. Barium, nickel, copper, silver, and niobium could be used for superconducting components of a mass driver [4]. If such an element is needed on the Moon, there remains an assessment to be made as regards the effort of recovering it from the regolith with a highly sophisticated processing plant and the effort of importing it from the Earth. Other valuable materials could be transferred for further use on the Earth.

A great disadvantage, compared to asteroids, is the lack of carbon on the Moon. Plastics which find use in almost any aspect of human life, cannot be produced with lunar material, and would have to be avoided to reduce the mass supply requirements from the Earth. A carbonaceous coating for a sunshade as proposed by McInnes [28] is therefore impractical.

Despite the large gravity well, extracting material from the Moon profits from the close

proximity to the Earth without having to move large amounts of asteroid mass initially. An efficient cis-lunar logistics network could be set up rapidly.

With the recent discoveries of frozen water in lunar polar regions, the Moon has received significant attention from international space exploration initiatives over the last decade [53]. The potential use of oxygen and water as propellant and resource for life-support systems [51, 54] – drinking, hygiene, agriculture – has driven space agencies to incorporate the Moon into their exploration roadmaps, serving as a central test-bed for technology demonstration, as refuelling station, communication and scientific observation relay outpost, as well as a demonstration site for infrastructure and operations of an independent off-world settlement on the path towards Mars [55, 56]. In the 2020 supplement to the Global Exploration Roadmap (GER) the International Space Exploration Coordination Group (ISECG) formulated common objectives for demonstrating sustained human exploration [56]. These include the demonstration of logistic operations to, from, and on the lunar surface, human long duration habitation capabilities, infrastructure for power and communication, and In-situ Resource Utilisation (ISRU) on the Moon. The GER as a guideline to support coordination efforts among space agencies reflects the large international interest in utilising the Moon. This momentum on the other hand can be utilised to incorporate the development of sunshade manufacturing capabilities, providing a use case for technologies in development, and inducing the creation of a lunar resource economy. Seen from another perspective, the dedication to and acceptance of space-based geoengineering has been almost non-existent on decision-making level in the space community. Affiliation and integration into the lunar exploration initiative might enable the idea of space-based geoengineering to remain feasible for the longest time.

Table 3.2 shows that making use of lunar resources for sunshade production is favourable. It presents the best alignment to international exploration efforts. This would enable timely opportunities for technology demonstration and optimisation with quick feedback time. The lunar gravity well to reach SEL_1 is significantly lower than the Earth's, but higher than that of an asteroid. This might however be countered by the use of lightweight metals. The Moon

	Earth	Asteroids	Moon
Material Availability	+ + +	+	+
Logistical Effort	-	+ +	+
Environmental Impact	- -	+	+
Timeliness	+ +	-	+
Spin-off Potential	+	+ +	+ +

Table 3.2: Evaluation of material sources

should therefore serve as primary material source for sunshade production. As soon as asteroid redirection and extraction technologies have matured the set of sunshade materials could be expanded.

Some materials might still need to be transferred from the Earth. Especially during early stages of sunshade production development there will be a dependency on Earth transportation. An analysis of future Earth-launch opportunities can be found in the parallel thesis [4].

3.4 Timeframe

At a certain point in the future, there will be a need for the sunshade to impact the climate. The benefit of investing in a giant sunshade would be reduced significantly if it is operational only after the climate is seriously damaged. The sunshade must be able to operate before that in order to be taken into consideration within the climate change mitigation efforts dialogue. A temperature rise of 2 °C above pre-climate warming temperatures has been defined as a barrier which, if exceeded, entails unacceptable probabilities for tipping points in the climate [8]. With the rate of temperature rise in the last decades, a reasonable expectation is that with current climate policies this barrier will be reached around 2060 [57]. At this point the sunshade must have an effect on the climate. It may not be implemented fully, but single sail modules must already influence the Earth's temperature to prevent further warming. 2060 is therefore assumed as deadline for operation of the first sunshades[2].

To examine if this timeframe is appropriate, the current state-of-the-art of technologies needed within the sunshade system, as well as trends for the future have to be assessed.

3.5 Sunshade System

The total sunshade system includes, besides the shade itself, also resource extraction systems, manufacturing systems, assembly, integration, and test systems, logistical systems for transportation, and auxiliary systems for power supply. Mission control, in-operation service strategies and regulations for international governance must be integrated as part of the mission operations. Figure 3.7 gives an overview of these critical system elements.

The following chapters will review the most critical technologies required for material supply and sunshade manufacturing, and their corresponding Technology Readiness Level (TRL). The TRL definitions can be found in the appendix. The second thesis performed in parallel considers logistical aspects of sunshade production, as well as sunshade attitude and orbit control [4].

[2]It should be noted that even if this timeframe cannot be maintained and in the meantime other means of solar radiation management are performed, the final goal of sunshade implementation should still be pursued. As soon as possible, the sunshades should substitute all SRM efforts optimising the climate effect and limiting adverse side-effects of large-scale Earth-based solar radiation management to few years.

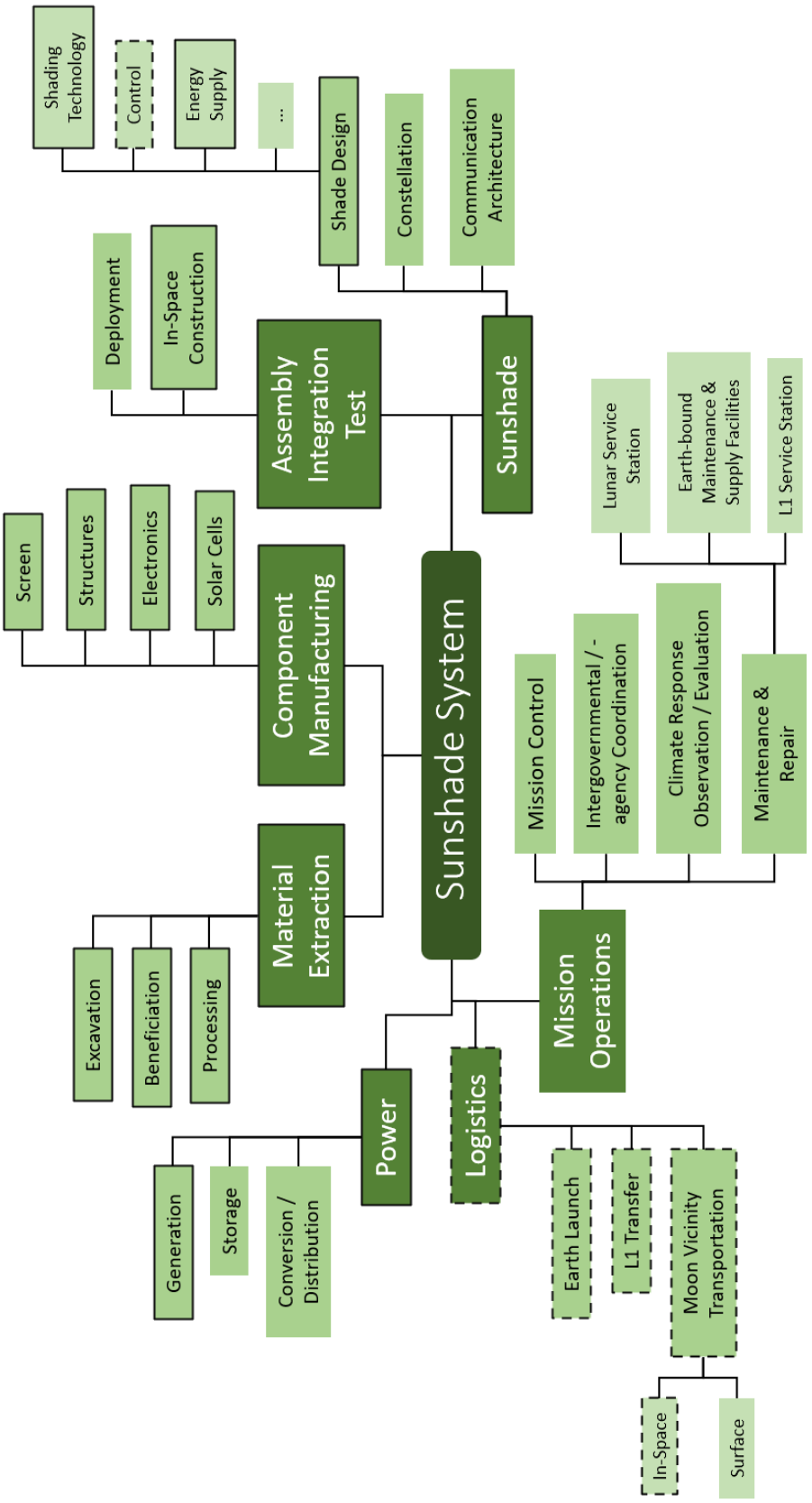

Figure 3.7: Sunshade system overview
(solid line: covered in this thesis; dashed line: covered in parallel thesis [4])

Chapter 4

Lunar In-situ Resource Utilisation

The objective of ISRU in space is to collect local material resources and convert them into products that can be used for space operations. This offers significant mass reductions, therefore the costs of space missions, and will be essential for sustained long-duration space activities [58].

An in-depth overview on lunar resources can be found in [51], where results from the analysis of the Apollo and Luna sample returns and recent remote sensing data are presented. With over 40%, oxygen accounts for the largest part of the lunar regolith. In several different compositions, this oxygen is bound to various metal elements with silicon as primary metal component. Depending on the location on the Moon, iron, aluminium, calcium, magnesium and titanium add to the mixture, as can be seen in figure 4.1. Lunar highland regolith has an increased amount of aluminium, whereas mare basalts are higher in iron and titanium. The different chemical surface compositions can even be recognised with bare eyes from the Earth, as high-iron mare regolith appears darker than lunar highland regolith. To the largest extent possible, the materials available on the Moon should be used for the production of sunshades.

In literature the process chain for ISRU usually consists of three elements, as can be seen in figure 4.2: excavation of raw material from the local soil, beneficiation of this material to create an optimised feedstock, and material processing to extract specific elements.

4.1 Excavation

The excavation of regolith is the first step in ISRU. To make use of a material it must be extracted from the local soil to be prepared for processing. Despite the essentiality of this step, it has received substantially less attention than would be expected. Recently a thorough review on existing regolith excavation systems has been performed [60].

Two significant issues with regolith excavation on the Moon can be pointed out. On one hand the gravity on the surface which is only a sixth of the Earth's gravity reduces the drawbar force of an excavation system. The maximum drawbar force is the force which an excavator

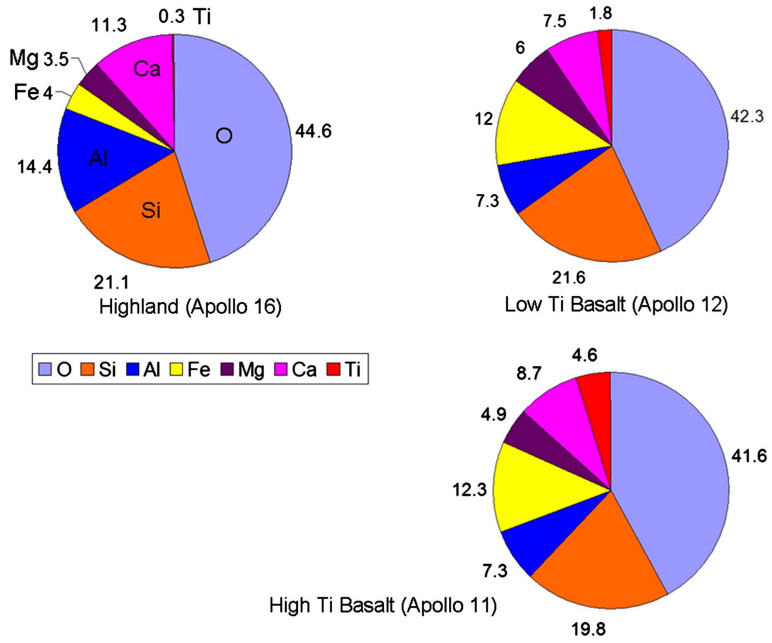

Figure 4.1: Chemical compositions of lunar highland minerals (Apollo 16), low-Ti basalts (Apollo 12), and high-Ti basalts (Apollo 11) [59]

is allowed to exert in order to haul its load without falling over. It depends on the weight of the excavator which is significantly smaller on the Moon. The second issue are the geotechnical properties of the regolith which strongly depend on the excavation site (mare, highland, poles, etc.). For dry regolith locations the excavation of deeper deposits will be more challenging due to the increase of regolith density [61]. Therefore, a general limitation of ISRU applications to the top few centimetres of the soil would be beneficial. Shallow cuts reduce the excavation force and therefore reduce the minimum-mass requirements for the excavation system. When extracting icy parts of regolith, the water content in frozen regolith simulants has shown the need for a greater drilling force for penetration and excavation. Research on percussive and vibrational operations combined with usual excavation techniques promise reductions in required excavation force. Another challenge pointed out is the interaction with lunar dust. The abrasive nature of the lunar regolith causes moving parts to wear out rather fast, which is why it is recommended to reduce their number. Bucket drums and pneumatic systems are the most promising considering that. Long-term behaviour of moving parts in the lunar environment however can only be estimated.

Except from NASA's RASSOR and Cratos platforms, as well as a pneumatic system, all of the investigated excavator concepts never exceeded the proof-of-concept state and are therefore below TRL-4. Meaningful publications are sparce. A lack of funding and discontinuation of research programs has been pointed out. Also, there are significant inequalities in test parameters

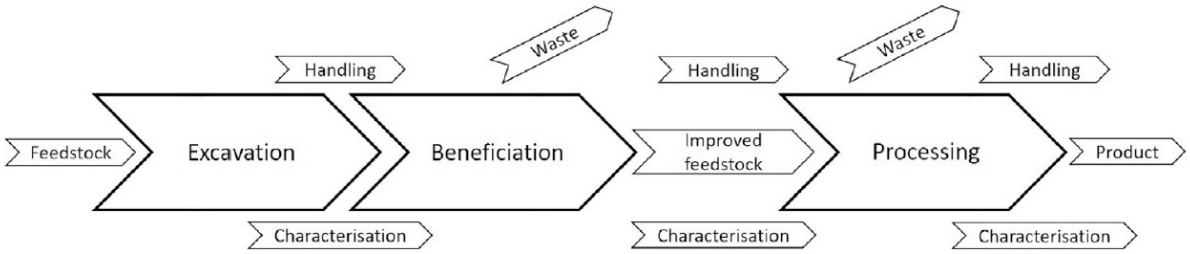

Figure 4.2: ISRU process chain [60]

and presented characteristics which make comparisons between the systems almost impossible. A need for consistency in provided data on the excavator systems for the objective assessment of the suitability of a system for extended operation on the lunar surface has been concluded [60].

In their 2006 solicitation funded within the US national Small Business Innovation Research (SBIR) programme the National Aeronautics and Space Administration (NASA) defined reasonable parameters for characterisation of excavation systems [62]. These metrics include excavation rate (kg/h), excavation efficiency (power required/excavation rate, i.e., W/kg/h), excavation depth, and berm height. Applying these parameters on investigated systems within future trade-off studies should serve as a proper basis for evaluation.

Considering NASA's metrics, the bucket ladder performed best, with a maximum excavation capability of 2400 kg/h and power requirements of under 200 W (0.083 W/kg/h). The excavation depth was one of the best, with 10 – 15 cm. The performance parameters of other regolith excavation systems are listed in Just, et al. [60].

When translating the state-of-the-art of lunar excavation concepts to sunshade production, a significant up-scaling of the excavation rate is needed. Large volumes can either be collected by deep excavation, or by collection over large areas with rather shallow material removal. It was pointed out that deep excavation is less efficient due to the higher regolith density in deep deposits [60]. They also point out that the inevitable interaction with abrasive charged lunar dust requires to reduce the number of moving parts, or on the other hand to reduce the distance transportation systems will have to move between excavation site and processing plant. With more knowledge on the power consumption for deep excavation and lunar transportation, as well as the interaction of lunar dust with mobile platforms, it must be analysed how the distribution of the regolith volume collected affects the excavation efficiency. An optimal combination of area and depth for lunar excavation must be found.

As the excavation volume, hence transportation distance and or height increases the importance of efficient and reliable transportation increases. A transportation system that has to carry, besides the regolith mass, the excavation equipment will have a higher power consumption. Systems that have to interrupt excavation activities for transportation and unloading reduce the

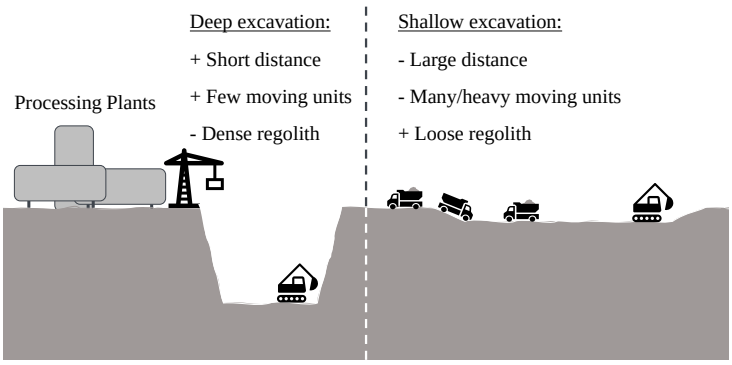

Figure 4.3: Effect of excavation depth

overall excavation rate. A separation of excavation and transportation systems therefore seems reasonable for large regolith volumes, where efficiency is central. A fleet of dump trucks could be employed to supply the processing plants with constant loads of regolith delivered from several bucket ladder excavators. In case of a failure of a truck, e.g., due to dust abrasion, excavation operations could continue, while the truck is repaired or replaced.

4.2 Beneficiation

Many regolith reduction processes have specific requirements for their feedstock to work at optimal efficiency. That can make beneficiation of the extracted regolith a very important step contributing to the quality of the final ISRU product. To reduce the volume of consumables required for the ISRU operations, dry separation processes that require no reactant or processing material are sought. Analysis of interaction between dry particles in literature considered van-der-Waals forces, adhesive forces, Coulomb forces, dielectrophoretic forces, and interparticle charging mechanisms. With this physical background several studies addressed the feasibility of manipulating lunar regolith and separating mineral phases. These processes have been reviewed, recently [63].

In general, dry separation techniques can be classified by electrostatic, magnetic, and gravitational separation. Gravitational separation however has not been considered for the Moon, due to the low lunar gravity. Some of the electrostatic techniques still make use of gravitational acceleration, but the main characteristic separating them from purely gravitational methods is the use of electrostatic fields to enhance manipulative authority. Electrostatic methods have been the largest subject of study so far. In the 1980s and early 1990s, slide separators have been investigated intensively. These machines separate particles by their level of electrical conductivity. Material is fed onto an earthed slide passing through a non-ionising electrostatic field.

The field polarises the particles. The conductive fraction delivers its negative charge onto the slide, resulting in positive net charge, while non-conductive particles keep no net charge. Differences in net charge make the particles diversely susceptible to the electrostatic field allowing for particle-path manipulation and collection into different containers at the lower end of the slide.

Plate separation with tribocharging employs an electrostatic field created by two vertically arranged parallel electrode plates onto tribostatically charged particles. The particles fall through pipes made from Polytetrafluorethylene (PTFE) or aluminium in which they are electrically charged by particle-particle and particle-wall interaction before entering the electric field chamber. Deflected by the field, particles of different charge (i.e., conductivity) can be collected in separate containers. This method is relatively advanced with tests in different environmental conditions. It is conceptually simple and consists of simple and light-weight components [63].

The Electrostatic Travelling Wave (ETW) technology uses tribostatic charge as well. While particles are conveyed horizontally, they charge each other and by interaction with the conveyor or vibrator surface. As they move through a non-uniform electrostatic field they are impelled vertically depending on their mass and charge. Hoppers above the conveyor belt can be used to collect particles of different size. As air drag and gravity reduce the ability to lift particles, this process is especially suitable for lunar environments. Beneficiation of simulated lunar material under vacuum has been demonstrated successfully [64].

Several magnetic beneficiation techniques for early-stage sizing and gangue removal have been presented. They make use of the ferromagnetic and paramagnetic components contained in the lunar regolith. Compared to the success of electrostatic separation methods with enrichment grades of up to 98%, magnetic separation demonstrations delivered moderate results. Purities achieved by mediocre electrostatic systems could be reached only by using heavy permanent magnets [63].

When characterising the viability of the beneficiation processes there are two tasks that have to be considered: mineral enrichment and size sorting. Most research however concentrated only on the first. As reported [63], the ranges of test parameters and presented results are small. Most studies focus on binary or ternary mineral mixtures. Finer fractions ($<$50 µm) of the regolith are not investigated often [63]. When working with actual lunar regolith all mineral fractions and sizes should be handled. As for regolith excavation, standards for data reporting must be implemented for reasonable process evaluation.

Beneficiation research on regolith-like material was rare, due to the unavailability of lunar samples and high cost for simulants. Since the chemical differences between lunar and terrestrial minerals is fundamental, the electromagnetic properties for lunar material must be determined intensively to be able to improve the maturity of beneficiation technology above proof-of-concept. The regolith on the Moon is naturally charged. This could complicate electrostatic separation techniques but may also be an advantage. Since electrostatic forces relative to gravitational pull are much stronger on the Moon than on the Earth and particle air interaction causes drag, the

presented techniques should work more efficiently in a lunar vacuum.

The processing volume for producing a sunshade is huge. Extensive beneficiation operations can be avoided with the choice of regolith processing technology. However, the opportunity of improving the processing efficiency for metal extraction or the specific manipulation of metal products by optimisation of the feedstock should not be neglected. Electrostatic separation methods require only simple elements. The results from preliminary studies seem very promising for the enrichment of specific lunar mineral phases.

4.3 Regolith Processing

Regolith processing is the chemical separation of oxides and silicates into pure oxygen and metal phases. By that, the brittle powder bulk material of the lunar surface can be separated into a vital oxygen stock and metallic building material with much higher performance [54]. Classical approaches that have been considered are based on chemical reduction, pyrolysis, acid treatment, or electrolysis of regolith melt [59]. The rather new molten salt electrolytic process has been studied intensively over the past decade [65]. For long-term scenarios biological options were studied [66, 67, 68]. The processes can be compared by the requirements on the feedstock used, needs for resupply, the complexity of the process, and the energy required. Since oxygen is easier to manipulate, most reduction processes are based on extracting oxygen, leaving behind not pure but at least purified metal by-products.

As a starting point, international efforts concentrate on the production of consumables [56, 69, 70]. The need for propellant and life support for human operations creates dependencies on Earth supply. Extracting oxygen from the regolith and frozen water from the lunar poles could create a local stock of these consumables and would reduce logistic efforts. Furthermore, the energy required to transport this propellant or supply for life support from the Moon to Earth orbits is much lower than launching it from the Earth [51, 71]. Therefore, lunar resource extraction could enable efficient life support and in-orbit refuelling operations for satellites or other spacecraft in lunar vicinity and around the Earth. Using metal by-products as construction material is emphasised as the following step [69, 70].

4.3.1 Advanced Methods

Hydrogen Reduction

The method of reducing lunar regolith with hydrogen utilises the iron oxide (FeO) fraction. Subsequently, the overall efficiency depends on the iron content, which is higher in lunar mare and lower for the polar highlands [51]. The process temperature is at 800 – 1000 °C [59, 72, 73]. The primary product of hydrogen reduction is water, which then may be electrolysed further into oxygen and hydrogen [59].

Hydrogen reduction is the most advanced regolith extraction process since its simplicity is favourable for early ISRU demonstration missions. Within the ISRU project in the Exploration Technology Development Program (ETDP) initiated by NASA in 2004 the oxygen extraction systems Precursor ISRU Lunar Oxygen Testbed (PILOT) and ROxygen were developed [74]. They were each designed to extract around 1 – 2% of oxygen from 10 kg of regolith. Both systems have been demonstrated during the 1st Lunar ISRU-Surface Operations Analog Field Test on Mauna Kea, Hawaii in 2008. While PILOT was able to produce oxygen at a rate of 250 kg/year, ROxygen produced oxygen at a rate of 660 kg/year. With additional parabolic flight tests the hydrogen reduction technology within the program reached TRL-5 [74].

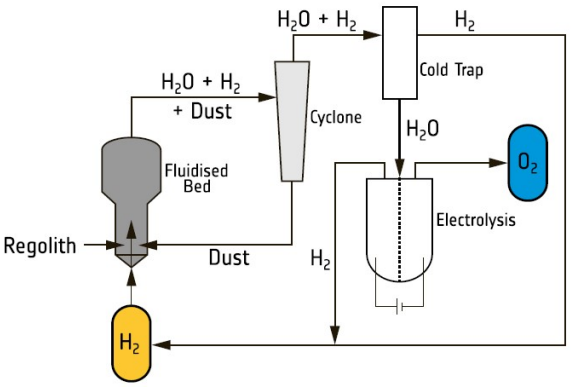

Figure 4.4: Hydrogen reduction process [72]

In 2017 an integrated system with a fluidised bed reactor for the reduction of ilmenite using concentrated solar power was presented [75].

The PROSPECT Sample Processing and Analysis (ProSPA) system of the European Space Agency (ESA) is able to produce small amounts of water using extracted oxygen and an internal hydrogen supply besides its primary task to characterise volatiles and analyse isotopes [76]. The feasibility of the simplified static system has been investigated, recently [73]. As part of the Package for Resource Observation and in-situ Prospecting for Exploration, Commercial exploitation and Transportation (PROSPECT) it is scheduled to launch in August 2025 with the Luna-27 mission to demonstrate ISRU on the Moon and more specifically volatiles extraction and hydrogen reduction, raising the maturity of the technology to TRL-6 [77].

Carbothermal Reduction

Within NASA's initiative, an oxygen reduction process was developed that is using methane as reactant [74]. By that it is possible to reduce silicon oxides as well [78]. While silicates (SiO_2) react to silicon carbide (SiC) at temperatures between 1600 °C and 2000 °C, pure silicon is achieved with temperatures higher than 2000 °C [72]. Besides the iron and silicon by-products, oxygen and methane are obtained, of which the latter can be reused for the process.

During the 2nd Lunar ISRU-Surface Operations Analog Field Test on Mauna Kea, Hawaii in 2010, a fully automatic carbothermal regolith reduction module developed by ORBITEC demonstrated the ability to extract oxygen from a lunar regolith simulant using methane [79]. The systems tested also included liquid oxygen and methane storage and a liquid oxygen/methane thruster [74].

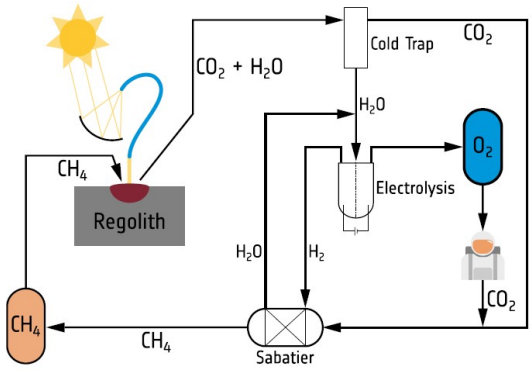

Figure 4.5: Carbothermal reduction process [72]

The maturity of carbothermal reduction is equal to that of hydrogen reduction [74]. While hydrogen reduction can reduce up to 10 wt.% [72, 80], carbothermal reduction yields up to 28 wt.% from lunar regolith [72, 79], due to the additional SiO fraction reduced. The multi-step nature, high operating temperatures, and potential need for methane resupply however, could prevent carbothermal reduction from large scale implementation.

Hydrogen reduction and carbothermal reduction are the most advanced technologies to extract oxygen from lunar regolith and the only ones with integrated system tests performed on the Earth. Hydrogen reduction is especially emphasised for the first demonstration on the Moon within the next five years by NASA [81], ESA and Roscosmos [77]. Both processes however deliver relatively impure metal products. Even with up to 28 wt.% of oxygen reduced by carbothermal reduction, more than 12 wt.% of oxygen would still be bound within the metal by-product and the range of purified metals would be small. While these simple processes seem favourable for early implementation and where only oxygen is needed, alternatives must be found that deliver more favourable high-purity metals to be able to manufacture lightweight components needed for a sunshade.

4.3.2 Thermal Methods

Techniques that use high process temperatures to directly dissolve metal oxides without reactants have been developed. Vapour Phase Pyrolysis (VPP) makes use of the dissociation of metal oxides in their vapour state. At temperatures between 2000 – 3000 °C regolith minerals are vaporised and dissociate into oxygen and metal suboxides, of which pure iron oxides are obtained at the lowest temperatures [72, 82]. Titanium and silicon oxides follow, while aluminium, magnesium, and calcium oxides are obtained at the highest temperatures [59, 82]. The reaction products appear in the gas phase and would have to be cooled actively to prevent back reactions. After cooldown, the oxygen phase is still vaporised so it can be collected easily.

With potential yields of up to 100 % of oxygen extracted from not beneficiated regolith [59, 82], vapour phase pyrolysis is a very simple process that does not require complex feedstock preparations or reactants and delivers high amounts of oxygen. To obtain pure metals an additional process step would be required since only metal suboxides are delivered by vapour

phase pyrolysis, increasing the process complexity.

Vapour phase pyrolysis has been demonstrated for a lunar volatile analysis and extraction application during the Desert RATS field test in 2011 [83], reaching TRL-5. The TRL for metal extraction remains at 3.

Plasma Separation goes even further in as it increases the temperature of the vaporised regolith to its plasma state [84]. As ionised plasma, the regolith species can be manipulated according to their charges, which allows to collect the species individually. The requirements for the regolith feedstock are low, while extraction capabilities and purity of the metal products are high. The application of a plasma to dissolve regolith components is still at a conceptual state with a corresponding TRL-2.

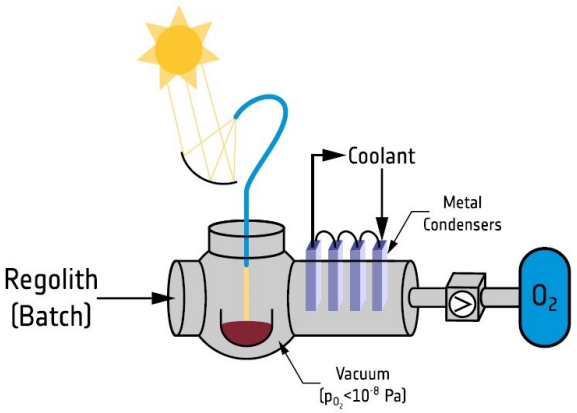

Figure 4.6: Vapour phase pyrolysis process [72]

Both thermally demanding processes promise high yields with no reactants needed, which may be very useful if high processing rates are required. The requirements for electrical power supply on the other hand make the use of these technologies unfavourable.

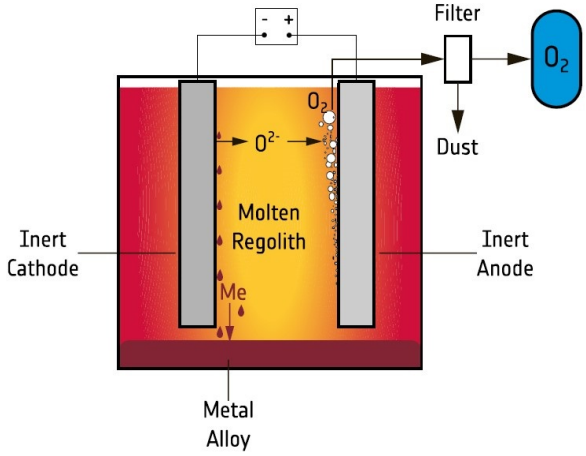

Figure 4.7: Molten regolith electrolysis process [72]

A process with more moderate temperatures is in development. Molten Regolith Electrolysis (MRE) is performed at 1600 – 2000 °C [72]. In an electrolytic cell a potential is applied to a regolith melt. The oxygen fraction evolves at the anode and remaining metal deposits at the cathode [59, 72, 85]. The metals can be collected according to their individual oxide stability as a function of the applied voltage in the order of Fe, Si, Ti, Al, Mg, Ca, of which iron is the metal with lowest voltage required and calcium the one with the highest [59, 72].

Problems concerning the longevity of the reactor material due to the corrosive oxide melt have been reported [86]. A cold-walled reactor was proposed, where the Joule-heating of the internal currents is utilised to maintain the molten state of the regolith in the centre, while at the sides the regolith is solid [85]. The

electrical and mechanical requirements for the electrodes in the corrosive environment remain a challenge. Platinum group metals and chromium-based alloys are studied in this context [86].

A thorough parametric sizing model of an MRE reactor has been set up numerically that provides a database of reactor designs and performance characteristics [87, 88]. For highland regolith, a production rate of 10 t of oxygen, about 2 t of aluminium, 5 t of silicon, and almost 1 t of iron per year for a reactor mass of under 600 kg and an electrical power of 35 kW were achieved within the simulations.

With that and the laboratory work performed by [85] and [86], currently the technology of molten regolith electrolysis is at TRL-4.

4.3.3 Chemical Methods

The high operating temperatures and high power demand have been a barrier for the implementation of the thermal methods described above. To increase the energy efficiency several technologies exist that utilise the chemical reaction potential of lunar minerals. Methods that use acidic liquids as reactant were developed. Sulphuric Acid Reduction (SAR) makes use of the acid's reaction with ilmenite into iron and titanium sulphates, that are then re-dissolved into pure metals and oxygen, while the sulphuric acid is recovered [59]. Drawbacks for the technology are low oxygen yield, and with only iron and titanium delivered, the small range of extractable metals [59]. Ionic Liquid Reduction (ILR) introduces a less toxic and less corrosive reactant, improving handling and lifetime of system components, as well as the range of metals and amount of oxygen extracted [89]. The process temperature of 150 °C is significantly lower than with other technologies. Both processes suffer from their complex multi-step nature, which may be unfavourable for large scale applications.

Molten Salt Electrolysis (MSE) is a very promising technology. It combines the chemical reactivity of salts with the electrochemical behaviour of metal oxides. The technique is based on the FFC-Cambridge process, a solid-state electrochemical reduction of metal oxides into metals in molten salt at temperatures of around 900 °C [90]. The company Metalysis improved the technology to be ready for industrial application for metal extraction (Metalysis-FCC). Theoretically, all lunar minerals can be reduced within MSE, which means that there would be low requirements on regolith beneficiation. The ability to separate oxygen and metals from lunar regolith simulant has been proven [65].

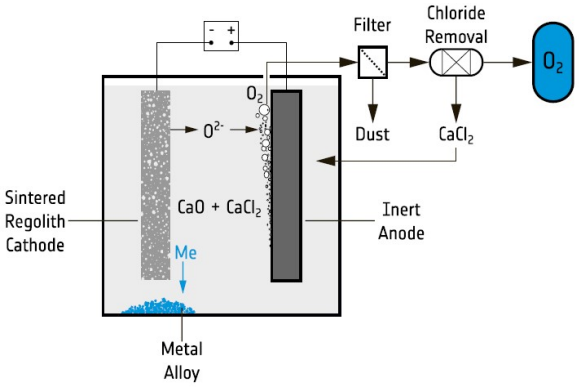

Figure 4.8: Molten salt electrolysis process [72]

Tests resulted in 96% of oxygen removed after 50 hours, while 100% are considered possible. The metal products obtained appeared in three distincts alloy groups: Al/Fe(/Si), Fe/Si(/Ti/Al), and Ca/Si/Al(Mg). Si and Mg were significantly depleted in the products. Depending on the usage of the obtained metals, an additional electrorefining process might be required to deliver the optimal metal alloy, but adjustments on the regolith feedstock might enable to directly produce specifically designed alloys [59, 65]. The recent proof-of-concept has raised the TRL of MSE to 3.

In cooperation with ESA, Metalysis is currently working on the optimisation of process parameters to lower the energy and mass required and increase the maturity for a lunar demonstration. Electrode lifetime and reuse of the $CaCl_2$ electrolyte are addressed as well as understanding the mechanisms leading to the depletion of Si and Mg.

4.3.4 Biological Methods

Utilising microorganisms to extract iron and silicon from lunar or martian regolith has been investigated [66, 68]. Laboratory experiments on the interaction between bacteria and lunar regolith simulants confirmed the potential of biomining for space exploration. Different bacteria were tested, and promising candidates were outlined. For martian surface missions, a theoretical bioreactor design to perform microbial mining activities has been created [66]. Advantages of biomining are the absence of a need for bulky hardware and extensive infrastructure, and no need for high processing temperatures or chemical treatment [91]. The payback time on the other hand, which is in the scope of years, is very long. The production rate of biological mining operations is by far too low for sunshade production operations and might only come into consideration for smaller lunar surface operations.

4.3.5 Discussion

Table 4.1 summarises advantages and disadvantages of the various regolith processing methods. It can clearly be seen that there is a distinction between simple high-effort, high-yield technologies and more complex low-effort, high-efficiency technologies. Molten salt electrolysis bridges the gap in between, providing highly-pure metals, with only moderate energy requirements and process complexity. It is therefore emphasised by ESA to be demonstrated on the Moon within this decade [69]. If successful, this would raise the technology's TRL to 6. NASA currently concentrates on the production of oxygen and water to support logistic operations and enable human missions. There is no focus on the quality of the metal by-products. In this context, the simple and reliable process of hydrogen reduction therefore is the optimal choice for a first ISRU implementation.

A large-scale application within sunshade production demands for a high mass throughput. Fast processes would reduce the number of processing units needed for the same total produc-

	HydRed	CarbRed	VPP	Plasma	MRE	SAR	ILR	MSE	Bio
Metal Products	- -	-	+ +	+ +	+ +	-	+	+ +	-
Process Complexity	+	-	+ +	+	+	-	-	+	+ +
Process Temperature	+ +	+	- -	- -	-	+	+ + +	+	+ + +
Process Duration	-	-	+	+	+ +	?	?	-	- - -
Feedstock Requirement	-	-	+ +	+ +	+ +	-	-	+	?
Consumables Requirement	-	-	+	+	+	-	-	-	+ +
TRL	+ +	+ +	- -	- -	-	-	- -	+	- -

Table 4.1: Evaluation of regolith processing technologies

tion rate. As seen in table 4.1, the processes with high production rates are usually the ones with high operating temperatures, consequently the ones with high energy demand. This in turn means a high mass for the power supply system, which may offset the advantage of fewer processing units. Molten regolith electrolysis provides high processing speed with low complexity. Out of the thermal methods it works at the lowest temperatures and has the highest TRL. Therefore, it would be the first choice, if production rate is more important than efficiency. Energy efficient methods usually involve chemical reactants which would need to be supplied from the Earth. Full recovery of these reactants is crucial. A detailed mass and cost analysis must conclude the optimal choice of ISRU processes.

Since the extracted metals for the sunshade have eventually to be transported to SEL_1, light materials such as aluminium, titanium, and silicon seem to be the optimal choice for sunshade manufacturing. As the reviewed processes for metal extraction have shown, iron is the element that is most easily extracted, either at the lowest temperatures or at the lowest voltages applied. The additional energy required to launch heavy iron may be compensated by a significant reduction in energy required for regolith processing when only iron is extracted. This however restricts the potential use of other metal by-products. When using primarily aluminium for sunshade production, the other elements extracted in the process, may for example be used for lunar construction projects. This creates spin-off potential and might help ramping up the production capabilities.

With the technologies reviewed in this chapter it can be concluded that the capabilities for lunar in-situ resource utilisation have yet to be proven. Relying on these technologies as baseline for sunshade production requires a significant maturation and demonstration effort. While simple processes of oxygen and metal separation that enable human life support and propellant production are ready for demonstration with missions planned for the next years, technologies that are able to deliver high quality metals needed for a sunshade are still only on laboratory scale. Demonstrating those must be the main focus within the sunshade development. With

ESA's commitment to molten salt electrolysis, first production of pure lunar metals might be performed within this decade. However, maturation and characterisation of processing technologies for increased metal production rate, such as with molten regolith electrolysis should be part of the demonstration effort as well.

The knowledge of the Moon's geology is based on the sample return of several surface missions and orbital remote-sensing and is therefore very incomplete. Extensive lunar in-situ surface characterisation and increasing the lunar material available for investigation and technology demonstration would accelerate developments for lunar excavation, beneficiation, and processing systems.

Chapter 5

Sunshade Manufacturing

The resources provided with the ISRU technologies that have been presented will be used for the manufacturing of sunshades. A screen that shades the Sun, electric control systems, elements for power supply, as well as structural support to integrate all elements are the most important components of a sunshade. Several potential ways to manufacture these components will be reviewed in this chapter. Components used for actuation of attitude control manoeuvres will be reviewed in the parallel thesis [4]. At first, the advantages of in-space manufacturing, as well as experiences that have been made will be presented.

5.1 In-Space Manufacturing

Developments in the field of In-space Manufacturing (ISM) indicate a fundamental paradigm shift for future space missions. The ability to manufacture parts in space promises several advantages over conventional space mission operations. Currently the most challenging environment for a spacecraft is the launch from the Earth. The strong accelerations, vibrations, and thermal loads constrain spacecraft structures to be designed with sufficient margin and redundancies. The requirements for the launch exceed the operational requirements by far. The restricted volume determined by the launcher fairing sets a limit for the size of spacecraft. This sometimes forces engineers to design complex mechanisms to unfold antennae or solar arrays. Mechanisms are sources of failure and are therefore usually oversized. Space stations such as the Mir and the International Space Station (ISS) had to be assembled modularly due to the maximum size of systems delivered in orbit.

If spacecraft structures were to be manufactured and integrated in space, theoretically, their feasible size would be unlimited. Large-scale antennae, large space telescopes, or space solar power satellites could be constructed [92]. The weight of the spacecraft could be reduced since they would not have to survive Earth launch. Heavy mechanisms would only be needed where nominal operation demands. The materials for production would have to be launched into space

only as feedstock. This allows for more efficient packaging. The cost for launching materials would be reduced due to the many mass savings. ISM also allows to use space resources that would reduce the cost for material supply even further.

For human missions, on-demand fabrication of parts increases the mission flexibility. The rapid response of ISM would enhance crew safety and allows for quick adaptation to unexpected situations, immediate repair, recycling, and maintenance. For ISS operations, 13 tonnes of spares are maintained on orbit, with additional 18 tonnes on the ground [93]. This mass could be reduced significantly since feedstock of base material could ideally be manufactured into any part. NASA states that 95% of available spares will never be used [94].

All in all, the many advantages of ISM would reduce the efforts for space operations. Especially mass reductions would lead to significant cost savings.

Space agencies have recognised this potential for a long time, however, it has been only recently that advancements in Additive Manufacturing (AM) have made ISM viable. Space agencies, especially NASA, have embraced the opportunities of AM for its affordability, shorter manufacturing times, and flexible design solutions [95]. The ISS has been used as critical testbed for demonstrating and validating capabilities to manufacture parts from different materials [93, 94, 96, 97, 98].

The many ISM demonstrations performed on the ISS, show the trend towards manufacturing components needed for space operations directly in space. Sunshades produced from space resources will have to be manufactured in space as well, and by that will benefit from the many advantages of ISM. It has been explained in chapter 3.2 that the mass of a sunshade depends on the properties of the sunshade surface. Minimising the shade mass can be achieved by reducing the reflectivity of the Sun facing surface, and hence being able to significantly reduce the areal density of the sails. Low mass would mean either early completion, or low production effort, which in turn means lower cost. The next section will explore ways to manufacture the thin screens required to shade the Sun and how the surface properties could be manipulated to improve the shade's mass efficiency.

5.2 Sunshade Screen

Previous studies proposed concepts that aimed to shade the solar light by means of absorption and re-emission, or refraction. Refractive or Fresnel lens type screens would scatter the light transparently and therefore would have very low reflectivity. The concept by Angel [29] is with $20{\times}10^6$ t the lightest proposal up to date, although it requires non-lunar materials and high-quality manufacturing, which might be available only on the Earth. The concept by McInnes [28] includes reflectivity reduction by a carbonaceous surface coating on thin iron foil. It would absorb most of the light and re-emit it diffusely. In case of lunar production, this carbon-coating would require either Earth supply or asteroid resources and is therefore not applicable. It is however

a concept that promises very simple manufacturing. A feasible sunshade concept should reduce the complexity of the manufacturing process. Therefore, it will be examined here how thin metal foil could be manufactured in space, using lunar resources and how the optical performance of this metal foil might be optimised.

Materials that are most abundant on the Moon should account for the largest parts of the shade in order to reduce the mass of regolith to be processed. Therefore silicon, aluminium, and iron should be examined as primary foil material. Some material properties for Si and Al are listed in table 5.1. Since the density of Fe (7,874 $\frac{\text{kg}}{\text{m}^2}$) is about three times the density of Al and Si, a shade made from iron foil can be expected to be much heavier than with aluminium or silicon, whereas there are no signs that iron could compensate that with much lower reflectivity. In chapter 4.3.5 the potential for secondary use of extracted iron has been mentioned. Iron is hence excluded as foil base material. However, iron as well as the other bulk material elements titanium, calcium, and magnesium can be added to form an optimised alloy. At this stage, it can be assumed, that the optical properties are defined by the main component of the respective alloy. Precise determination of the optical behaviour of an alloy of choice should be performed later to optimise the accuracy of the system model.

The efforts of developing the capability for ISM mostly focused on AM. The lowest resolution of current terrestrial printing systems is in the range of 20 – 100 µm and therefore not suitable to produce metal sheets with very-low areal density, as it would be required for a sunshade [99]. An alternative manufacturing process for thin metal foil must be found.

The natural reflectivity of silicon is much lower than that of aluminium. Therefore, techniques of silicon foil production will examined now.

Element	ρ [$\frac{\text{kg}}{\text{m}^3}$]	η [-]	ϵ [-]
Aluminium	2,699	94% [100]	0.03 [40, 101]
Silicon	2,329	40% [102, 103]	0.7 [104, 105]

Table 5.1: Properties of lunar materials: Density ρ, Reflectivity over the total solar spectrum η, NIR-Emissivity ϵ

5.2.1 Silicon Foil Spalling

The conventional technique of slicing silicon wafers to obtain thin foil comes with costly material losses of more than 40% during the cutting process [106]. Within the field of solar cell production, new ways to cheaply manufacture ultra-thin junction layers for thin film solar cells are developed. As an approach to reduce the material losses, foil spalling was developed [107, 108]. This technique is based on controlledly breaking off layers from a metal substrate. Figure 5.1 shows the required process steps. A stress inducing layer of different material is added to the substrate,

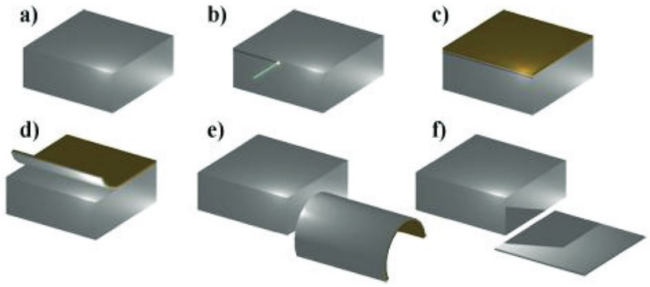

Figure 5.1: Spalling of silicon from a substrate [107]

while at the side of the substrate a laser or cutter creates a notch. Thermal stress as consequence of different thermal expansion is created so that a thin layer cracks from the substrate, as can be seen in figure 5.1 d). Afterwards the stress inducing layer can be removed with a thermochemical process and a separate foil element is obtained.

In the presented studies an epoxy-based layer was used for inducing thermal stress. A foil thickness of around 100 µm was achieved, while the required thickness of the epoxy layer was up to more than three times higher [107, 108]. Silicon foils of 5×5 cm^2 were obtained and classified as large area thin silicon foils [108]. A laser welding process to overcome area restrictions in the production of thin film silicon wafers was developed [109]. This allows to join many foil elements and create large area silicon foil, as it would be needed for a sunshade (see fig. 5.2). Different laser welding techniques were investigated [110]. Keyhole welding of silicon foil with operational power of 260 W was demonstrated enabling a join speed of 550 $\frac{\text{mm}}{\text{s}}$ for a single seam.

The process of producing large area silicon foil is a rather new technology with most of the processes still under investigation on laboratory scale. The brittle nature of silicon results in a complex multi-step process that requires assembly of an enormous multitude of foil elements to obtain a significant sail size. The joining speed of a single laser device and the small size of foil elements result in a huge amount of welding units needed, or in turn slow production. The brittleness of silicon also complicates the handling of foil and lowers the sunshade robustness. Most of all, the high usage of consumable epoxy during foil production disqualifies silicon foil for lunar-built sunshades.

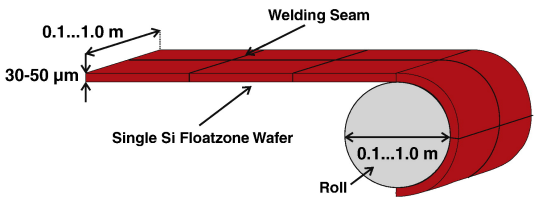

Figure 5.2: Silicon foil made from individual Si wafers, which are welded together [109]

5.2.2 Aluminium Foil Rolling

The production of thin aluminium foil is much easier since it is a malleable metal. A quick technique to fabricate sheets of malleable metals like copper, aluminium, iron, gold, silver, titanium, and many more, is Twin Roll Casting (TRC). Metal melt is poured in between two rolls where it solidifies into a thin sheet with thickness in the low millimetre range [111]. To further reduce the foil thickness, several steps of cold and hot rolling, and annealing have to be added to the process [112]. This is common for the production of household aluminium foil, where thicknesses of 16 – 24 µm are standard [100]. However, a thickness down to 6.3 – 10 µm is producible with aluminium depending on the cast alloy [112]. The maximum strip width can be found at about 2 m [112].

The effect of the casting speed on surface quality and strength of the final foil product has been examined [113]. Although high casting speeds of up to 180 $\frac{\mathrm{m}}{\mathrm{min}}$ can be achieved for sheets in the mm range [114], low casting speed is preferable for thin foil production [113]. The best 7 µm aluminium foil was rolled at a speed of 100 $\frac{\mathrm{m}}{\mathrm{min}}$.

To apply this process of foil rolling to production on the Moon, it would have to be adapted to the lunar environment. Foil stock properties and impurities are the main reasons for pinholes and strip breaks during aluminium roll casting, of which the likelihood increases as the foil thickness is reduced [112]. Lunar dust contamination may represent a significant source of impurities when rolled into the sheets. During manned lunar missions and in laboratory characterisations this dust has been reported to be electrically charged, sticking to any surface. Its irregular shape also makes lunar dust very abrasive wearing down any moving parts [61]. Thus, it may be beneficial to move the foil production from the lunar surface into orbit to prevent foil damage and increased facility maintenance services.

There is no atmosphere on the Moon or in orbit, which may interfere with cooling processes during roll casting. Grain formation in the metal can be limited when cooled quickly [112]. Forced cooling has been introduced and a suppression of defects in thin foil has been verified [115]. The process in figure 5.3 includes forced cooling using water. Novel approaches to handle the temperature of cast strips in space might need to be introduced to enable the production of very-thin aluminium foil without dependency on consumables.

During construction of the production facilities, the rolls for aluminium foil production would present significant mass to be transported into orbit. It should be examined if those rolls could be manufactured in-situ from lunar metals and ceramics.

Roll casting to produce thin aluminium foil is a low-complexity process that has been used for decades and is well understood, constituting a mass production industry on the Earth [111]. The high level of technology maturity promises a timely lunar application, with only the discussed adaptations to the space environment presenting a challenge.

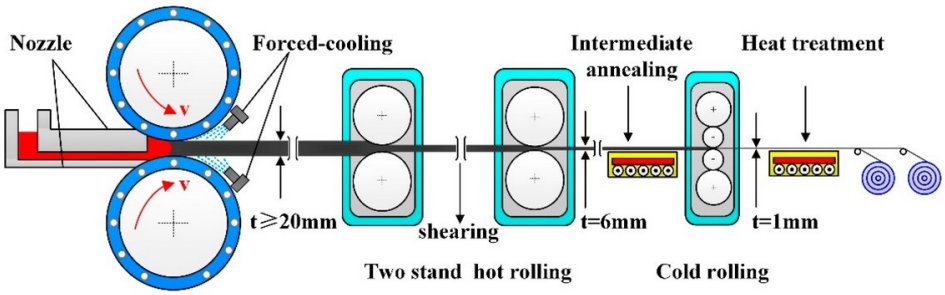

Figure 5.3: Schematic of twin-roll casting process with forced-cooling (FC-TRC) [115]

5.2.3 Aluminium Foil Evaporation

Very-thin metal foil production has been examined as part of solar sail design. Instead of reducing the thickness of roll cast metal sheets where a lower limit is reached at around 7 µm, the manufacturing concepts that have been developed are based on growing thin films by vapour deposition onto a substrate.

Physical Vapour Deposition

During Physical Vapour Deposition (PVD) atoms or molecules are removed from a source (liquid or solid) in a vacuum and deposited on a solid surface where a film of material is epitaxially grown [116]. Removal from the source is achieved by thermodynamic evaporation, or physical sputtering. For evaporative removal, electron beam heating is most commonly applied to dissolve atoms. Laser or a cathodic arc can also be used. Vapour pressure causes the free particles to move towards the deposition substrate in the line of sight. The mean free path of the vapour flux must be larger than the distance to the substrate. This results in a maximum pressure for PVD applications. Co-evaporation to produce alloys is possible, if two material sources are provided. The deposition material may also be ionised by the electron beam or cathodic arc, to allow influencing the deposition flux. Sputtering employs ions, atoms, molecules, or photons to bombard the source material. With a multi-atom kinetic collision process the source material is removed. Usually, a plasma or an ion beam is used. The kinetic energies of the atoms are higher than when evaporated. This causes already deposited atoms to be rearranged on the substrate and creates a very dense and smooth film. Evaporation on the other hand results into a columnar microstructure that is prone to absorption. When producing mirrors or reflectors that require very smooth surfaces with low absorption, sputtering may be favourable. For solar cells it is an advantage if the light is trapped and absorbed within the junction material, so evaporation might be more favourable.

PVD was adapted and successfully performed in space within the Wake Shield Facility Program [117]. The Wake Shield Facility is an atmospheric shield that in its wake creates a very

clear vacuum of about 10^{-14} Torr when deployed in LEO. It was flown during three different Space Shuttle missions from 1994 to 1996. As a payload a PVD system was operated that was able to produce ultra-low impurity semi-conductor thin films.

The technology has been developed further by Lunar Resources, Inc. They have developed a system that is able to produce different metal, semi-conductor, and hybrid films. It will be demonstrated on the OSAM-1 mission scheduled for launch in 2022 [117]. Within one hour a 0.5×0.5 m glass substrate will be deposited with a 0.7 µm aluminium film, requiring an operational power of 1 kW. The company's goal is to provide a permanent in-space service for production of coatings of different type and solar cells, as well as maintenance operations.

With the success during the Wake Shield Facility Program the TRL of PVD in space was raised to 7. The developments of Lunar Resources, Inc. promise commercial vapour deposition operations that will create great experience for future applications.

With the high maturity of PVD, evaporative production of thin aluminium foil comes into consideration. The challenge of producing freestanding foil with PVD lies in the damage-free separation of the foil from the substrate. Laboratory studies demonstrated the separation of 25 µm thick aluminium foil from a steel substrate roll on which it was evaporated [118]. The process is shown in figure 5.4. Despite the relatively high thickness, which simplifies the peeling of the foil, the results indicated that the process might be suitable for the production of thin solar sails in space. The only damages after separation were observed at locations where there were scratches on the steel roll.

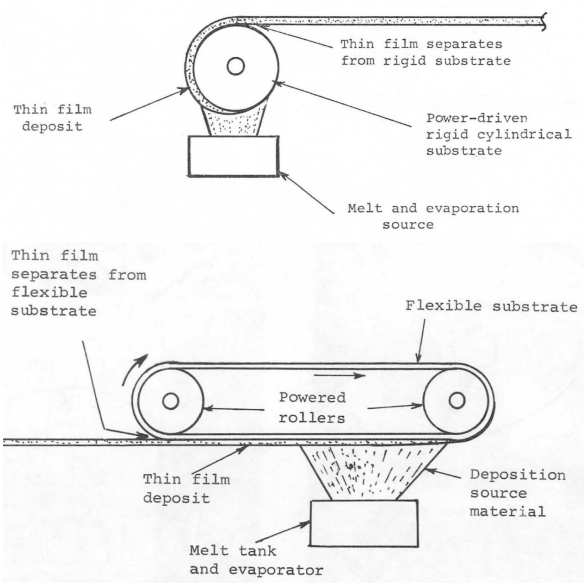

Figure 5.4: Schematic of evaporation processes for foil production [118]

In another experiment a similar procedure was investigated that included a flexible copper ribbon, rotating around two rollers, on which the aluminium is evaporated, as can also be seen in figure 5.4. There were no cracks observed during separation [118]. A very preliminary power estimation for these two processes resulted in 2640 W for a deposition rate of 0.2 $\frac{\text{kg}}{\text{h}}$.

The interlaminar bond of substrate and foil creates a limitation of the separation forces exerted onto very-thin films. A concept was proposed which would allow the production of aluminium foil even below this limit [119]. It includes evaporating a sublimable wax on the substrate

belt before the aluminium is evaporated on top of it. After that, the wax is heated to sublimation condition in an evaporation chamber. It leaves through holes in the substrate belt and is collected and reused. The separated foil product is extruded, while the substrate belt re-enters the cycle. The end-to-end process presented also includes a stamping and cutting step creating slits that prevent the spreading of tears in the foil. There are losses expected during the several evaporation steps that would require considerable replenishment of the wax substrate for high production volumes. Because of the many process steps and the handling of substrate wax in different physical states, it is a complex process which on the other hand allows for manufacturing of ultra-thin metal foil down to several nanometres. Small sheets of aluminium foil with a thickness of 40 nm have been produced within laboratory tests that show enough mechanical strength to bear loads expected during manufacturing and operation of solar sails [119]. A 3 t total system was estimated that produces 1 m wide, 100 nm thick aluminium foil at a speed of 1 $\frac{\mathrm{m}}{\mathrm{s}}$ with a power demand of 62 kW.

The few experiments performed on the evaporative production of thin metal foil have proven the potential of the technology for solar sail manufacturing in space. However, since the 1970s there were no further technological advancements reported and the readiness level of thin foil manufacturing in space remains at TRL-3.

Earlier in this section, silicon foil was pursued initially for its low reflectivity. With the use of highly reflective aluminium as shading foil, other means of reducing the reflectivity must be found.

5.2.4 Surface Texturing

Developments in the field of solar cells showed significant reductions in reflectivity by three-dimensional texturing of silicon junction surfaces. This might be translated to aluminium surfaces as well. When irradiated perpendicularly the light is not reflected directly back to the source, it is reflected onto another surface irregularity that absorbs a part and reflects a part. Figure 5.5 shows how with every surface contact more light is absorbed and the total reflectivity decreases.

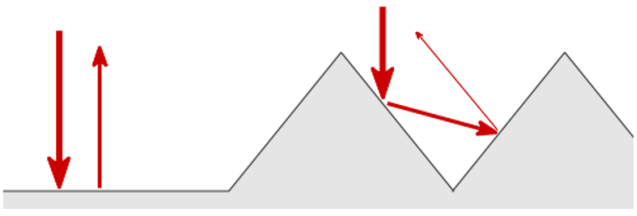

Figure 5.5: Effect of surface texturing on light reflection [120]

The effect of upright pyramids, inverted pyramids and honeycomb structures have been investigated [121, 122]. Also texturing of the backside of solar cell junctions is able to reduce the reflectivity and by that increase the solar cell's efficiency by 10 – 40% [123, 124]. The creation of a nanostructure even further reduced the reflectivity [125]. While a flat silicon surface was reported to have a reflectance of 37.3%, the pyramid textured surface had 12.3%, the nano-textured surface 6.4%, and with creating a two-scale textured surface by etching an additional nanostructure onto the pyramid structure 3.8% reflectance was achieved [126]. Black silicon is a surface modification that creates nano-pillars on silicon surfaces. This form of texturing was reported to achieve reflectances of around 1% [127]. An additional 3D-nanostructure placed on the nano-pillars resulted in further improvements and reflectances of around 0.5% over the total light spectrum from ultraviolet to infrared could be measured [102].

The nanostructures needed to create such low reflectances require complex manufacturing processes. Usually, the surfaces are modified by chemical etching. If it is possible to create high-tech nanostructured metal foil with lunar resources, it would be reasonable to instead of absorbing foil rather manufacture ultra-lightweight refractive screen shades as proposed by Angel [29]. Satisfying results from manufacturing experiments of such screens by chemical etching have been presented [128]. Dependency on such high-tech manufacturing processes to achieve a very low reflectivity however should be avoided to reduce the sunshade production complexity. Furthermore, applying an etching step to the foil production would reduce the manufacturing speed, for it takes several minutes to achieve the required effect on the foil surface [127]. The durability of the surface in a high radiation environment is questionable as well. Long operation might result in a significant increase of reflectivity. But the achievements of ultra-low reflectances of silicon surfaces show the potential of surface texturing on the reflectivity of naturally reflective metals. If a surface texturing process is applied to sunshade foil, it would have to be a very simple one.

In this aspect, advantage can be taken from the ductility of aluminium. It has been found out, that while the hemispherical reflectance of two differently rough aluminium samples were the same, the one with higher roughness had significantly lower spectral reflectance [129]. 95% specular reflectance were measured for an rms height of 0.2 µm and 30% specular reflectance for an rms height of 0.6 µm. Characterisation on the reflectance of matte side and bright side of household aluminium foil have shown similar results [100]. For the whole range from 250 – 2500 nm wavelength a specular reflectance of 19.8% and diffuse reflectance of 76.2% was measured for the matte side. These results show that even with a standard industrial rolling process the specular reflectance of aluminium foil can be influenced significantly.

With the sunshade facing the Sun at a perpendicular angle it is not important to create a surface that has low reflectivity even at small angles of incidence. Only the back-reflection of perpendicular incoming light is of importance. To reduce the impulse in the Sun-Earth-line direction, it would be optimal if the perpendicular incoming sunlight would be reflected parallel

to the foil surface. The ellipse in figure 5.6 should be as flat as possible, or even have a more complex shape. Randomly created roughness may reduce the reflectivity to a certain extent, but a specifically designed surface texturing might minimise the perpendicular reflectivity even further. If the foil is produced by rolling, the texture could be printed into the aluminium foil in a final rolling step. The surface of the corresponding rolls would have to be manufactured with a certain surface texture that is then imprinted into the foil. The effort for texturing of the rolls is justified, since it would have to be performed only once during facility construction, or in case a roll needs to be replaced.

Alternatively, if the foil is produced by evaporation, the substrate belt could have a textured surface on which the aluminium grows. This has been mentioned together with the ability to create wrinkles in the foil for local stress relief [119].

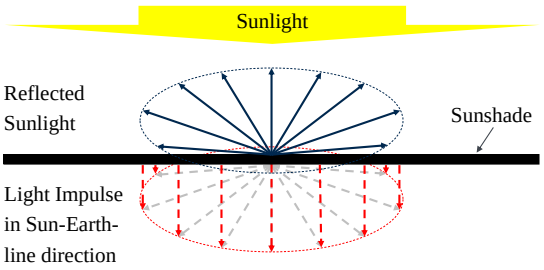

Figure 5.6: Light reflection and impulse pattern by a matte surface

It has been shown that even simple pyramid texturing on the surface of silicon could reduce the reflectivity by a factor of three [122, 127]. If the same is assumed for aluminium foil a perpendicular reflectivity of about 30% can be achieved instead of over 90%. The total impulse in sunlight direction would have to be determined by detailed hemispherical characterisation of the scattered light. It would also have to be considered that by texturing a surface in order to reduce the reflectivity, the emissivity of this surface increases [130]. As seen in equation 3.11 this influences the impulse budget and increases the optical factor κ. Consequently the position, area, and mass of the sunshade are affected.

Table 5.2 compares the foil production processes reviewed in this section. Despite the lower reflectivity, silicon foil can be excluded because of the high consumable requirements and the

	Si Spalling	Al TRC	Al Evaporation	Al Evaporation + Wax
Foil Thickness	-	-	+	+ +
Production Rate	- -	+ +	+	+
System Complexity	-	+	+	-
Power Requirement	-	+	+	-
Consumables Requirement	- - -	+	+	-
TRL	-	+	-	-

Table 5.2: Evaluation of technologies to manufacture thin metal foil

fact that aluminium foil with comparably effective reflectivity might be producible by optimised texturing. The aluminium foil production processes can best be evaluated by the thickness required for the sunshades. If ultra-low thickness is preferred, the complexity of evaporation with wax-assisted foil separation can be justified. If a thickness in the high nanometre until low micrometre range is needed, the separation of foil and substrate could be performed by simple peeling without the complexity of the handling of sublimated wax. If even higher thickness would suffice, foil rolling should be considered, since it combines low complexity with a high production rate.

5.3 Sunshade Structure

Any screen that shades the Sun will be very thin to lower the mass of the sunshade and therefore the production effort. Still a certain stiffness is required for the sunshade to maintain its shape and position in the solar wind environment between the Sun and the Earth. To allow for attitude control, actuation forces must be sustained. A support structure for the thin foil and for the integration of subsystems is needed. While for foil manufacturing very low thickness was crucial, this truss structure allows for more voluminous elements, but still as lightweight as possible.

The manufacturing of large structures in space opens the doors for new space activities including large antennae, solar power satellites, and large telescopes. NASA is funding companies to enhance systems that enable the production and assembly of space structures with different materials [131].

The SpiderFab process has been developed to enable rapid construction of very large lattice-like structures with high strength-per-mass [132]. The automated construction systems would combine techniques of Fused Deposition Modelling (FDM) with robotic assembly technologies to manufacture truss structures that enable large space systems with low mass, as shown in figure 5.7. Proof-of-concept level testing was performed to establish TRL-3 [132]. As part of further development NASA has granted Tethers Unlimited funds to develop the Trusselator, a system that will create carbon composite beams in orbit with a final goal of TRL-7 [133].

SPace Infrastructure DExterous Robot (SPIDER) is designed to enable robotic self-assembly of satellites in Earth orbit [134]. NASA has funded the development of a satellite mission to demonstrate this technology [135]. On board, the satellite OSAM-1 will assemble seven antenna elements to form a large communication array. The satellite will also manufacture a composite beam using the Trusselator technology.

With the Archinaut project, Made In Space developed a system that will 3D-print two beams of about 10 m, each that will then unfurl two solar arrays. In 2017, the printing equipment was demonstrated in a thermal vacuum test. 2018 followed the demonstration of the robotic arm to perform assembly in a simulated space environment. With the name OSAM-2 the system will be launched for in-space demonstration no earlier than 2022 [136]. Successful demonstration

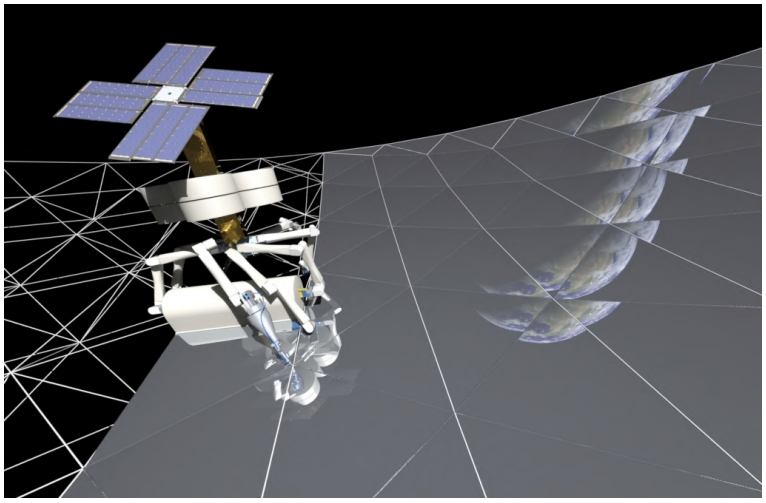

Figure 5.7: Illustration of a SpiderFab bot [132]

of the two On-orbit Servicing, Assembly, and Manufacturing (OSAM) missions will raise the capability to manufacture and assemble spacecraft components in space to TRL-7.

With Phoenix by DARPA and Orbital ATK's Mission Extension Vehicle (MEV) and Mission Robotic Vehicle (MRV) satellites, several other projects are or have been in development to provide commercial satellite servicing, upgrading or refurbishing.

With the large amount of funding and the integration of commercial partners it can be assumed that operations to robotically service, manufacture, and assemble satellite components will be performed frequently and will reach high maturity within the next few years.

The systems developed for demonstration of ISM use the AM process of fused deposition modelling (FDM). FDM operates by feeding a plastic filament feedstock through a heated nozzle where it melts before controlled deposition [137]. Chopped carbon fibres can be added to the feedstock to enable manufacturing of carbon composites, and recently manufacturing of continuous-fibre composites by FDM was developed [138]. The low melting temperatures of plastics and the high strength-to-mass ratio of carbon composite structures have driven several companies to adapt the relatively simple and cheap technology to the space environment. Microgravity printing has been performed frequently on the ISS and space vacuum printing will be proven by the by the OSAM satellites.

FDM does however not allow to directly print metal parts. Some processes have been developed that employ a polymeric binder for fused deposition of powdery metal [139, 140]. An additional sintering step removes the binder to create a pure metal part. With the aim to mainly use lunar resources and to minimise the material supply from the Earth, the technology of FDM is not suitable for sunshade manufacturing.

Several processes capable of additively manufacturing metal parts have been developed. On the Earth Selective Laser Melting (SLM) or Selective Laser Sintering (SLS) are established technologies. A layer of metal powder is deposited in a bed and selectively fused within the part geometry by a high energy laser [141]. After the melting/sintering step a new layer of powder is deposited and fused again. At the end, the loose powder is removed, and the fused metal part remains. A clear disadvantage of this process in a microgravity environment is the powder principle of SLS. In µg the powder cannot be efficiently controlled. Artificial gravity by rotation or powder control by electromagnetic fields could be explored, but the complexity of the manufacturing process would be increased significantly, which disqualifies the technology for ISM application [93].

Ultrasonic Additive Manufacturing (UAM) is a process that joins thin layers of metal foil with ultrasonic vibrations under pressure [142]. Solid-state welding enables operation at temperatures far below the melting point. This creates minimal residual stress in the fabricated parts, however, brings along the typical inter-laminar bonding challenges. The manufacturing of parts with complex geometries is possible. A great advantage of UAM is the ability to easily bond dissimilar materials [143]. This allows to manufacture hybrid structures and the integration of embedded electronics, such as microprocessors and sensors [142].

With its patented UAM process, the company Fabrisonic promises to manufacture parts at a rate of 97 to 194 $\frac{\text{cm}^3}{\text{hr}}$ [144]. The production-scale printing system operates at 9 kW.

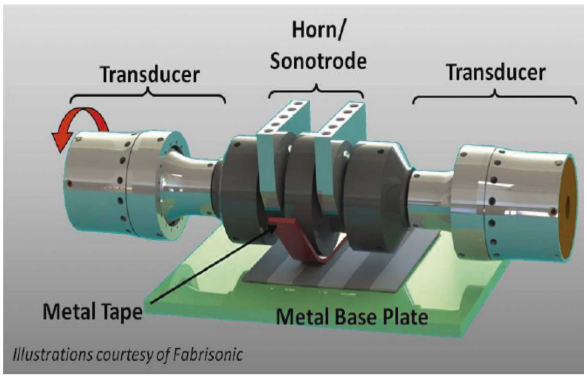

Figure 5.8: UAM welding machine [142]

Phase II funding within the SBIR programme was granted by NASA for increasing the efficiency and scaling of the UAM process for ISS demonstration as part of the Multi-Material Fabrication Laboratory (FabLab) development [93].

A metal deposition process similar to FDM was developed at NASA Langley Research Center. Electron-beam Free-form Fabrication (EBF3) uses metal wire as feedstock fed into a molten pool that is created by a focused electron beam in a vacuum environment [145]. It is a rapid deposition process and works well with any electrically conductive material. EBF3 enables manufacturing of defect-free products without inclusions of non-metallic material or pores [146]. Structures produced were reported to have mechanical properties comparable to handbook data for wrought plate products [145, 146]. Deposition rates of 300 – 2500 $\frac{\text{cm}^3}{\text{hr}}$ depending on the level of detail of the printed part have been demonstrated [145]. The power provided to melt the metal defines the possible deposition rate.

Feeding a 1 mm steel wire with a speed of 10 $\frac{mm}{s}$ required 700 W operational power [146]; feeding 1 mm aluminium wire at a speed of 100 $\frac{mm}{s}$ required 3 – 5 kW of power [147]. Image processing using Near-infrared (NIR) cameras and closed-loop control has been introduced to the process recently, improving the deposition accuracy to 0.2 mm [148, 149]. In a partnership with Lockheed Martin, EBF3 is used to manufacture titanium spars for vertical tails of the F-35 fighter resulting in less material waste and shorter machine times [150].

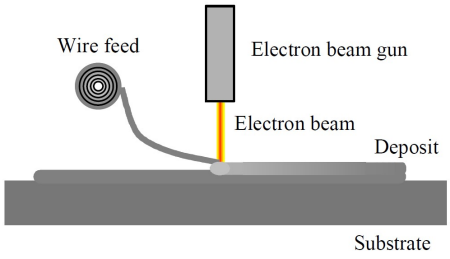

Figure 5.9: Schematic of the EBF3 process [145]

The requirement for a vacuum facilitates the adaptation of the EBF3 process to space. Parabolic flight tests were performed and concluded that microgravity has no effect on the deposition quality, if the wire feeder is close enough to the substrate [147]. This advances the maturity of EBF3 to TRL-5.

A study initiated by ESA identified technologies of AM that are most interesting for manufacturing of components on the Moon using in-situ resources. Solar sintering was selected for bulky infrastructure construction (habitat, landing pads, dust protection walls), FDM as a versatile manufacturing process with experience in the space environment, Stereo Lithography (SLA)-based ceramics manufacturing from lunar soil, and EBF3 for the production of large metal parts [151].

EBF3 and UAM are promising technologies for the manufacturing of metal structures in space. Due to the high deposition rate achievable and the lower power requirements, EBF3 is most suitable for large parts that require no high accuracy, while UAM may be applied when more detailed metallic parts are required, or for example when foil elements must be joined and attached to a support structure to create large sails.

Just as for the metal extraction processes, the technologies to manufacture metallic structures have high energy consumption. Mainly due to the high melting and dissolution temperatures of metals. The power system to supply these production processes in space or on the Moon will be of significant size. To reduce the mass that has to be launched from the Earth, it is interesting to know how large power generation systems could be manufactured with lunar resources.

5.4 Power Supply

Sunshade production facilities and the sunshade itself need to be supplied with electrical power. The conventional source of power in space is the Sun. Solar cells have been supplying satellites and space stations since the beginning of space flight. The Moon is rich in silicon [51]. This enables solar cell production with lunar resources. Nuclear energy sources promise high energy

densities to provide large amounts of energy in relatively small systems [40]. With thorium a suitable radioactive material is locally available [51]. The integration of nuclear systems may however cause problems regarding the public perception during political discussions. A system that aims to help saving the Earth's environment should not include systems that pose a risk for radioactively contaminating the space environment. Initially, the focus of power supply should be on photovoltaic systems. If solar power is declared infeasible, nuclear power sources may be considered.

Lunar Solar Cells

Silicon solar cells have been used intensively for space missions and on the Earth. Next generation multi-junction cells and advanced solar cell concepts promise higher efficiencies, but with recent developments to increase the efficiency of cells with crystalline silicon to over 25%, the global market share of silicon solar cells is about 90% [152].

Basic crystalline cells can be designed with a simple layer by layer concept: an insulating substrate as base layer, a p/n-junction in between two metallic conductive contacts, on the surface an Anti-reflection Coating (ARC) that increases the light trapping capability and therefore the efficiency, and protects the cell from the environment [153].

Within lunar exploration efforts, there have been studies on the feasibility of lunar material as well as in-space production processes that enable manufacturing of solar cells for sustainable lunar exploration [154, 155]. Despite the lower efficiency compared to crystalline silicon cells, amorphous silicon solar cells were preferred due to the lower mass of silicon required. The amount of hydrogen required for the hydrogenation step during amorphous silicon cell production (2 – 10 atm.%) was assumed to be low enough to allow Earth supply. For sunshade production this would certainly be different. In this case the use of lunar water ice could enable the manufacturing of ultra-thin amorphous silicon solar cells. However, with the likely large mass of aluminium extracted from the lunar soil for sunshade production, there might be enough silicon by-product available to manufacture crystalline silicon cells without the need for hydrogen. Analysis on the power requirements for sunshade production and the subsequent requirement for silicon material must confirm that assumption.

In 2000, a study supported within the NASA Innovative Advanced Concepts (NIAC) programme was performed with the goal to prove the concept and the economic viability of manufacturing solar cells on the Moon using local resources [156]. The ability to extract silicon material from lunar regolith, the design of the solar cell, a feasible production process, and cost/benefit ratios were assessed.

The cell design shown in figure 5.10 was proposed. It includes a glass substrate made from molten lunar regolith, a bottom electrode made from aluminium, the p-type silicon junction layer doped with native aluminium (20 – 50 ppm), the n-type junction layer doped with arsenic or phosphorus (100 – 200 ppm), an ARC made from titanium oxide which may as well be

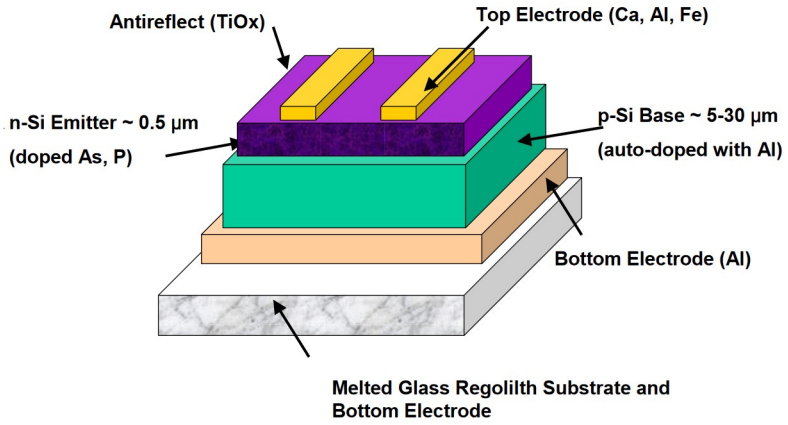

Figure 5.10: Lunar Silicon Solar Cell [157]

substituted or combined with aluminium oxide or silicon oxide, and top electrodes made from aluminium, iron, or calcium. Except the dopants for the n-Si emitter all materials would be readily available on the Moon. Experiments on the properties of silicon extracted from lunar simulant have been performed. The impurities resulting from the carbothermal reduction process suggested a solar cell efficiency of 6 – 9% [157]. As presented in chapter 4 the purity of metals extracted by methods of molten regolith electrolysis or molten salt electrolysis is expected to be higher, so an improvement in solar cell efficiency might be possible.

For the production of the presented lunar solar cells, a thermal evaporation process was proposed [156]. A lunar rover concept was created that, while driving, is able to collect regolith, extract the required materials, and evaporate the solar cells on the ground, continuously. This concept could be reversed into an extrusion-based manufacturing process. With the evaporation temperatures and the mass of different materials used they obtained the total energy required to produce lunar solar cells by thermal evaporation. Mass and volume of the evaporation equipment were also estimated. According to the study report, comparison with other solar cell production technologies showed that in terms of energy, volume and mass, evaporation of thin film solar cells exceeded all other production technologies by factors of 50 to 1000 [156]. It was mentioned that by adjusting the evaporation characteristics a crystal structure that is on the edge of the amorphous to microcrystalline phase transition could lower the required silicon junction thickness to 1 – 2 µm, thereby reduce material demand and production time [158].

Laboratory tests of components manufactured according to the proposed process have been performed as well [159]. Lunar regolith simulant has been melted to create the glassy substrate for the solar cells. With a thickness of 1 mm, it shows a resistivity of more than 10^4 Ωm, which are good properties for an insulating base layer.

Tested glass substrate was imprinted with a texture on one side. Reflectivity measurements showed 16% specular reflectivity for the smooth side and less than 1% for the textured side [159].

This can be explained by the oxidic nature of the regolith, just like usual ARCs. The regolith melt has been evaporated onto a substrate and very low thickness down to 500 Å was achieved [158]. This enables to use the molten raw regolith glass as simple ARC instead of extracting and applying pure silicon, aluminium, or titanium oxide.

Evaporated silicon junctions have been tested [159]. Diode behaviour was verified, however there was no measurable response to light. Challenges with doping the silicon correctly during evaporation have been pointed out. An optimised calibration of dopant co-evaporation is needed.

With the few laboratory examinations, lunar regolith derived solar cell components could be manufactured and examined. Diode behaviour of lunar simulant silicon junctions could be demonstrated. Since power generation through light interaction has not been demonstrated yet, the technology of lunar solar cells has not reached TRL-3, yet. As presented earlier, the maturity of the evaporation technology however is promising.

5.5 Electronic Components

A sunshade that is controlled actively requires an appropriate and reliable electric control system: communication hardware for telemetry and telecommand, computer hardware for data handling, as well as power control to operate sensors and actuators and to manage power generated by solar cells. This hardware must be manufactured and then integrated inside one or several sunshade control units.

The complexity of these systems presents a challenge for ISM with lunar resources. Carbon material would have to be supplied from the Earth and highly sophisticated manufacturing units implemented in space. The mass of the electronic control systems, even when integrated redundantly, is expected to be very small compared to the total sunshade mass. To ensure reliability of these components and fault-free sunshade operation, it is advisable therefore to rely on the high-quality manufacturing capabilities available on the Earth. Depending on the number of sunshades produced and the appropriate level of redundancy, several of these control units would have to be supplied from the Earth.

Wires and power lines to transfer sensor data, actuation commands or electric power over large distances on the other hand could be manufactured from lunar material. Aluminium and iron have very good electrical conductivity. Insulation could be made from lunar oxide material.

In this chapter technologies to manufacture key elements for a sunshade have been explored. Production of the foil that shades the solar light, structural components to support the foil, solar cells to power the sunshade as well as manufacturing and resource extraction facilities, and the manufacturing of electronic systems have been assessed. The next chapter will examine how the knowledge gathered in the previous chapters will influence the design of the sunshade and subsequently the requirements for the sunshade production infrastructure.

Chapter 6

Sunshade Concepts

Chapter 3 has defined shading requirements for sunshades. 0.52% of solar light reduction would reduce the global mean temperature by 1 K. Definitions for sunshade area, position, and mass were obtained with basic geometric derivations. The technology review in chapter 5 explored ways to manufacture these sunshades.

To give an impression on the scale of production necessary, a MATLAB® script has been created for the preliminary modelling of the sunshades, according to the derivations made in chapter 3. With the input of feasible shade design parameters derived from the technologies reviewed in the previous chapter, resulting sunshade area, position, mass, etc. can be determined. The sunshade concepts that have been created will be outlined now.

6.1 Minimum Mass Sunshade

In order to reduce the production requirements, concepts that enable minimal mass for the sunshades with a given shading requirement are favourable. The concept of shading the Sun with easily manufactured metal foil was proposed. From the abundant lunar metals aluminium and iron are the easiest to transform into foil. Iron has been excluded for its higher density compared to aluminium. Aluminium can be rolled into foil as thin as ∼7 µm. It is now assumed, that with technological adaptations to the space environment and the use of space resources a minimum thickness of 10 µm can be achieved. With micro-textured rolls the perpendicular reflectivity of thin aluminium foil might be as low as 30%. It is important to note that this is not the specular reflectivity, but the projection of every reflected light vector onto the Sun-Earth line integrated hemispherically. Thereby the impulse in Sun-Earth direction of widely scattered light is not neglected, and equation 3.11 which assumes a specular reflector is still applicable. The emissivity of aluminium at 100°C is ∼0.03 [160]. Examination of aluminium surfaces have shown a significant increase of the emissivity when the surface roughness is higher, i.e., textured [130]. Therefore, an emissivity of 0.3 is assumed for the textured front side of the sunshades while the

backside emissivity is 0.03. With perpendicular reflectivity, front side and backside emissivity, equation 3.11 delivers $\kappa = 0.84$. While this value is still very high it is one that is achieved with a simple roll process without further treatment. It allows the sunshade areal density to be as low as 37.1 $\frac{g}{m^2}$ to reach minimal total shade mass. With help of the MATLAB® script, it was determined that, to achieve this for the whole sunshade, the foil would need to have a thickness of ∼8.6 µm. As explained in chapter 3.2.2, very-low areal densities are only feasible with low κ. This is not the case for textured aluminium foil. Therefore the low foil thickness achieved with evaporation production technologies is not required. Employing evaporation for foil production might even reduce the production rate due to the long time required to grow such a relatively thick foil.

Technologies to produce a supporting structure for this foil made mainly from aluminium have been reviewed. Several large solar sail craft concepts have been developed [161, 162, 163, 164]. Minimisation of structural mass is essential for solar sail acceleration, hence very low-density structural concepts were developed. After comparing those studies an increment of the sail areal density through the sail structural mass of about 70% is a good orientation. The concepts developed however consider launching from the Earth. Earlier the many mass savings by in-space manufacturing and avoiding Earth launch have been discussed. Therefore, sunshades manufactured in space are expected to have even lower relative structural mass.

Kennedy, et al. [30] presented a more detailed distribution of the sunshade mass. For different sunshade areas they estimated the structural mass to support the sunshade sails to 37%, 40% and 51% of additional sail mass, where the largest area required the largest relative structural mass. To have a conservative estimation, 60% of additional mass for the support structure, electronic systems, as well as actuation and sensor systems will be assumed for the present example. With more knowledge of operational forces, control torques, and the sunshade configuration a generic structural optimisation model taking reliability and serviceability into account is needed to obtain precise values for the structural mass.

With the density of aluminium (2699 $\frac{kg}{m^3}$) the sunshade areal density including 10 µm foil and 60% additional mass results to 43.2 $\frac{g}{m^2}$ [1]. Shade density and optical factor κ can now be applied to the derivations of chapter 3 in the MATLAB® script. Resulting sunshades would be positioned at 2.199×10^9 m from the Earth, would have a cumulative area of 1,707,600 km^2 and a total mass of 73.74×10^6 t [2]. A complete list of sunshade parameters can be found in table 6.1.

With more knowledge on the manufacturing process parameters, it could be examined whether increased aluminium foil thickness is favourable due to reduced manufacturing effort during foil rolling. The mass to be extracted and transported however would increase.

The regolith would be excavated and processed on the Moon. The aluminium would then be

[1] The 60% additional structural mass is a rough estimation. If lower structural mass can be achieved, the areal density might be reduced to the 37.1 $\frac{g}{m^2}$ for minimal total sunshade mass

[2] It must be noted, that the mass for production systems and their corresponding power supply is not included

Structural Design		Optical Design	
Density aluminium	2699 $\frac{kg}{m^3}$	Reflectance front	0.3
Aluminium foil thickness	10 µm	Emissivity front	0.3
Foil areal density	27 $\frac{g}{m^2}$	Emissivity back	0.03
Additional structural mass	+60%	Optical factor κ	0.84
Areal density	43.2 $\frac{g}{m^2}$		
Sunshades Total Size			
Distance to the Earth	2.199×10^9 m		
Total area	1,707,600 km^2		
Total mass	73.74×10^6 t		
Solar light reduction	0.52%		

Table 6.1: Minimum mass sunshades properties

launched into space, where it is manufactured into sunshades. Strategies for the lunar launch are assessed in the parallel thesis [4]. Within logistical analyses it was also found there, that instead of manufacturing the shades in a lunar orbit and transferring them to SEL_1 making use of sail accelerations, it is more favourable to transfer the extracted material directly to SEL_1 and manufacture the sunshades there. It should be analysed whether it is favourable to produce the shading foil on the Moon, before launching it to the orbital manufacturing facilities. The circular shape of coilgun capsules, could be utilised perfectly by a roll of aluminium foil.

The sunshade mass would almost completely be aluminium, with small fractions of other materials within control systems and power supply components. If the sunshades were to be built in a period of 20 years this would mean that an aluminium mass of 422 $\frac{t}{h}$ would have to be extracted from lunar regolith, launched into space, and manufactured into thin foil sunshades. This is about ∼6% of the average terrestrial aluminium production in December 2020 [165]. The production effort and the power required to operate sunshade production at that rate would clearly be enormous. Setting up the production capability would require a significant effort as well. If all technologies were to be matured successfully, the ramp up of sunshade production capabilities is limited primarily by the amount of energy available. If production ramp-up and sunshade production were to be combined, this could save much time. An alternative concept that combines power generation and Sun shading can be outlined.

6.2 Photovoltaic Sunshade

Powering the production of sunshades at the necessary rate with solar cells requires large areas of solar arrays for regolith processing at the Moon and sunshade manufacturing in space. What also requires large areas of solar light interaction is shading the Earth to halt global warming.

The solar array area for powering sunshade production could directly be used as a sunshade. An initial area of solar arrays would have to be brought from the Earth to power the production of the first lunar photovoltaic cells. As soon as enough sunshade area is produced and enough additional power is available, a new production line can be put into operation. The production rate is doubled and exponential growth of production capability and simultaneously sunshade area is induced. Figure 6.1 shows a schematic of a possible bootstrapping process for the production of photovoltaic sunshades. With this strategy the gap between starting the production ramp-up and production of the first sunshade, i.e., the gap between money spent and effect created, can be closed. Sunshade production can be started immediately.

An additional challenge concerning this photovoltaic concept is to transfer the power generated by the sunshade to the ISM facilities and if efficient, to the ISRU plants on the Moon.

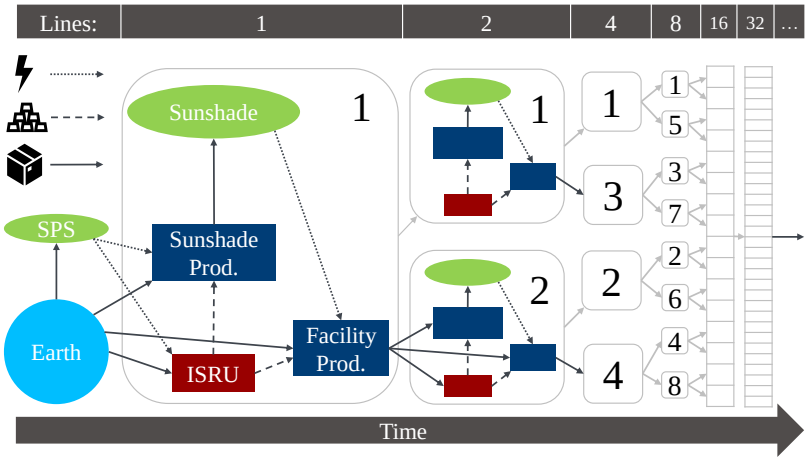

Figure 6.1: Schematic of a photovoltaic sunshade production bootstrapping process (Arrows for energy and resource transfer, and delivery of manufactured products)

Wireless Power Transmission in Space

Wireless Power Transmission (WPT) in space has been a field of research for several decades [166]. Applications for powering orbital manufacturing [167], electric thrusters [168], or laser beam propulsion [169], which utilise transmission of power through free space and sometimes the Earth's atmosphere were presented. Solar Power Satellites (SPS) that would provide renewable energy for terrestrial use have been considered more and more and concepts have been advanced [170, 171]. Especially the U.S., Japan, and China were investing in the development of SPS [172]. Just recently the British government has appointed an engineering consultancy to perform a thorough study to assess the technical and economic feasibility of SPS as major power supply for the UK [173]. ESA released a public call to gather and support new technologies and concepts to advance SPSs [174].

There are two principles of wireless power transmission: Microwave and laser transmission [175]. Microwaves are not largely affected by atmospheric clouds or fog but require large apertures to transmit and receive energy. Laser transfer on the other hand allows much more compact systems but is affected significantly by atmospheric disturbances.

In 2020, the U.S. Naval Research Laboratory (NRL) conducted a first test of SPS hardware in space [176]. A small module was designed to transform power collected by solar cells into a Radio Frequency (RF) microwave. The U.S. National Space Society (NSS) proposed a public/private partnership to further advance SPS technology and perform a high-level demonstration mission to reach TRL-7 [170]. This shall promote the technology and attract commercial energy providers to build first pilot plants. Currently, the SPS technology is at TRL-4/-5 [170]. With the many studies that are being performed and space agencies and governments involved in SPS development, the technology can be expected to be matured to at least TRL-7. This momentum will help the development of photovoltaic sunshades.

For a quick assessment of the application of WPT on photovoltaic sunshades it is important to know the mass and the efficiency of power conversion and transmission systems. McSpadden and Mankins have presented a review on microwave SPS developments and predictions for the future [166]. The technologies presented let assume, that a relative mass of 1.3 – 1.5 $\frac{\text{kg}}{\text{kW}}$ transmitted with efficiencies of 80% are possible. Additionally, this mass may be reduced, since systems manufactured for a sunshade would not have to survive Earth launch. The value of 1 $\frac{\text{kg}}{\text{kW}}$ that has been assumed by Kennedy, et al. [30] is thus reasonable.

For the manufacturing of photovoltaic sunshades solar cells and microwave/laser arrays have to be added to the previous example of a foil shade. A complete list of sunshade parameters can be found in table 6.2. Reduction of reflectivity is a natural goal during solar cell development. ARCs, texturing, and inter-crystalline scattering have been enhanced for the solar cells to absorb as much energy as possible. Investigations on textured oxidic surface coatings on solar cells have shown that, for crystalline silicon solar cells with a junction thickness of 300 µm to maximise light absorption, a reflectance of 10.5% can be achieved with a polished surface, and 3.5% with a textured surface [177]. The significantly lower thickness of the lunar solar cells proposed make very low reflectance infeasible. With random texturing and the typical microstructure resulting from evaporation combined with the very low reflectance observed for molten regolith substrates, 10% reflectance might be achieved. Measurements of standard solar cells were performed and an emittance of 0.52 was reported for silicon cells [178].

The 10 µm aluminium foil serves as base foil for the sunshades. It is assumed that 90% of the sunshade area can be covered with solar cells, while the other 10% may be needed for control surfaces, power lines, and others. The solar cell design with 9% efficiency presented in chapter 5 is then vacuum deposited on the front side. The regolith glass substrate may as well be fixed onto the base foil with ultrasonic additive manufacturing. The production rate is expected to be

lower due to the high power demand and low deposition rates of PVD, however the early delivery of shading area and exponential ramp-up of the production capability promises to counter that.

A cell areal density of 107 $\frac{g}{m^2}$ was obtained. Together with the aluminium base foil and structural support, this increases to 197.5 $\frac{g}{m^2}$. Adding the power transmission systems to the sail increases the sail mass and moves it closer to SEL_1. This reduces the sunshade area, hence the power generated by the solar cells, hence the power transmitted, hence the mass for the power transmission system. An iterative process was added to the MATLAB® script and the final position of the sunshades was estimated to 1.558×10^9 m from the Earth. The sunshades would have a cumulative area of 857,128 km^2 and a total mass of 286×10^6 t [3]. With an efficiency of 75% applied for internal power transfer and conversion, the sunshade would transmit 72,899 GW of microwave power. This would be a massive source of energy. Again, the total average energy consumption on the Earth is currently about 18 TW, so even with increased power demand, a photovoltaic sunshade would have a central role in powering a future carbon free world.

The thickness of the solar cells on the sunshade have been 20 µm in this report. The efficiency could be higher with more silicon junction thickness. More efficient solar cells would provide more energy but would on the other hand result in more system mass and production time. It could also be explored if it is more efficient to place fewer thick solar cells at certain locations on the sunshades instead of covering all the sunshade area with thin ones.

For the power transmission system, it remains to be seen if microwaves or laser transmission is the optimal way. A combination might be the optimum as well.

The mass of the photovoltaic sunshades would not only consist of aluminium as for the previous concept, but also large amounts of silicon and even bulk regolith for the solar cell substrate and coating. However, the regolith processing demand would not increase as much as the sunshade mass, since with aluminium foil sunshades, all the silicon and other elements would still be extracted from the regolith and be available for other purposes. Now a significantly higher fraction of the lunar regolith would be used for the photovoltaic sunshade. The rate of lunar launches and the in-space manufacturing demand however would increase. Due to the higher fraction of regolith used and the large amounts of energy available in the vicinity of SEL_1, rather than processing regolith on the Moon, it may be beneficial to launch the unprocessed regolith, transfer it to SEL_1, and process it with the sunshade energy. In case the regolith processing and material launch was powered by an independent lunar power supply, the size of this lunar power system might be reduced, despite higher launch rates. In case the regolith processing and material launch was powered by energy transmitted to the Moon from the SEL_1 sunshades, power losses due to the transmission over the large distance to the Moon might be reduced. This trade is a matter of energy efficiency that requires in-depth knowledge of technology performance. An appropriate scenario could also be the gradual relocation of regolith processing after a basic

[3] Unlike the total mass of the minimum mass sunshade, this value now includes most of the mass for power supply (solar cells, power transmission system)

processing capability was established during early lunar demonstration stages. The materials not used for the sunshades could be used as building material for production and service facilities and would therefore not be transported to SEL_1 in vain.

If the sunshades were to be built in a period of 20 years the proposed photovoltaic sunshade concept would require an average production rate of about 1636 $\frac{t}{h}$ of material extracted from the lunar regolith, launched, and manufactured into sunshades. Again, it must be mentioned, that the production rate is limited primarily by the amount of energy provided. Since the solar cell area is also used for shading the Sun, power generation can be increased excessively and energy availability should not be a problem. When no more, or less sunshade manufacturing is needed, the energy left over can be delivered to the Earth to help powering a sustainable economy. Even if the sunshades are not required to shade the Sun anymore, the same amount of energy could be generated and transmitted to the Earth from a higher parking orbit.

Position and mass of the sunshade concepts presented in this chapter are plotted in figures 6.2 and 6.3. Resulting total sunshade area and mass for the different amounts of shading presented in chapter 3 are outlined in table 1 in the appendix.

The two designs are based on very different strategic production principles. The sunshade concept with minimal mass requires a certain production capability to be produced in a timely manner. This requires setting up a corresponding production infrastructure that ensures the required production rate. The photovoltaic sunshade combines sun shading with bootstrapping of the production systems. By that, sunshades can be produced earlier, although with low production rate, initially. Photovoltaic sunshades would form a much heavier system that would have to be produced until the same deadline. Due to the higher system mass, the production rate for a certain sunshade area is expected to be lower, or on the other hand for the same production rate the mass for the production systems is expected to be higher. However, the continuous ramp-up of energy generation allows to implement a significant sunshade production rate that could potentially negate the disadvantage of increased system mass, while opening up opportunities further beyond the scope of preventing the global warming. In further studies it must be determined which production strategy is more efficient. Again, a system combining different sunshade concepts, or a gradual transition from one concept to another could optimise the total efficiency. This, and other strategic considerations will be assessed in the next chapter.

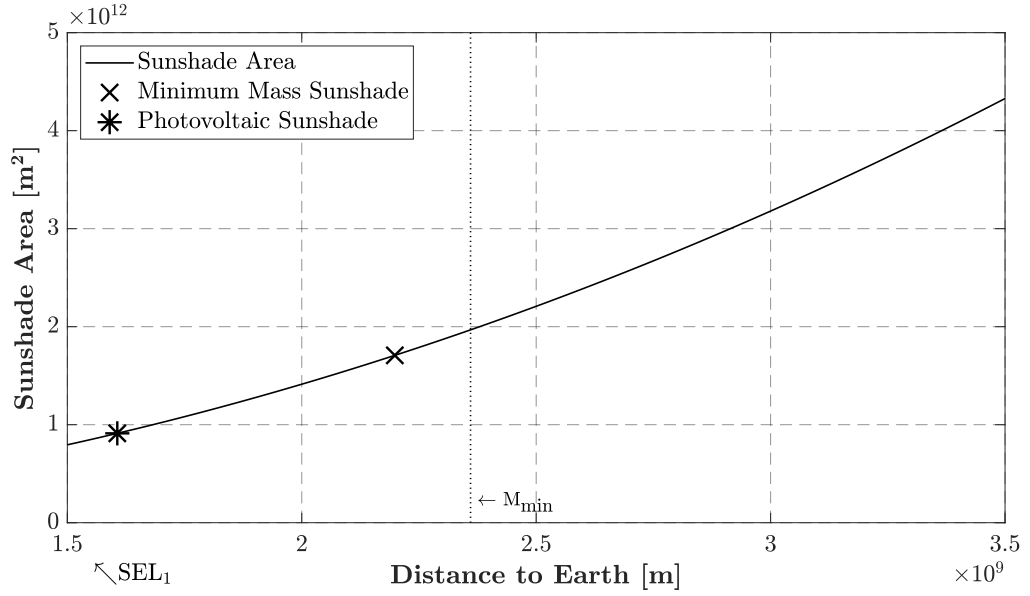

Figure 6.2: Position and area of both sunshade concepts for 0.52% solar light reduction

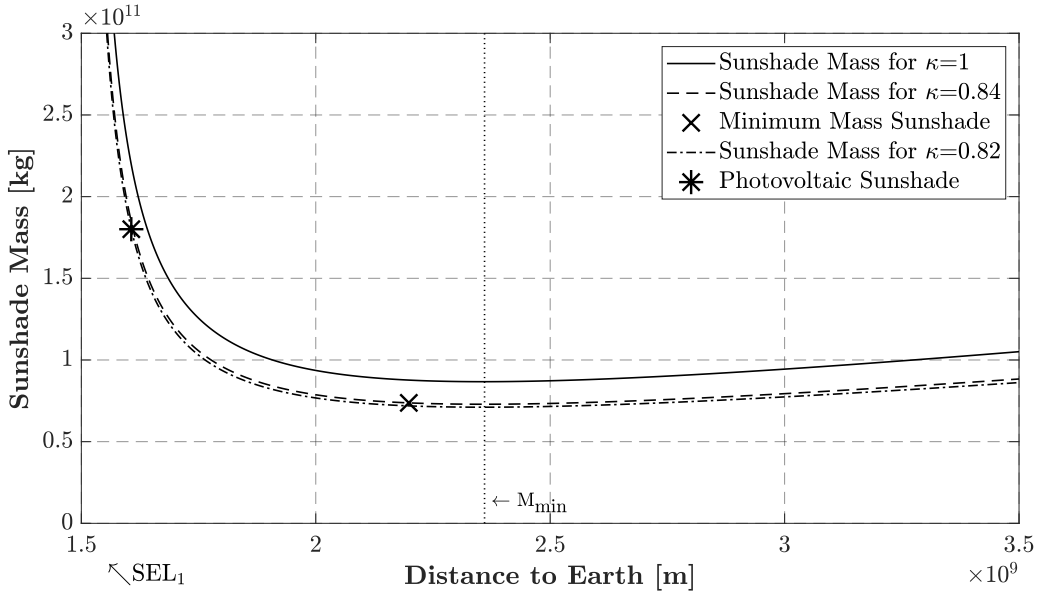

Figure 6.3: Position and mass of both sunshade concepts for 0.52% solar light reduction

Solar Cell Design			
Thickness substrate (Reg)	20 µm	Density aluminium	2699 $\frac{kg}{m^3}$
Thickness back contact (Al)	2 µm	Density silicon	2329 $\frac{kg}{m^3}$
Thickness silicon junction (Si)	20 µm	Density calcium	1550 $\frac{kg}{m^3}$
Thickness regolith ARC (Reg)	0.4 µm	Density fused regolith [156]	2700 $\frac{kg}{m^3}$
Thickness front contact (Ca)	0.5 µm		
Front contact coverage	10%	Reflectance front	0.1
Solar cell areal density	107 $\frac{g}{m^2}$	Emissivity front	0.52
Aluminium Base Foil			
Foil thickness	10 µm	Reflectance front	0.3
Foil areal density	27 $\frac{g}{m^2}$	Emissivity front	0.3
		Emissivity back	0.03
Aluminium Foil with Solar Cells			
Solar cell coverage	90%	Reflectance front	0.12
Areal density of photovoltaic foil	123.4 $\frac{g}{m^2}$	Emissivity front	0.50
Additional structural mass	+60%	Emissivity back	0.03
Areal density of photovoltaic sail	197.5 $\frac{g}{m^2}$	Optical factor κ	0.82
Power Transmission System			
Solar radiation flux	1400 $\frac{W}{m^2}$		
Solar cell efficiency	9%		
Power generated by solar cells	97,198 GW		
Internal efficiency	75%		
Power transmitted	72,899 GW		
Power transmission relative mass	1 $\frac{kg}{kW}$		
Power transmission system mass	72.899×10^6 t		
Additional structural mass	+60%		
Power trans. system mass final	116.6×10^6 t		
Sunshades Total Size			
Total areal density	334 $\frac{g}{m^2}$		
Distance to the Earth	1.558×10^9 m		
Total area	857,128 km^2		
Total mass	286×10^6 t		
Solar light reduction	0.52%		

Table 6.2: Photovoltaic sunshades properties

Chapter 7

Roadmap

While the sunshade concepts presented above are mainly qualitative and the numbers presented a result of preliminary trade-offs and assumptions, the most important technologies required for sunshade production have been reviewed. Promising technologies and trends for the near-term future without the inclusion of a sunshade production scenario were presented. A summary can be found in figure 2 in the appendix. With the state-of-the-art review of crucial technologies for a sunshade production, and the review on aspects of logistics and sunshade control performed in parallel [4], a roadmap was created that defines critical mission phases and a timetable for action. When creating this roadmap several strategic philosophies were central to find the most feasible way towards the sunshade implementation:

- **Spin-Ins**: Recognising current trends and finding opportunities to accelerate sunshade development
- **Efficiency**: Exploiting the environment and local resources in an optimal way
- **Spin-offs**: Making sunshade development interesting for as many parties as possible (public or private)
- **Knowledge**: Creating experience through extensive research, frequent demonstration, and continuous operation
- **Adaptation**: Starting with what is available while developing and integrating improved technologies

It is important to align with current development trends. Using the momentum of ongoing space exploration efforts will give the sunshade development a significant head start. Therefore, technologies have been reviewed and the most useful and advanced ones have been pointed out, to allow for fast demonstration. Following the international space exploration trend, the Moon should be integrated as testbed for the demonstration of Earth-independent sunshade production operations. An summarised overview of the possible spin-ins will be given in section 7.2.

To maximise the efficiency, locally available resources should be used for sunshade development and production. This includes construction material from the Moon and energy provided by the Sun, as well as technical and operational expertise provided by space agencies.

To accelerate sunshade development, spin-offs should be created that provide a use case and safety for investments even if large-scale sunshade production should not be started. Section 7.3 outlines the most notable spin-offs that would come along with sunshade development and operation.

Fast technology development requires quick feedback of operational behaviour. A trial-and-error approach for technology demonstration and sunshade operation will create profound experience that in turn will result in a reliable sunshade system. Already during the early stages of sunshade development, small simple sunshades should be manufactured on the Earth or with early lunar manufacturing capabilities and launched into space to create knowledge on solar sail operational behaviour in the SEL_1 environment. If further technologies are matured, the complexity of the small sunshades can be increased demonstrating the manufacturing capabilities and Earth-independence incrementally. The same should occur for the production systems. With frequent testing and demonstration, production technologies will mature and efficiencies can be improved quickly.

Development and construction of sunshades is a matter of decades. The expertise will grow, and technologies will improve. Therefore strategies, models, and designs must be constantly adapted and improved. Different approaches should be investigated and the sunshade architecture should provide sufficient flexibility for the adaptation of processes. This includes the application of different extraction and manufacturing techniques, at some point the potential availability of asteroidal resources, adaptation of logistical strategies, and as a consequence new sunshade designs that require flexible sunshade constellation configuration.

7.1 Mission Phases

In chapter 3.3, the Moon has been chosen as material source. The ability to utilise lunar resources must be developed, demonstrated, and matured to sufficient reliability. Considering the timeframe defined in chapter 3.4, several mission phases can now be defined. Table 7.1 gives a short overview of the phases describing the location of payload manufacturing, the schedule for each phase, and the respective objectives. A graphical representation of the proposed activities can be found in figure 3 of the appendix.

Phase 1 At the beginning, the momentum of lunar exploration will be used for technology development. Many systems within resource utilisation, in-space manufacturing, and logistics that are already in development might be incorporated. Some technologies might need to be added to the portfolio, and the focus within several fields might need to shift towards systems

	Phase	P/L Manuf.	Time	Objectives
1	Technology Development	Earth	2021 – 2040	Development of mission critical technologies, manufacturing on the Earth
2	Technology Demonstration	Moon	2035 – 2045	Demonstration of the production capabilities using lunar resources
3	Sunshade Production	SEL_1	2045 – 2070	Demonstration of large-scale sunshade production, continuous shade production
4	Sunshade Operation	SEL_1	**2060** – 20xx	Shade operation, climate monitoring, optimisation of climate effect

Table 7.1: Mission phases for sunshade development

that allow for significant scaling. Demonstration systems for resource utilisation, shade manufacturing, launchers, and preliminary small-scale sunshade demonstrators would be manufactured on the Earth and then be transported to their respective demonstration environment, following the standard procedures of technology maturation.

Phase 2 The second phase should concentrate on shifting the production of small-scale demonstration shades towards the Moon. When resource extraction capabilities are matured, the manufacturing of shade components using lunar in-situ resources will be demonstrated with the final goal of a fully integrated, independent small-scale sunshade production line including resource extraction, launch capabilities, component manufacturing, assembly, and power supply on and around the Moon.

Phase 3 After the in-space production capabilities are demonstrated, a crucial political decision would have to decide to kick off phase 3. Within the third phase of sunshade development the production would now be scaled up and shifted towards SEL_1. A full-size manufacturing line would need to be implemented at the Lagrange Point. The dependency on Earth materials should be minimised by manufacturing the bulk components of the facility from lunar metal. Therefore, there would have to be a significant extraction ramp-up for the resource extraction systems on the Moon. A first large-scale sunshade would be manufactured and demonstrated after the production line is operational. Following the operational demonstration of the large-scale sail, or if need be directly after the production of it, further shades could be manufactured or in parallel new production lines could be set up.

Phase 4 The fleet of large shades would then form a flexible constellation in the vicinity of SEL_1 which can be actively controlled delivering the optimal climate feedback until the Earth is self-sustainable again.

7.2 Early Spin-In Possibilities

The first stage of sunshade development focuses on maturing technologies by manufacturing on the Earth. The ability to extract pure metals from lunar soil, manufacture sunshade components in space, operate, and control the sunshades, as well as the capabilities to launch and transport materials or systems must be demonstrated. While some technology developments are already in place, others will need increased attention. The general goal should be TRL-6/-7 for all sunshade system technologies.

Light-weight sunshade designs capable of controlled operation at SEL_1 must be developed. Strategies for SEL_1 sail constellation control, swarm dynamics and debris management must be created. Experience gained from flown or conceptually developed solar sail missions can be integrated. First small demonstration sails can be manufactured on the Earth and launched to space to demonstrate sunshade stabilisation, AOCS, operations and control from the Earth. When several small sails are launched, constellation operation can be optimised.

The ongoing technology developments in the space sector can be taken advantage of. ESA has declared its goal to demonstrate molten salt electrolysis on the Moon. Currently, they also are constructing a large lunar analogue facility with 1000 m^2 of simulated lunar soil [179]. This could serve as a useful testbed for ISRU operations before demonstration on the Moon.

The two OSAM satellites to be launched over the course of the next few years, will demonstrate robotic manufacturing and assembly of satellite parts in space. Additionally, concepts developed for construction of large structures in space such as the SpiderFab process could be built on. EBF3 has already been demonstrated in a space environment and process parameters are being optimised. High-quality UAM parts for aerospace applications are commercially available. ISM systems have not yet been realised. A new PVD system will also be demonstrated on OSAM-1. Following the trend with developments of Solar Power Satellite technologies, power conversion and transmission of small photovoltaic demonstration sunshades can be demonstrated over short distances.

Yet, challenges will be posed by the development of lunar photovoltaics and metal foil production in space. Currently, there are no development goals formulated for both sunshade technologies; they currently are the ones with the lowest TRL. The development of lunar solar cells must be picked up. Since they are crucial to power a lunar sunshade production industry, it is essential to solve the remaining manufacturing problems and prove light energy conversion. The terrestrial process of aluminium foil production must be adapted to the space environment. The long-time experience of the aluminium foil industry should be integrated.

For the second phase, it may be beneficial to set up a technology demonstration hub on the Moon in cooperation with international partners, that will provide the opportunity to demonstrate technologies for space exploration, commercial lunar activities, and sustainable space operations. Sunshade development could be the neighbour of crewed lunar habitation opera-

tions, scientific exploration, and commercial mining demonstrations. For that, easy access and sufficient energy supply is required. More advanced regolith reduction processes may early be implemented on the Moon. A lunar propellant infrastructure that makes the lunar surface accessible for scientific and demonstration operations should be created. A collaborative study including members of American industry, government, and academic experts has been performed to lay out a commercial lunar propellant architecture [71]. The technical and economical analysis presented there should serve as guideline for laying the groundwork for further lunar operations in an economically self-sustaining way. Initial energy for surface operations may be provided by photovoltaic systems launched from the Earth. Recent advancements of perovskite solar cells are interesting, since they are highly efficient, lightweight and printable [180]. Just recently a new record in light conversion efficiency by a single cell has been set with a perovskite solar cell [181]. The common perovskite material however is not part of the bulk lunar regolith. Still, a material feedstock could be brought from the Earth and set up an on-demand fabrication capability to extend the power generation volume for initial technology demonstration operations flexibly before the Earth-independence is increased by producing lunar silicon solar cells.

These plans largely align with goals defined by space exploration initiatives such as the ISECG or the Moon Village Association, which aim to coordinate sustainable exploitation of the lunar environment for development of sustainable space operations [56, 182]. Cooperation with these initiatives might facilitate lunar surface demonstrations during phase 2 of sunshade development.

Utilising the trends in space exploration and the paradigm shift towards in-space manufacturing will help to accelerate sunshade development. Figure 2 outlines this with the high TRL or the near-term goals defined for the most important sunshade production technologies and gives an impression of the required development effort to reach the goals of phase 1 & 2 within time. It can be seen, that in many ways sunshade development is in accord with efforts and investments already made. In principle, it would just represent a new use case for the many efforts made and would shift further investments to a new goal, of which previous programmes will only profit. This enables timely demonstration of specifically adjusted sunshade production technologies.

7.3 Spin-off Potentials

To make sunshade development attractive for investments it is important to enable second uses for the technologies developed. This creates security for investors. At any time, the money spent should not be lost in case sunshade activities are terminated and should be paid off as early as possible.

The ability to efficiently manufacture solar cells in space by PVD with only a feedstock of material would reduce the cost for space-based solar power and could enable serious competition

to power generation on the Earth. In the same sense, the development and demonstration of wireless power transmission technology could be a catalyst for the implementation of solar power satellites. First small demonstration sunshades equipped with WPT technology could provide power for lunar surface operations, such as polar crater exploration.

The technologies to manufacture and assemble large metal structures in orbit would increase the flexibility of in-space manufactured spacecraft. While currently mainly carbon composite structures are emphasised, this would provide robust and reliable alternatives. As a first case of mega-structure production in space, other large-scale concepts could profit from the experiences of sunshade construction. Large space telescopes, SPSs, or solar sails for interstellar travel could be produced by repurposed facilities initially planned or used for sunshade manufacturing. Metal structure and thin reflective aluminium foil products would be highly useful for that.

The ability to extract large masses of lunar metals and launch them into space would reduce the cost of ISM activities even further. Mature ISRU technologies would also provide the capability for human exploration missions to generate important oxygen stock and high-quality building materials. The technologies might even be adapted to the environment of Mars. Increased lunar surface activities and transportation capabilities would create an infrastructure that enables simple integration of new scientific or commercial activities on the Moon and support for exploration missions further into the solar system. Figure 4 in the appendix gives an overview of spin-in opportunities and spin-off potential for the early development phase.

An operating sunshade could provide a wide range of thermal environments in the vicinity of SEL_1. Constant solar radiation could be replaced by ultra-low temperatures in the shadow of a sunshade. When equipped with solar cells, the temperature range from ultra-low to very-high could be artificially created with electrical power provided by the sunshade. This opens opportunities for thermally demanding space operations. In case the sunshade is built and operated with lunar solar cells, the energy provided by sunshade photovoltaics could potentially help powering a carbon-free economy on the Earth and supply various types of space operations at SEL_1 or around the Earth with electrical power. Additionally, after the sunshade production is completed, a functioning manufacturing infrastructure and supply chain for raw materials would be left over. Powered with the vast amount of sunshade energy, this could provide shipyard production services and serve as a gateway for future endeavours of exploration and habitation of the solar system. Even after the shading operations are finished, these secondary uses could still be provided, or even extended.

7.4 Coordination and Governance

Initial coordination of international research and development for a sunshade should be guided by a framework association similar to the Moon Village Association which aims to create international cooperation of public and private entities, enabling sustainable lunar exploration. The

sunshade initiative should support and coordinate development efforts while providing a potential use case for technologies in development. A framework concept especially for space-based sun shading has been proposed [183].

Shading the Earth with a sunshade would affect not only a few space fairing nations, but the whole planet. Therefore, a critical number of countries and companies/organisations must agree to an international governance, at some point. A treaty organisation similar to NATO into which the major emitting nations are paying, could address issues of governance and funding to reach a global strategy. National entities may drive forward the development of different technologies and concepts within a scientific initiative, but eventually an international strategy must converge, combining efforts and expertise. This would form an International Planetary Sunshade (IPSS) system, similar to the development and operation of the ISS.

The presented roadmap serves as first orientation of how future development efforts should be addressed. It must not be seen as a fixed project plan, but as an architecture from which an optimised sunshade system evolves while aligning with international development trends.

Chapter 8

Conclusions

The aim of this thesis was to assess the technical feasibility of a sunshade in the vicinity of SEL_1. Several space-based sunshade concepts have been reviewed and discussed, pointing out differences in terms of overall mass, research, development and production effort, and the effect on the Earth's climate. A sail sunshade close to SEL_1 has been confirmed as the concept with the best climate effect which should make implementation more feasible. The technological challenges have been addressed afterwards.

The requirements for a sunshade at the Lagrange Point L1 have been defined. A target of 0.52% of solar light reduction has been defined in order to limit the global warming to an extent that would make the Paris Agreement goals feasible again. Geometrical sizing and the influence of the solar radiation pressure on position, area, and mass of such a sunshade have been presented. With the scale of space-based sun shading in mind, the source of manufacturing materials has been discussed. Material supply from the Earth would pollute the atmosphere significantly. Despite the larger gravity well, the Moon was chosen rather than asteroids. It enables the use of lightweight materials, silicon for solar cells, and water for generation of propellant. Due to the international trend towards lunar exploration, the Moon should also serve as testbed for sunshade production technology demonstration. The close proximity to the Earth allows for fast feedback.

As a reasonable timeframe for the sunshade development and production, 2060 was defined as goal for the operation of a first large sunshade. Elements that must be involved in sunshade development, production, and operation were identified. These include the sunshade itself, manufacturing systems, resource supply, logistics, power supply, servicing systems and mission control overseen by an international governance.

To assess the feasibility of the timeframe, the technologies required within the system elements for sunshade production were reviewed. The state-of-the-art of in-situ resource utilisation technologies, in-space manufacturing technologies, lunar solar cells, and wireless power transmission was examined. With the most promising technologies, two examples of sunshades producible

in space using lunar resources were presented with rough quantification, serving as orientation on the scale of SEL_1 sunshades. The first is an assembly of very lightweight sails primarily consisting of thin textured aluminium foil attached to a mass-optimised aluminium structure. To block 0.52% of the solar light the sunshades would have a total area of $\sim 1.7 \times 10^9$ km^2 and a total mass of $\sim 74 \times 10^9$ t. The second design combines shading the Sun with the generation of solar power. Lunar solar cells attached to most of the sunshade sail surface would generate enough power to supply the ramp-up of production capabilities exponentially. Even with low-efficiency thin-film photovoltaics power in the order of ~70 TW could be generated. Such sunshades would be about four times heavier and therefore located closer to the Earth. The total sunshade area would need to be ~857,000 km^2 to block 0.52% of solar light.

The results of the technology review also allowed to define a roadmap strategy comprising four specific mission phases. Within the first phase all sunshade related technologies should be developed on the Earth and demonstrated in space. The goal of the second phase is to demonstrate the end-to-end small-scale sunshade production using lunar resources. Within phase 3 the sunshade production should be ramped up, shifted towards SEL_1, and full-scale sunshades should be produced. During the fourth phase the sunshades are operated, providing solar light reduction for the Earth, and potentially also electric power.

Several spin-in possibilities and spin-off potentials for sunshade technologies could be identified. The paradigm shift towards in-space manufacturing might facilitate sunshade development. The same accounts for the international efforts for sustainable lunar exploration as well as the interest in green energy production concepts for the Earth of which space-based solar power receives increased attention. Few technological challenges have been pointed out. The production of solar cells and thin aluminium foil from lunar material will have to be addressed intensively to prevent them from becoming a showstopper. Phase 1 of the sunshade development must start now. Due to the many spin-in possibilities, the early sunshade development effort is smaller than would be expected, but must be pursued near-term for the timeframe for technology demonstration to remain feasible. Computer models for sunshade production and operation should be set up and improved continuously with the results of constant technology maturation. A sound quantification of sunshade production models requires a sound quantification of process parameters.

Chapter 9

Outlook

The state-of-the-art-review performed presents a baseline for further sunshade investigations. A quantification of the presented systems must be achieved to improve the viability of the roadmap that has been outlined. The sunshade design concepts serve as a technically feasible orientation that requires significant optimisation. A dynamic system model combining all aspects of sunshade production; logistics, lunar ISRU activities, ISM processes, a detailed sunshade model, and models to predict the climate feedback should be implemented to allow for early quantification and optimisation, to make sophisticated predictions. This system model would be able to assess the large trade space and the various interconnections to create optimised sunshade production processes. The creation of the system model should comply to the same philosophies as the roadmap: Spin in technologies, gather knowledge on how to employ them, and adapt the system to maximise spin-off capabilities and efficiency.

The accuracy of the computer models depends on the knowledge of the technologies employed and the environment exploited. The technology developments recommended with the roadmap should deliver more and more precise data on certain process parameters.

The TRL review has shown that several technologies require increased attention. The production of aluminium foil in space and the ability to manufacture solar cells from lunar material pose the greatest challenges for successful sunshade production. Aluminium foil production has been a standard on the Earth for several decades. An ISM process with minimal use of consumables must be developed. Manufacturing the heavy rolls on or around the Moon with lunar resources should be examined. In parallel, evaporation technologies to produce thin aluminium foil should be investigated as an option in case, rolling can not be adapted to space. The effect of surface roughness or texturing should be investigated then. Hemispherical reflection and emission characterisation must be performed to improve the sunshade simulation models. The ability to convert photon energy into electrical power by PVD produced silicon solar cells must be proven. Remaining doping challenges must be solved.

In order to advance the production capabilities to the use of space resources during phase 2,

a critical milestone is the ability to provide pure lunar metals by ISRU. Regolith extraction must be advanced to highest purity, to allow for thin foil production. Besides molten salt electrolysis, molten regolith electrolysis should be added to the portfolio as an alternate metal extraction process due to its higher production rates.

The knowledge on the lunar geology depends on few samples and remote sensing data. Further sample returns or continuous robotic surface characterisation to expand the database would help maximising the efficiency of processes in development. Especially data on the lunar poles is interesting since they present favourable locations for early lunar surface operations.

An early sunshade manufacturing demonstration satellite could be developed. OSAM-3 (US mission) or OSAM-E (European mission) could succeed the first two ISM demonstration satellites by demonstrating the ability to print different parts from aluminium feedstock with EBF3, assemble a small structure, weld aluminium foil onto the structure with UAM, and coat it with different materials by PVD. If the technologies are developed far enough, it could also include a foil production step, as well as the vacuum deposition of a fully functioning solar cell. An EBF3 printer for space could also be used on the ISS where currently only polymer, ceramic and first bioprinting printing capabilities are available.

In parallel a lunar surface mission, to demonstrate new scalable regolith excavation and beneficiation technology, could be conducted within the next few years. Preliminary demonstration of the equipment could be performed in ESA's Luna facility, the lunar landing could be performed with ESA's European Large Logistics Lander (EL3) lander. This could be achieved in combination with further ISRU demonstrations.

Bibliography

[1] W. Seifritz. Mirrors to halt global warming? *Nature*, 340(6235):603, 1989.

[2] United Nations Environment Programme (UNEP). *Emissions Gap Report 2020*. Nairobi.

[3] D. Keith, O. Morton, Y. Shyur, et al. Reflections on a Meeting about Space-based Solar Geoengineering; <https://geoengineering.environment.harvard.edu/blog/reflections-meeting-about-space-based-solar-geoengineering> [accessed: 23.12.2020].

[4] T. Maheswaran. *Analysis of logistical construction aspects of a sunshade concept in the vicinity of the Sun Earth L1 Lagrange Point (IRS-21-S-017)*. Master Thesis, University of Stuttgart, 2021.

[5] Intergovernmental Panel on Climate Change (IPCC). *Climate change 2014: Synthesis Report: Contribution of Working Groups I, II and III to the Fifth Assessment Report of the Intergovernmental Panel on Climate Change*. [Core Writing Team, R.K. Pachauri and LA Meyer (eds.)] IPCC, Geneva, Switzerland, 2014.

[6] United Nations Office for Disaster Risk Reduction (UNDRR). *Human Cost of Disasters 2000-2019*. 2020.

[7] World Meteorological Organization (WMO). *Provisional Report on the State of the Global Climate 2020*. Geneva, Switzerland, 2021.

[8] C. A. Horowitz. Paris Agreement. *International Legal Materials*, 55(4):740–755, 2016.

[9] K. Caldeira, B. Govindasamy, and L. Cao. The Science of Geoengineering. *Annual Review of Earth and Planetary Sciences*, 41(1):231–256, 2013.

[10] I. Dicaire. Climate Engineering: Which Role for Space? *Proceedings of the 64th International Astronautical Congress 2013*, pages 9233–9241, IAC-13,D4,4,5,x20121, 2013.

[11] A. Ridgwell, J. S. Singarayer, A. M. Hetherington, and P. J. Valdes. Tackling regional climate change by leaf albedo bio-geoengineering. *Current biology : CB*, 19(2):146–150, 2009.

[12] C. E. Doughty, C. B. Field, and A. M. S. McMillan. Can crop albedo be increased through the modification of leaf trichomes, and could this cool regional climate? *Climatic Change*, 104(2):379–387, 2011.

[13] H. Akbari, S. Menon, and A. Rosenfeld. Global cooling: Increasing world-wide urban albedos to offset CO2. *Climatic Change*, 94(3-4):275–286, 2009.

[14] S. Menon, H. Akbari, S. Mahanama, et al. Radiative forcing and temperature response to changes in urban albedos and associated CO 2 offsets. *Environmental Research Letters*, 5(1):014005, 2010.

[15] R. Seitz. Bright water: Hydrosols, water conservation and climate change. *Climatic Change*, 105(3-4):365–381, 2011.

[16] J. Latham, P. Rasch, C. Chen, et al. Global temperature stabilization via controlled albedo enhancement of low-level maritime clouds. *Philosophical transactions. Series A, Mathematical, physical, and engineering sciences*, 366(1882):3969–3987, 2008.

[17] P. J. Rasch, J. Latham, and C. Chen. Geoengineering by cloud seeding: Influence on sea ice and climate system. *Environmental Research Letters*, 4(4):045112, 2009.

[18] P. J. Rasch, S. Tilmes, R. P. Turco, et al. An overview of geoengineering of climate using stratospheric sulphate aerosols. *Philosophical transactions. Series A, Mathematical, physical, and engineering sciences*, 366(1882):4007–4037, 2008.

[19] A. Robock, A. Marquardt, B. Kravitz, and G. Stenchikov. Benefits, risks, and costs of stratospheric geoengineering. *Geophysical Research Letters*, 36(19):1369, 2009.

[20] T. M. Lenton and N. E. Vaughan. The radiative forcing potential of different climate geoengineering options. *Atmospheric Chemistry and Physics*, 9(15):5539–5561, 2009.

[21] P. J. Irvine, A. Ridgwell, and D. J. Lunt. Climatic effects of surface albedo geoengineering. *Journal of Geophysical Research: Planets*, 116(D24):n/a–n/a, 2011.

[22] L. Burns, D. Keith, P. Irvine, J. Horton, and B. . Ed. Belei. Technology Factsheet Series: Solar Geoengineering, Paper. *Belfer Center for Science and International Affairs*, Harvard Kennedy School, June 2019.

[23] Z. Dai, D. K. Weisenstein, and D. W. Keith. Tailoring Meridional and Seasonal Radiative Forcing by Sulfate Aerosol Solar Geoengineering. *Geophysical Research Letters*, 45(2):1030–1039, 2018.

[24] J. Shepherd. *Geoengineering the climate: Science, governance and uncertainty*, volume 10, 2009 of *Excellence in science*. The Royal Society, London, 2009.

[25] J. P. Sánchez and C. R. McInnes. Optimal Sunshade Configurations for Space-Based Geoengineering near the Sun-Earth L1 Point. *PloS one*, 10(8):e0136648, 2015.

[26] J. T. Early. Space-based solar shield to offset greenhouse effect. *Journal of The British Interplanetary Society*, 42:567–569, 1989.

[27] C. R. McInnes. Minimum Mass Solar Shield for Terrestrial Climate Control. *Journal of The British Interplanetary Society*, 55:307–311, 2002.

[28] C. R. McInnes. Space-based geoengineering: Challenges and requirements. *Proceedings of the Institution of Mechanical Engineers, Part C: Journal of Mechanical Engineering Science*, 224(3):571–580, 2009.

[29] R. Angel. Feasibility of cooling the Earth with a cloud of small spacecraft near the inner Lagrange point (L1). *Proceedings of the National Academy of Sciences of the United States of America*, 103(46):17184–17189, 2006.

[30] R. G. Kennedy, K. I. Roy, and D. E. Fields. Dyson Dots: Changing the solar constant to a variable with photovoltaic lightsails. *Acta Astronautica*, 82(2):225–237, 2013.

[31] Our World in Data. Primary energy consumption <https://ourworldindata.org/explorers/energy?tab=chart&xScale=linear&yScale=linear&stackMode=absolute&endpointsOnly=0&time=earliest..latest&country=United%20States~United%20Kingdom~China~World~India~Brazil~South%20Africa&region=World&Total%20or%20Breakdown%20=Total&Select%20a%20source%20=Low-carbon&Energy%20or%20Electricity%20=Primary%20energy&Metric%20=Annual%20consumption> [acessed: 27 January 2021], 2021.

[32] R. Bewick, J. P. Sanchez, and C. R. McInnes. The feasibility of using an L1 positioned dust cloud as a method of space-based geoengineering. *Advances in Space Research*, 49(7):1212–1228, 2012.

[33] R. Bewick, J. P. Sanchez, and C. R. McInnes. Gravitationally bound geoengineering dust shade at the inner Lagrange point. *Advances in Space Research*, 50(10):1405–1410, 2012.

[34] C. Struck. The Feasibility of Shading the Greenhouse with Dust Clouds at the Stable Lunar Lagrange Points. *Journal of The British Interplanetary Society*, 60, 2007.

[35] R. Bewick, C. Lücking, C. Colombo, et al. Heliotropic dust rings for Earth climate engineering. *Advances in Space Research*, 51(7):1132–1144, 2013.

[36] M. Mautner. A Space-Based Solar Screen Against Climatic Warming. *Journal of The British Interplanetary Society*, 44:135–148, 1991.

[37] J. Pearson, J. Oldson, and E. Levin. Earth rings for planetary environment control. *Acta Astronautica*, 58(1):44–57, 2006.

[38] D. J. Lunt, A. Ridgwell, P. J. Valdes, and A. Seale. Sunshade World: A fully coupled GCM evaluation of the climatic impacts of geoengineering. *Geophysical Research Letters*, 35(12), 2008.

[39] D. G. MacMartin, D. W. Keith, B. Kravitz, and K. Caldeira. Management of trade-offs in geoengineering through optimal choice of non-uniform radiative forcing. *Nature Climate Change*, 3(4):365–368, 2013.

[40] E. Messerschmid and S. Fasoulas. *Raumfahrtsysteme*. Springer Berlin Heidelberg, Berlin, Heidelberg, 2017.

[41] B. Govindasamy and K. Caldeira. Geoengineering Earth's radiation balance to mitigate CO2 -induced climate change. *Geophysical Research Letters*, 27(14):2141–2144, 2000.

[42] National Oceanic and Atmospheric Administration (NOAA). Climate Change: Atmospheric Carbon Dioxide; <https://www.climate.gov/news-features/understanding-climate/climate-change-atmospheric-carbon-dioxide> [accessed: 10.11.2020], 2020.

[43] S. C. Sherwood, M. J. Webb, J. D. Annan, et al. An Assessment of Earth's Climate Sensitivity Using Multiple Lines of Evidence. *Reviews of geophysics (Washington, D.C. : 1985)*, 58(4):e2019RG000678, 2020.

[44] National Aeronautics and Space Administration (NASA). SLS Fact Sheets; <https://www.nasa.gov/exploration/systems/sls/factsheets.html> [accessed: 07. January 2021].

[45] A. Zak. Everything You Need To Know About Russia's Super Heavy Rocket <https://www.popularmechanics.com/space/rockets/a30705512/yenisei-rocket-russia/> [accessed: 07. January 2021].

[46] SpaceX. Starship; <https://www.spacex.com/vehicles/starship/> [accessed: 07. January 2021].

[47] H. S. Hudson. A space parasol as a countermeasure against the greenhouse effect. *Journal of The British Interplanetary Society*, 44:139–141, 1991.

[48] R. Bewick, J. P. Sánchez, and C. R. McInnes. Usage of Asteroid resources for Space-Based Geoengineering. In V. Badescu, editor, *Asteroids*, pages 581–603. Springer, Heidelberg and New York, 2013.

[49] J. P. Sánchez and C. McInnes. Asteroid Resource Map for Near-Earth Space. *Journal of Spacecraft and Rockets*, 48(1):153–165, 2011.

[50] D. S. McKay, G. Heiken, A. Basu, et al. The Lunar Regolith. In Heiken, G.H., Vaniman, D., French, B.M., editor, *The Lunar Source Book*. Cambridge University Press, 1991.

[51] I. A. Crawford. Lunar resources. *Progress in Physical Geography: Earth and Environment*, 39(2):137–167, 2015.

[52] L. A. Haskin and P. Warren. Lunar Chemistry. In Heiken, G.H., Vaniman, D., French, B.M., editor, *The Lunar Source Book*, pages 357–474. Cambridge University Press, 1991.

[53] S. Li, P. G. Lucey, R. E. Milliken, et al. Direct evidence of surface exposed water ice in the lunar polar regions. *Proceedings of the National Academy of Sciences of the United States of America*, 115(36):8907–8912, 2018.

[54] L. A. Haskin. Toward a Spartan Scenario for Use of Lunar Materials. In W. W. Mendell, editor, *Lunar bases and space activities of the 21st Century*. Lunar and Planetary Institute, Houston, Tex., 1985.

[55] International Space Exploration Coordination Group (ISECG). *The Global Exploration Roadmap*. 2018.

[56] International Space Exploration Coordination Group (ISECG). *The Global Exploration Roadmap: Supplement August 2020: Lunar Surface Exploration Scenario Update*. NASA, Washington, 2020.

[57] National Oceanic and Atmospheric Administration (NOAA). Climate Change: Global Temperature <https://www.climate.gov/news-features/understanding-climate/climate-change-global-temperature> [accessed: 15 January 2021], 2021.

[58] M. Anand, I. A. Crawford, M. Balat-Pichelin, et al. A brief review of chemical and mineralogical resources on the Moon and likely initial in situ resource utilization (ISRU) applications. *Planetary and Space Science*, 74(1):42–48, 2012.

[59] C. Schwandt, J. A. Hamilton, D. J. Fray, and I. A. Crawford. The production of oxygen and metal from lunar regolith. *Planetary and Space Science*, 74(1):49–56, 2012.

[60] G. H. Just, K. Smith, K. H. Joy, and M. J. Roy. Parametric review of existing regolith excavation techniques for lunar In Situ Resource Utilisation (ISRU) and recommendations for future excavation experiments. *Planetary and Space Science*, 180:104746, 2020.

[61] W. D. Carrier, G. R. Olhoeft, and Mendell W. Physical Properties of the Lunar Surface. In Heiken, G.H., Vaniman, D., French, B.M., editor, *The Lunar Source Book*, pages 475–594. Cambridge University Press, 1991.

[62] National Aeronautics and Space Administration (NASA). Lunar Regolith Excavation and Material Handling <https://sbir.nasa.gov/content/lunar-regolith-excavation-and-material-handling-1> [accessed: 14 January 2021], 2006.

[63] J. N. Rasera, J. J. Cilliers, J. A. Lamamy, and K. Hadler. The beneficiation of lunar regolith for space resource utilisation: A review. *Planetary and Space Science*, 186:104879, 2020.

[64] M. Adachi, K. Hamazawa, Y. Mimuro, et al. Vibration transport system for lunar and Martian regolith using dielectric elastomer actuator. *Journal of Electrostatics*, 89:88–98, 2017.

[65] B. A. Lomax, M. Conti, N. Khan, et al. Proving the viability of an electrochemical process for the simultaneous extraction of oxygen and production of metal alloys from lunar regolith. *Planetary and Space Science*, 180:104748, 2020.

[66] B. Lehner. *To new frontiers: Microbiology for nanotechnology and space exploration.* Doctoral Thesis, University of Technology, Delft, 2019.

[67] R. Volger, M. J. Timmer, J. Schleppi, et al. Theoretical bioreactor design to perform microbial mining activities on mars. *Acta Astronautica*, 170:354–364, 2020.

[68] R. Volger, G. M. Pettersson, S.J.J. Brouns, et al. Mining moon & mars with microbes: Biological approaches to extract iron from Lunar and Martian regolith. *Planetary and Space Science*, 184:104850, 2020.

[69] European Space Agency (ESA). *Space Resources Strategy.* 2019.

[70] National Aeronautics and Space Administration (NASA). *Artemis Plan: NASA's Lunar Exploration Program Overview.* 2020.

[71] D. Kornuta, A. Abbud-Madrid, J. Atkinson, et al. Commercial lunar propellant architecture: A collaborative study of lunar propellant production. *REACH*, 13(12):100026, 2019.

[72] A. Cowley. Astronautics and Space Exploration: Space Resources and Space Analogues for Spaceflight [Lecture Slides], Institute of Space Systems, Stuttgart, 16 January 2020.

[73] H. M. Sargeant, F.A.J. Abernethy, M. Anand, et al. Feasibility studies for hydrogen reduction of ilmenite in a static system for use as an ISRU demonstration on the lunar surface. *Planetary and Space Science*, 180:104759, 2020.

[74] G. B. Sanders and W. E. Larson. Progress Made in Lunar In Situ Resource Utilization under NASA's Exploration Technology and Development Program. *Journal of Aerospace Engineering*, 26(1):5–17, 2013.

[75] Denk, T., González-Pardo, A., Cañadas, I., Vidal, A. Design and Test of a Concentrated Solar Powered Fluidized Bed Reactor for Ilmenite Reduction. *International Annual SolarPACES Conference*, Santiago de Chile, 2017.

[76] R. Trautner, S. J. Barber, J. Carpenter, et al. Development of the PROSPECT Payload Package for Subsurface Sample Acquisition and Analysis of Lunar Volatiles [Presentation Paper], Lunar ISRU, Columbia, MD, USA, 15-17 July 2019.

[77] R. Trautner, S. J. Barber, J. Carpenter, et al. Development of the PROSPECT Payload Package for Subsurface Sample Acquisition and Analysis of Lunar Volatiles [Presentation Slides], Lunar ISRU, Columbia, MD, USA, 15-17 July 2019.

[78] Rosenberg, S., Musbah, O., Rice, E. Carbothermal Reduction of Lunar Materials for Oxygen Production on the Moon: Reduction of Lunar Simulants with Methane. *Lunar and Planetary Science*, 27:1105, 1996.

[79] A. Muscatello. The 2010 Field Demonstration of the Solar Carbothermal Reduction of Regolith to Produce Oxygen [Presentation Slides], First Joint Meeting of the Space Resources Roundtable and the Planetary & Terrestrial Mining Sciences Symposium, Colorado School of Mines, Golden, Colorado, 8-10 June 2010.

[80] H. M. Sargeant, F.A.J. Abernethy, S. J. Barber, et al. Hydrogen reduction of ilmenite: Towards an in situ resource utilization demonstration on the surface of the Moon. *Planetary and Space Science*, 180:104751, 2020.

[81] D. Linne, G. B. Sanders, S. O. Starr, et al. Overview of NASA Technology Development for In-situ Resource Utilization (ISRU). *Proceedings of the 68th International Astronautical Congress 2017*, pages 10382–10381, IAC-17-D3.3.1, 2017.

[82] W. Steurer. Vapor phase pyrolysis. In F. A. McKay, D. S. McKay, and M. B. Duke, editors, *Space Resources*, pages 210–213. Lyndon B Johnson Space Center, Houston, TX, 1992.

[83] D. P. Glavin, C. Malespin, I. L. Kate, et al. Volatile Analysis by Pyrolysis of Regolith for planetary resource exploration. In *2012 IEEE Aerospace Conference*, pages 1–11, Piscataway, NJ, 2012. IEEE.

[84] W. Steurer. Plasma Separation. In F. A. McKay, D. S. McKay, and M. B. Duke, editors, *Space Resources*, pages 214–217. Lyndon B Johnson Space Center, Houston, TX, 1992.

[85] D. Sadoway, A. Ignatiev, and P. Currieri. Regolith Extraction Through Molten Regolith Electrolysis [Presentation Paper], Lunar ISRU, Columbia, MD, USA, 15-17 July 2019.

[86] L. Sibille, S. S. Schreiner, and J. A. Dominguez. Advnaced Concepts for Molten Regolith Electrolysis: One-Step Oxygen and Metals Production Anywhere on the Moon [Presentation Paper], Lunar ISRU, Columbia, MD, USA, 15-17 July 2019.

[87] S. S. Schreiner, J. A. Hoffman, G. B. Sanders, and K. A. Lee. Integrated modelling and optimization of lunar In-Situ Resource Utilization systems. In *IEEE Aerospace Conference, 2015*, pages 1–11, Piscataway, NJ, 2015. IEEE.

[88] S. S. Schreiner, L. Sibille, J. A. Dominguez, and J. A. Hoffman. A parametric sizing model for Molten Regolith Electrolysis reactors to produce oxygen on the Moon. *Advances in Space Research*, 57(7):1585–1603, 2016.

[89] M. S. Paley. Oxygen Production from Luanr Regolith using Ionic Liquids. In *Space, Propulsion & Energy Sciences International Forum SPESIF 2009*, AIP conference proceedings. AIP American Inst. of Physics, Melville, NY, 2009.

[90] D. J. Fray, T. W. Farthing, and Z. Chen. *Removal of Oxygen from Metal Oxides and Solid Solutions by Electrolysis in a Fused Salt*. Cambridge University, 1999.

[91] J. U. Navarrete, I. J. Cappelle, K. Schnittker, and D. M. Borrok. Bioleaching of ilmenite and basalt in the presence of iron-oxidizing and iron-scavenging bacteria. *International Journal of Astrobiology*, 12(2):123–134, 2013.

[92] M. McRobb, B. Robb, S. Ridley, and C. McInnes. Emerging space technologies: macro-scale on-orbit manufacturing. *Journal of The British Interplanetary Society*, 72(12):431–434, 2019.

[93] T. Prater, N. Werkheiser, and F. Ledbetter. Toward a Multimaterial Fabrication Laboratory: In-Space Manufacturing as an Enabling Technology for Long-Endurance Human Space Flight. *Journal of The British Interplanetary Society*, 71(1), 2018.

[94] National Aeronautics and Space Administration (NASA). In-Space Manufacturing <https://www.nasa.gov/oem/inspacemanufacturing> [accessed: 13 August 2020], 2019.

[95] R. G. Clinton, JR. Overview of Additive Manufacturing Initiatives at NASA Marshall Space Flight Center - In Space and Rocket Engines [Presentation Slides], Additive Manufacturing for Aerospace, Defense & Space Conference, London, United Kindom, February 21-23, 2017.

[96] Made In Space Inc. Made In Space to Launch First Ceramic Manufacturing Facility to the International Space Station <https://madeinspace.us/blog/press-releases/made-in-space-to-launch-first-ceramic-manufacturing-facility-to-the-international-space-station/> [accessed: 14 January 2021], 2020.

[97] B. O'Neal. Bioprinting on the ISS: Russian Cosmonaut 3D Prints Cartilage in Space <https://3dprint.com/270522/bioprinting-on-the-iss-russian-cosmonaut-3d-prints-cartilage-in-space/> [accessed: 14 January 2021], 2020.

[98] M. Garcia. Christina Koch activated the new BioFabrication Facility <https://www.nasa.gov/image-feature/christina-koch-activates-the-new-biofabrication-facility> [accessed: 14 January 2021], 2019.

[99] C. Y. Yap, C. K. Chua, Z. L. Dong, et al. Review of selective laser melting: Materials and applications. *Applied Physics Reviews*, 2(4):041101, 2015.

[100] V. Pozzobon, W. Levasseur, K. Do, et al. Household aluminum foil matte and bright side reflectivity measurements: Application to a photobioreactor light concentrator design. *Biotechnology reports (Amsterdam, Netherlands)*, 25:e00399, 2020.

[101] D. Giulietti and M. Lucchesi. Emissivity and absorptivity measurements on some high-purity metals at low temperatures. *Journal of Physics D: Applied Physics*, 14(5):877–881, 1981.

[102] S. J. Cho, T. An, and G. Lim. Three-dimensionally designed anti-reflective silicon surfaces for perfect absorption of light. *Chemical communications (Cambridge, England)*, 50(99):15710–15713, 2014.

[103] H. Kanda, A. Uzum, N. Harano, et al. Al 2 O 3 /TiO 2 double layer anti–reflection coating film for crystalline silicon solar cells formed by spray pyrolysis. *Energy Science & Engineering*, 4(4):269–276, 2016.

[104] T. Satō. Spectral Emissivity of Silicon. *Japanese Journal of Applied Physics*, 6(3):339–347, 1967.

[105] N. M. Ravindra, B. Sopori, O. H. Gokce, et al. Emissivity Measurements and Modeling of Silicon-Related Materials: An Overview. *International Journal of Thermophysics*, 22(5):1593–1611, 2001.

[106] T. Y. Wang, Y. C. Lin, C. Y. Tai, et al. A novel approach for recycling of kerf loss silicon from cutting slurry waste for solar cell applications. *Journal of Crystal Growth*, 310(15):3403–3406, 2008.

[107] R. Martini, M. Gonzalez, F. Dross, et al. Epoxy-Induced Spalling of Silicon. *Energy Procedia*, 27:567–572, 2012.

[108] P. Bellanger and J. Serra. Room Temperature Spalling of Thin Silicon Foils Using a Kerfless Technique. *Energy Procedia*, 55:873–878, 2014.

[109] M. T. Hessmann, T. Kunz, I. Burkert, et al. Laser process for extended silicon thin film solar cells. *Thin Solid Films*, 520(1):595–599, 2011.

[110] M. T. Hessmann, T. Kunz, M. Voigt, et al. Material Properties of Laser-Welded Thin Silicon Foils. *International Journal of Photoenergy*, 2013:1–6, 2013.

[111] N. S. Barekar and B. K. Dhindaw. Twin-Roll Casting of Aluminum Alloys – An Overview. *Materials and Manufacturing Processes*, 29(6):651–661, 2014.

[112] O. Keles and M. Dundar. Aluminum foil: Its typical quality problems and their causes. *Journal of Materials Processing Technology*, 186(1-3):125–137, 2007.

[113] A. U. Malcioglu, C. Dogan, C. Inel, and C. Gode. Effects of Casting Speed on Thin Gauge Foil Surface Quality of 8079 Aluminum Alloy Produced by Twin Roll Casting Method. *Transactions of the Indian Institute of Metals*, 72(4):1001–1011, 2019.

[114] T. Haga, K. Tkahashi, M. Ikawaand, and H. Watari. Twin roll casting of aluminum alloy strips. *Journal of Materials Processing Technology*, 153-154:42–47, 2004.

[115] Y. Li, C. He, J. Li, Z. Wang, Di Wu, and G. Xu. A Novel Approach to Improve the Microstructure and Mechanical Properties of Al-Mg-Si Aluminum Alloys during Twin-Roll Casting. *Materials (Basel, Switzerland)*, 13(7), 2020.

[116] S. M. Rossnagel. Thin film deposition with physical vapor deposition and related technologies. *Journal of Vacuum Science & Technology A: Vacuum, Surfaces, and Films*, 21(5):S74–S87, 2003.

[117] A. Ignatiev and R. S. Polidan. The in-space vacuum deposition of reflective mirror coatings (Conference Presentation). In T. Hull, D. W. Kim, and P. Hallibert, editors, *Astronomical optics*, Proceedings of SPIE, page 18, Bellingham (Wash.), 2019. SPIE.

[118] M. E. Lippman. *In-space fabrication of thin-film structures.* National Aeronautics and Space Administration, Washington, D.C., 1972.

[119] K. E. Drexler. *Design of a high performance solar sail system.* Massachusetts Institute of Technology (MIT), Boston, MA, USA, 1979.

[120] pveducation.org. Surface Texturing <https://www.pveducation.org/pvcdrom/design-of-silicon-cells/surface-texturing> [accessed: 20 January 2021], 2021.

[121] A. Parretta, A. Sarno, P. Tortora, et al. Angle-dependent reflectance measurements on photovoltaic materials and solar cells. *Optics Communications*, 172(1-6):139–151, 1999.

[122] S. Manzoor, M. Filipič, A. Onno, et al. Visualizing light trapping within textured silicon solar cells. *Journal of Applied Physics*, 127(6):063104, 2020.

[123] L. Forbes. Texturing, reflectivity, diffuse scattering and light trapping in silicon solar cells. *Solar Energy*, 86(1):319–325, 2012.

[124] D. Kray, M. Hermle, and S. W. Glunz. Theory and experiments on the back side reflectance of silicon wafer solar cells. *Progress in Photovoltaics: Research and Applications*, 16(1):1–15, 2008.

[125] D. Z. Dimitrov and C.-H. Du. Crystalline silicon solar cells with micro/nano texture. *Applied Surface Science*, 266:1–4, 2013.

[126] Y. Xiu, S. Zhang, V. Yelundur, et al. Superhydrophobic and low light reflectivity silicon surfaces fabricated by hierarchical etching. *Langmuir : the ACS journal of surfaces and colloids*, 24(18):10421–10426, 2008.

[127] C.-H. Hsu, J.-R. Wu, Y.-T. Lu, et al. Fabrication and characteristics of black silicon for solar cell applications: An overview. *Materials Science in Semiconductor Processing*, 25:2–17, 2014.

[128] G. Vdovin, P. Sarro, O. Soloviev, et al. Structured film for compensation of anthropogenic radiative forcing. *Optics letters*, 40(8):1702–1704, 2015.

[129] M. Rönnelid, M. Adsten, T. Lindström, et al. Optical scattering from rough-rolled aluminum surfaces. *Applied optics*, 40(13):2148–2158, 2001.

[130] P. M. Reynolds. Spectral emissivity of 99.7% aluminium between 200 and 540°C. *British Journal of Applied Physics*, 12(3):111–114, 1961.

[131] National Aeronautics and Space Administration (NASA). NASA Funds Demo of 3D-Printed Spacecraft Parts Made, Assembled in Orbit <https://www.nasa.gov/press-release/nasa-funds-demo-of-3d-printed-spacecraft-parts-made-assembled-in-orbit>[accessed: 14 January 2021], 2019.

[132] R. Hoyt, J. Cushing, and J. Slostad. *SpiderFab: Process for On-Orbit Construction of Kilometer-Scale Apertures*. Tethers Unlimited, Inc., 2013.

[133] D. Werner. Tethers Unlimited expands to fulfill additive manufacturing orders <https://spacenews.com/tethers-unlimited-expands-to-fulfill-additive-manufacturing-orders/> [accessed: 14 January 2021], 2017.

[134] National Aeronautics and Space Administration (NASA). OSAM-1 <https://nexis.gsfc.nasa.gov/osam-1.html> [accessed: 14 January 2021], 2020.

[135] National Aeronautics and Space Administration (NASA). NASA Funds Demonstration of Assembly and Manufacturing in Space <https://www.nasa.gov/press-release/nasa-funds-demonstration-of-assembly-and-manufacturing-in-space> [accessed: 14 January 2021], 2020.

[136] National Aeronautics and Space Administration (NASA). OSAM-2 <https://www.nasa.gov/mission_pages/tdm/osam-2.html> [accessed: 14 January 2021], 2020.

[137] B. Bhushan and M. Caspers. An overview of additive manufacturing (3D printing) for microfabrication. *Microsystem Technologies*, 23(4):1117–1124, 2017.

[138] R. Matsuzaki, M. Ueda, M. Namiki, et al. Three-dimensional printing of continuous-fiber composites by in-nozzle impregnation. *Scientific reports*, 6:23058, 2016.

[139] M. K. Agarwala, R. van Weeren, A. Bandyopadhyay, et al. Fused Deposition of Ceramics and Metals: An Overview. *International Solid Freeform Fabrication Symposium*, 1996.

[140] Fraunhofer Institut für Fertigungstechnik und Angewndte Materialforschun (IFAM). Metallischer 3D-Druck mittels Fused Filament Fabrication <https://www.ifam.fraunhofer.de/de/Institutsprofil/Standorte/Dresden/Zellulare_ metallische_Werkstoffe/fused-filament-fabrication.html> [accessed 15 January 2021], 2021.

[141] S. L. Sing and W. Y. Yeong. Laser powder bed fusion for metal additive manufacturing: Perspectives on recent developments. *Virtual and Physical Prototyping*, 15(3):359–370, 2020.

[142] A. K. Gujba and M. Medraj. Power Ultrasonic Additive Manufacturing: Process Parameters, Microstructure, and Mechanical Properties. *Advances in Materials Science and Engineering*, 2020(5):1–17, 2020.

[143] S.-H. Tang, C.-W. Cheng, R.-Y. Yeh, and R.-Q. Hsu. Direct joining of 3D-printed thermoplastic parts to SLM-fabricated metal cellular structures by ultrasonic welding. *The International Journal of Advanced Manufacturing Technology*, 99(1-4):729–736, 2018.

[144] Fabrisonic. Fabrisonic's 3D Metal Printing Design Guide and Frequently Asked Questions <https://fabrisonic.com/3dprinting/wp-content/uploads/2018/03/FAQ-Design-Guide_S.pdf> [accessed: 15 January 2021], 2021.

[145] K. M. B. Taminger and R. A. Hafley. Electron beam freeform fabrication: A rapid metal deposition process. *Proceedings of the 3rd Annual Automotive Composites Conference, Troy, MI, USA*, 2003.

[146] K. N. Kalashnikov, K. S. Khoroshko, T. A. Kalashnikova, et al. Structural evolution of 321 stainless steel in electron beam freeform fabrication. *Journal of Physics: Conference Series*, 1115:042049, 2018.

[147] R. Hafley, K. Taminger, and R. Bird. Electron Beam Freeform Fabrication in the Space Environment. In *45th AIAA Aerospace Sciences Meeting and Exhibit*, page 857, [Reston, VA], 2007. [American Institute of Aeronautics and Astronautics].

[148] K. M. Taminger, C. S. Domack, J. N. Zalameda, et al. In-process thermal imaging of the electron beam freeform fabrication process. In *SPIE Commercial + Scientific Sensing and Imaging, 2016, Baltimore, MD, USA*.

[149] S. Chang, H. Zhang, H. Xu, et al. Closed-Loop Control of Droplet Transfer in Electron-Beam Freeform Fabrication. *Sensors (Basel, Switzerland)*, 20(3), 2020.

[150] National Aeronautics and Space Administration (NASA). Electron Beam Freeform Fabrication <https://www.nasa.gov/topics/technology/features/ebf3.html> [accessed: 15 January 2021], 2011.

[151] European Space Agency (ESA). 3D printing our way to the Moon <https://www.esa.int/Enabling_Support/Preparing_for_the_Future/Discovery_and_Preparation/3D_printing_our_way_to_the_Moon> [accessed 09. January 2021], 2019.

[152] C. Battaglia, A. Cuevas, and S. de Wolf. High-efficiency crystalline silicon solar cells: Status and perspectives. *Energy & Environmental Science*, 9(5):1552–1576, 2016.

[153] A. Goetzberger, J. Knobloch, and B. Voss. *Crystalline silicon solar cells*. Wiley, Chichester and New York, 1998.

[154] G. A. Landis. Lunar production of space photovoltaic arrays. In *Conference Record of the Twentieth IEEE Photovoltaic Specialists Conference*, pages 874–879 vol.2. IEEE, 1988.

[155] G. A. Landis and M. A. Perino. Lunar production of solar cells. *Princeton Conference on Space Manufacturing*, 1989.

[156] A. Ignatiev, A. Freundlich, S. Rosenberg, D. Makel, and M. Duke. *New Architecture for Space Solar Power Systems: Fabrication of Silicon Solar Cells Using In-Situ Resources: NIAC-Program - Final Report*. Houston, 2000.

[157] A. Ignatiev. New Architecture for Space Solar Power Systems: Fabrication of Silicon Solar Cells Using In-Situ Resources [Presentation Slides]. *NIAC 2nd Annual Meeting*, June 6-7 2000.

[158] C. Horton, C. Gramajo, A. Alemu, et al. Design Issues in Fabricating Nanocrystalline Silicon Solar Cells Using In-Situ Lunar Resources. *NanoTech 2002 - At the Edge of Revolution*, 9-12 September 2002, Houston, TX, USA.

[159] C. Horton, C. Gramajo, A. Alemu, et al. First demonstration of photovoltaic diodes on lunar regolith-based substrate. *Acta Astronautica*, 56(5):537–545, 2005.

[160] J. Bartl and M. Baranek. Emissivity of aluminium and its importance for radiometric measurement. *Measurement of Physical Quantities*, 2004.

[161] A. Lyngvi, P. Falkner, and A. Peacock. The interstellar heliopause probe technology reference study. *Advances in Space Research*, 35(12):2073–2077, 2005.

[162] M. Macdonald, G. W. Hughes, C. R. McInnes, et al. Solar Polar Orbiter: A Solar Sail Technology Reference Study. *Journal of Spacecraft and Rockets*, 43(5):960–972, 2006.

[163] M. Leipold, H. Fichtner, B. Heber, et al. Heliopause Explorer—a sailcraft mission to the outer boundaries of the solar system. *Acta Astronautica*, 59(8-11):785–796, 2006.

[164] T. Appourchaux, P. Liewer, M. Watt, et al. POLAR investigation of the Sun—POLARIS. *Experimental Astronomy*, 23(3):1079–1117, 2009.

[165] The International Aluminium Institute. Primary Aluminium Production, December 2020 <https://www.world-aluminium.org/statistics/> [accessed: 24 January 2021], 2021.

[166] J. O. McSpadden and J. C. Mankins. Space solar power programs and microwave wireless power transmission technology. *IEEE Microwave Magazine*, 3(4):46–57, 2002.

[167] W. C. Brown and E. E. Eves. Beamed microwave power transmission and its application to space. *IEEE Transactions on Microwave Theory and Techniques*, 40(6):1239–1250, 1992.

[168] W. C. Brown. *LEO to GEO Transportation System Combining Electric Propulsion with Beamed Microwave Power from Earth.* American Astronautical Society, 1987.

[169] I. Levchenko, K. Bazaka, S. Mazouffre, and S. Xu. Prospects and physical mechanisms for photonic space propulsion. *Nature Photonics*, 12(11):649–657, 2018.

[170] National Space Society. *A Public/Privaet COTS-Type Program to Develop Space Solar Power [Position Paper].* 2020.

[171] Y. Yang, Y. Zhang, B. Duan, et al. A novel design project for space solar power station (SSPS-OMEGA). *Acta Astronautica*, 121:51–58, 2016.

[172] J. C. Mankins. New Developments in Space Solar Power. *NSS Space Settlement Journal*, 2017.

[173] T. Bawden. Millions of homes could be powered by solar power beamed down from space by 2050 <https://inews.co.uk/news/science/millions-uk-homes-solar-power-beamed-down-from-space-2050-759491> [accessed: 17 January 2021], 2020.

[174] European Space Agency (ESA). Clean Energy - New Ideas for Solar Power from Space <https://ideas.esa.int/servlet/hype/IMT?documentTableId=45087625530300097&userAction=Browse&templateName=&documentId=514a8db636ea637f6e27069183966350> [accessed: 17 January 2021], 2020.

[175] D. Goto, H. Yoshida, H. Suzuki, et al. The Overview of JAXA Laser Energy Transmission R&D Activities and the Orbital Experiments Concept on ISS-JEM. *Proceedings of the International Conference on Space Optical Systems and Applications (ICSOS), Kobe, Japan*, May 7-9 2014.

[176] U.S. Naval Research Laboratory. NRL conducts first test of solar power satellite hardware in orbit <https://www.nrl.navy.mil/news/releases/nrl-conducts-first-test-solar-power-satellite-hardware-orbit> [accessed: 20 January 2021], 2020.

[177] F. Fertig and E. Franklin. Titanium Diocide as Anti-reflective Coating for Crystalline Silicon Solar Cells. *Proceedings of the European Photovoltaic Solar Energy Conference, Milan, Italy*, September 3-7 2007.

[178] L. Granados, N. Takamure, J. Bing, et al. Direct Determination of Total Hemispherical Emittance of Perovskite and Silicon Solar Cells. *Cell Reports Physical Science*, 1(1):100008, 2020.

[179] European Space Agency (ESA). Luna facility brings Moon to Earth <https://www.esa.int/About_Us/EAC/Luna_facility_brings_Moon_to_Earth> [accessed: 19 January 2021], 2018.

[180] A. Lydon. Forget silicon. This material could be a game-changer for solar power <https://edition.cnn.com/2020/10/14/energy/solar-energy-perovskites-spc-intl/index.html> [accessed: 29 January 2021], 2020.

[181] Oxford PV. Oxford PV hits new world record for solar cell <https://www.oxfordpv.com/news/oxford-pv-hits-new-world-record-solar-cell> [accessed: 01 February 2021], 2020.

[182] Moon Village Association. Home <https://moonvillageassociation.org/> [accessed: 04 February 2021], 2021.

[183] International Space Univerisity (ISU). *EC2LIPSE: Exploring Climate Change Lagrangian 1 Point Solutions for Earth.* Strasbourg, France, 2012.

[184] National Aeronautics and Space Administration (NASA). Technology Readiness Level <https://www.nasa.gov/directorates/heo/scan/engineering/technology/txt_accordion1.html> [accessed: 01 February 2021], 2017.

Appendices

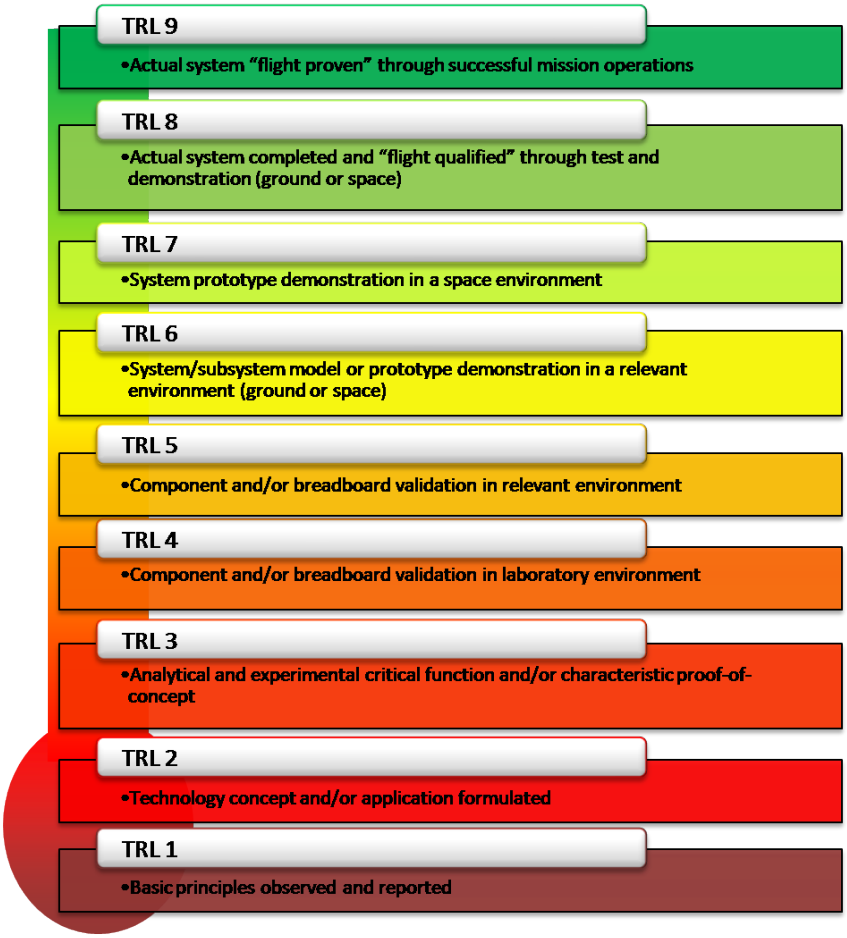

Figure 1: Definition of TRL levels by NASA [184]

	Shading f	Sunshade Position	Sunshade Area	Sunshade Mass	Power
Minimum Mass Sunshade	0.52%	2.199×10^9 m	1.707×10^6 km^2	73.74×10^9 kg	
	1.1%	2.199×10^9 m	3.612×10^6 km^2	155.99×10^9 kg	
	1.77%	2.199×10^9 m	5.812×10^6 km^2	251.00×10^9 kg	
	1.9%	2.199×10^9 m	6.239×10^6 km^2	269.44×10^9 kg	
	2.6%	2.199×10^9 m	8.537×10^6 km^2	368.70×10^9 kg	
	3.6%	2.199×10^9 m	11.492×10^6 km^2	496.33×10^9 kg	
Photovoltaic Sunshade	0.52%	1.558×10^9 m	0.857×10^6 km^2	286.00×10^9 kg	72.90 TW
	1.1%	1.558×10^9 m	1.813×10^6 km^2	604.99×10^9 kg	154.21 TW
	1.77%	1.558×10^9 m	2.918×10^6 km^2	973.49×10^9 kg	248.14 TW
	1.9%	1.558×10^9 m	3.132×10^6 km^2	$1{,}045.00\times10^9$ kg	266.36 TW
	2.6%	1.558×10^9 m	4.286×10^6 km^2	$1{,}430.00\times10^9$ kg	364.49 TW
	3.6%	1.558×10^9 m	5.769×10^6 km^2	$1{,}925.00\times10^9$ kg	490.67 TW

Table 1: Overview of sunshade sizes for different amounts of shading

	Sunshade Technologies	2021 - 2024	2025 - 2029	2030 - 2034	2035 - 2039	2040 - 2044	2045 - 2049
ISRU	Regolith Excavation	TRL-4 Analog Tests, NASA Excavation Contests, RASSOR	TRL-5 ESA Luna Facility	TRL-6 ESA Goal	TRL-7	TRL-8	
	Regolith Beneficiation	TRL-3 Slide/Plate Separation, ETW	TRL-5 ESA Luna Facility	TRL-6	TRL-7	TRL-8	
	Metal Extraction	TRL-3 MRE, MSE	TRL-5 Metalysis-FFC	TRL-6 ESA Goal	TRL-7	TRL-8	
ISMA	Thin Foil Production	TRL-3 Evaporation, TRC [TRL-9]	TRL-5	TRL-6	TRL-7	TRL-8	
	Metal Structure Printing	TRL-4/-5 UAM / EBF3		TRL-6	TRL-7	TRL-8	
	In-Space Vacuum Deposition	TRL-6 Lunar Resources, Inc.	TRL-7 OSAM 1			TRL-8	
	Automated Assembly	TRL-6 SpiderFab, Archinaut, Phoenix ...	TRL-7 OSAM 1, OSAM 2			TRL-8	
Power	Lunar Photovoltaics	TRL-2 NIAC Studies	TRL-3	TRL-6	TRL-7	TRL-8	
	Wireless Power Transmission	TRL-4/-5 NRL, JAXA Demos		TRL-7		TRL-8	
Logistics	SEL_1 Solar Sailing	TRL-6 IKAROS RCD, LightSail 2, NEA Scout	TRL-7 Solar Cruiser	TRL-8			
	Reusable Rockets	TRL-6 Starship	TRL-9 Starship				
	Lunar Mass Driver	TRL-4 EMRG [TRL-9], EMM, EMALS			TRL-6	TRL-8	
	Laser Beam Propulsion	TRL-4 US Navy SSL [TRL-6]					TRL-7

Figure 2: Sunshade technology status and outlook (Phase 1: 2021 - 2040 | Phase 2: 2035 - 2045 | Phase 3: 2045 - 2070)

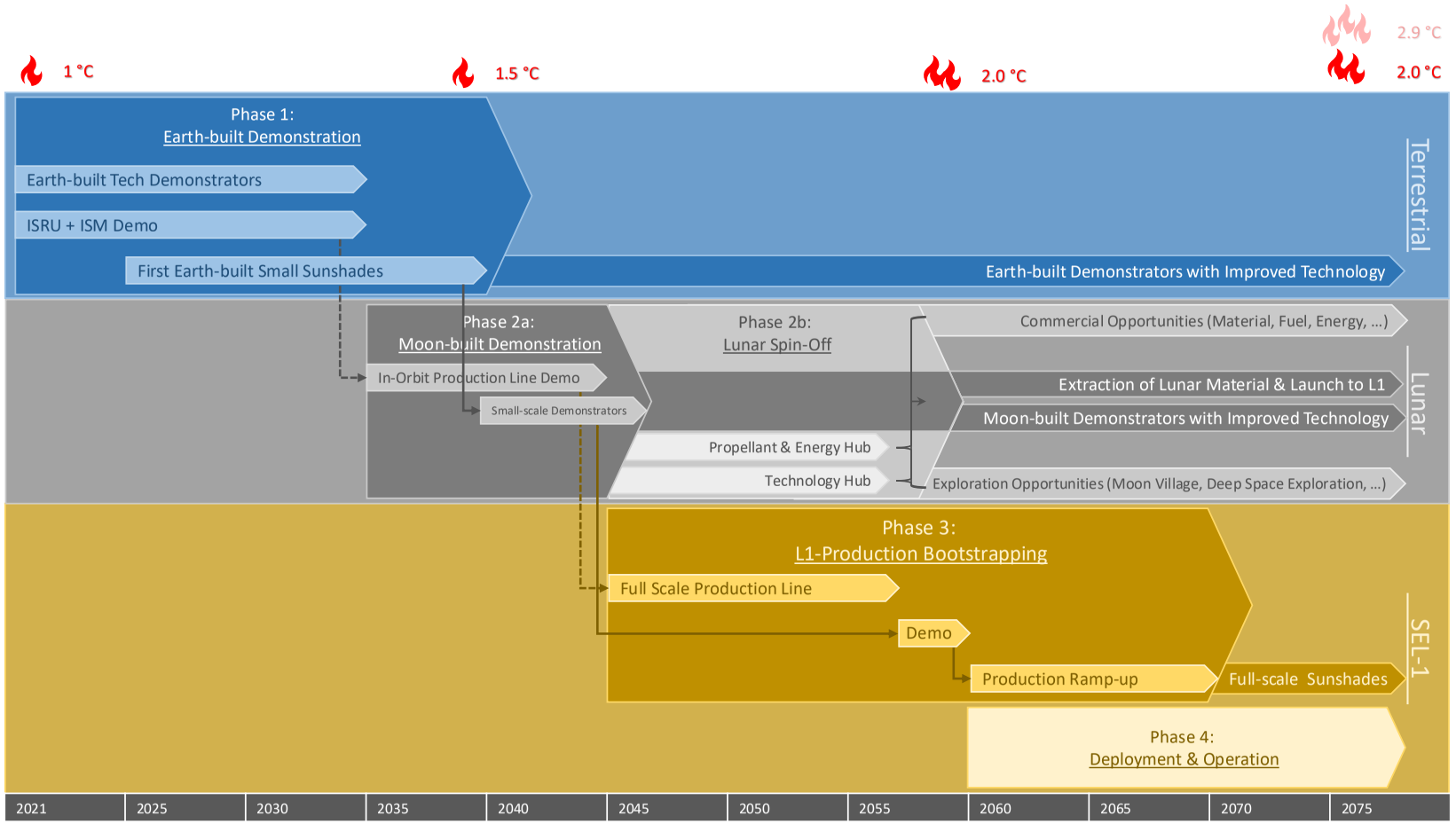

Figure 3: Roadmap towards a sunshade at SEL_1

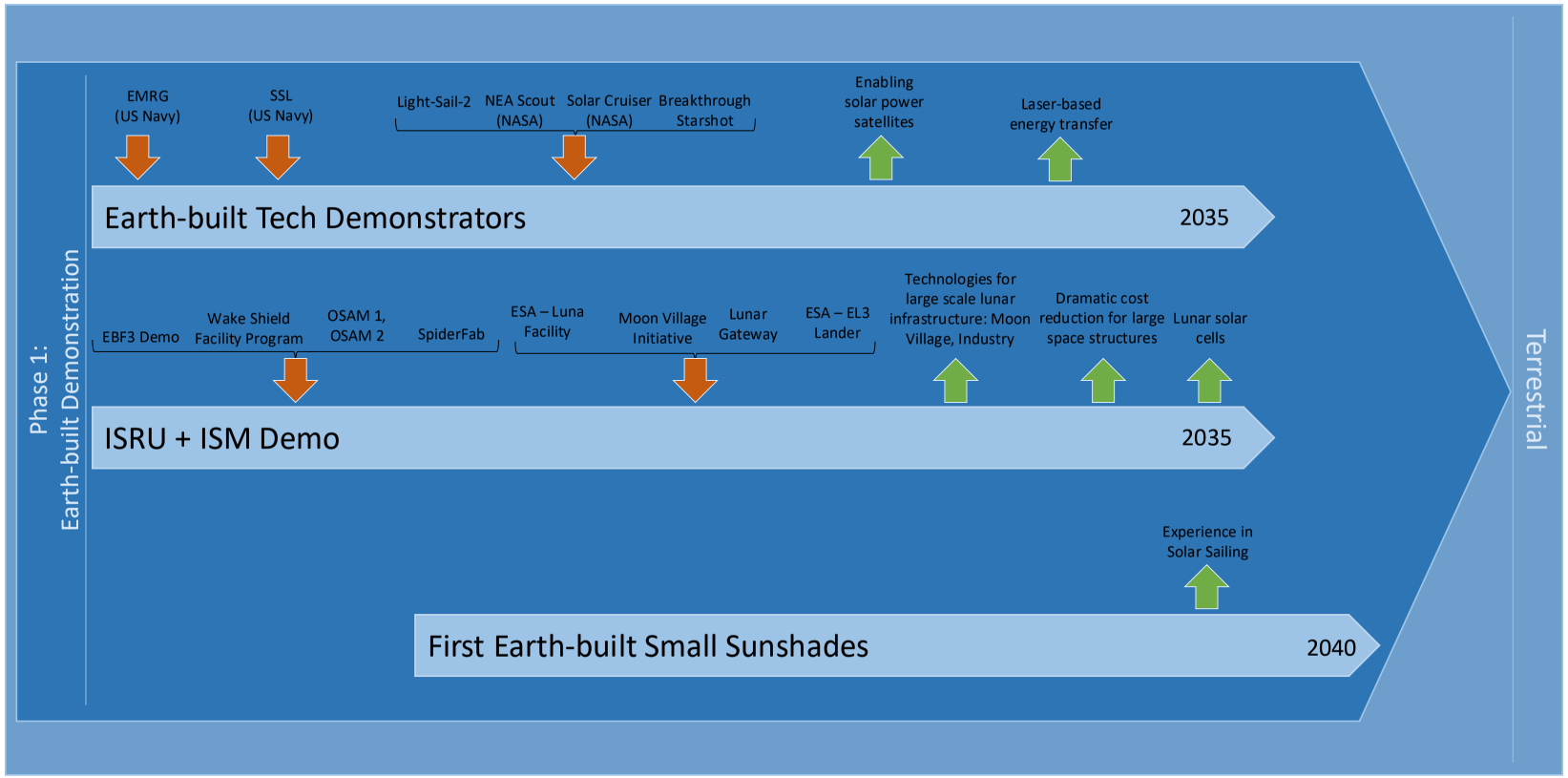

Figure 4: Early spin-in and spin-off potentials during phase 1 of sunshade development